Terr. Atmos. Ocean. Sci., Vol. 29, No. 2, 149-186, April 2018 doi: 10.3319/TAO.2017.08.29.01

Zircon U-Pb and Hf isotopic constraints on the magmatic evolution of the Northern Luzon Arc

Yu-Ming Lai[1,*], Mei-Fei Chu[2], Wen-Shan Chen[3], Wen-Yu Shao[3], Hao-Yang Lee[4], and Sun-Lin Chung[3,4]

[1] *Department of Earth Sciences, National Taiwan Normal University, Taipei City, Taiwan*
[2] *Institute of Oceanography, National Taiwan University, Taipei City, Taiwan*
[3] *Department of Geosciences, National Taiwan University, Taipei City, Taiwan*
[4] *Institute of Earth Sciences, Academia Sinica, Taipei City, Taiwan*

Article history:
Received 5 July 2017
Revised 17 August 2017
Accepted 29 August 2017

Keywords:
Taiwan, Zircon, U-Pb geochronology, Hf isotope, Magma, Northern Luzon Arc

Citation:
Lai, Y.-M., M.-F. Chu, W.-S. Chen, W.-Y. Shao, H.-Y. Lee, and S.-L. Chung, 2018: Zircon U-Pb and Hf isotopic constraints on the magmatic evolution of the Northern Luzon Arc. Terr. Atmos. Ocean. Sci., 29, 149-186, doi: 10.3319/TAO.2017.08.29.01

ABSTRACT

The complete volcanic sequences restored in the Coastal Range of Taiwan are key archives for better understanding the magmatic and tectonic evolution of the Northern Luzon Arc. This paper reports (1) new zircon U-Pb ages and Hf isotopic data of fourteen volcanic samples from different sequences of four major volcanoes in the Coastal Range, (2) Hf isotopic data of dated magmatic and detrital zircons from two offshore volcanic islands, Lutao and Lanyu. These data indicate that the arc magmatism in the Coastal Range started at ~15 Ma, most active at ~9 Ma, and ceased at ~4.2 Ma. Magmatic zircons from the arc rocks show a significant variation in Hf isotopic composition, with $\varepsilon_{Hf}(T)$ values varying from +24.9 to +4.8. As pointed out by our previous studies, old continental zircons that show Cathaysian-type ages and Hf isotope features are common in samples from the Yuemei, Chimei, and Lanyu volcanoes, supporting the notion for the influence of the existence of an accreted micro-continent or continental fragment plays a role in the petrogenesis. Such inherited zircons are not observed in the Chengkuang'ao and Tuluanshan volcanoes and uncommon in Lutao, implying the discontinuity or a limited extent of the accreted continental fragment. The $\varepsilon_{Hf}(T)$ values are high and positive from ~15 - 8 Ma (+25 to +15; ±5ε-unit variation), and became lower from ~6 to 4.2 Ma (+20 to +8; ±6ε units) and the lowest from ~1.3 Ma (+19 to +5; ±7ε units). Such a temporal variation in zircon Hf isotopic ratios can be also identified in whole-rock Hf and Nd isotopic compositions, which decrease from ~6 Ma when the Northern Luzon Arc may have started colliding with the Eurasian continental margin.

1. INTRODUCTION

The Northern Luzon Arc (NLA) consists of the Coastal Range (CR) of Taiwan and volcanic islands between Taiwan and Luzon Island, e.g., the Lutao and Lanyu Islands (Fig. 1a). The CR refers to the region that has collided with the Eurasian continental margin, and it consists of volcanoes with complete volcanic sequences that can be used to study the magmatic and tectonic evolution of the NLA. From north to south, the four major volcanoes in the CR were recognized as the Yuemei, Chimei, Chengkuang'ao, and Tuluanshan volcanic groups by Lai and Song (2013) (Fig. 1b). Previous studies have produced abundant dating results for the volcanic rocks in the CR; however, geologists need to use these data carefully because of two major questions. The first problem with many geochronological studies is the inaccuracy of the K/Ar results, due to the low-temperature alteration experienced by these samples (Lo et al. 1994). Another problem is that the dating results from the same location are inconsistent with each other (Ho 1969; Juang and Bellon 1984; Richard et al. 1986; Yang et al. 1988, 1995; Song 1990; Lo et al. 1994; Song and Lo 2002). This is because volcanic sequences were not established until Song and Lo (1988), and volcanic rocks from different sequences may yield various ages even in the same outcrop. Consequently, these previous ages are considered for reference only. Recently, Shao et al. (2015) used the results of

* *Corresponding author*
E-mail: ymlai@ntnu.edu.tw

zircon U-Pb dating to constrain the beginning of the main magmatism of the Chimei volcano to ~9 Ma; on the other hand, Lai et al. (2017) reported that the $^{40}Ar/^{39}Ar$ ages from the top sequences of each volcano in the CR represent the time of its latest eruption.

Zircon is a mineral that is physically and chemically robust under wide-ranging conditions and is widespread in volcanic rocks. The closure temperature of the U-Pb isotopic system in zircon is very high; therefore, it can still yield accurate age information following hydrothermal alteration. For these reasons, the zircon U-Pb dating method is suitable for the analysis of volcanic rocks in the CR. In this paper, we report the in situ analyses of zircon U-Pb ages and Lu-Hf isotopes for volcanic rocks from individual volcanic sequences of these four major volcanoes in the CR. These results reflect the occurrence of several significant and different volcanic processes in each volcano. Moreover, we combine the ages and Hf isotopic compositions of volcanic rocks from the Lutao and Lanyu Islands. The inherited zircons from the Yuemei, Chimei, and Lanyu volcanoes yield Cathaysian-type ages and Hf isotopic compositions. Based on the ages and isotopic compositions of these six volcanoes, the petrogenesis of the NLA can be determined.

2. GEOLOGICAL BACKGROUND

The NLA was formed when the South China Sea Plate subducted beneath the Philippine Sea Plate from approximately 35 - 17 Ma (Taylor and Hayes 1983). The CR includes four major volcanoes, named the Yuemei, Chimei, Chengkuang'ao, and Tuluanshan volcanic groups, which have already become a part of Taiwan, as well as two volcanic islands located near Taiwan, which are named Lutao and Lanyu Islands (Fig. 1). Previous studies of the magmatic rocks in the CR have focused on their mineralogy and petrology (Wang 1966; Yen 1967), volcanology (Song and Lo 2002; Lai and Song 2013), geochemistry (Chen 1975; Lan 1982; Chen et al. 1990; Song 1990; Yang 1992; Lai et al. 2008, 2017; Lai and Song 2013), and geochronology (Ho 1969; Juang and Bellon 1984; Richard et al. 1986; Yang et al. 1988, 1995; Song 1990; Lo et al. 1994; Song and Lo 2002; Shao et al. 2015; Lai et al. 2017). Among these studies, the establishment of volcanic sequences and geochronologic analyses of volcanic rocks are the two main methods that have been used to understand the relationships between geochemical variations and time.

Volcanic sequences in the CR were first established by Hsu (1956); they were then revised by later geologists several times. The sequences used in this paper were established by Song and Lo (1988). These volcanic sequences include the Chimei Igneous Complex (CM) in the lower part and the Tuluanshan Formation in the upper part (Ho 1969; Song and Lo 1988). The Chimei Igneous Complex is composed of basaltic to andesitic lava flows and some volcaniclastic rocks (Yen 1967; Song and Lo 1988; Chen 1997). During the period of CM sequence, the volcanic island erupted below the volatile fragmentation depth and formed lava flows that were several thousand meters thick. The previous dating of volcanic

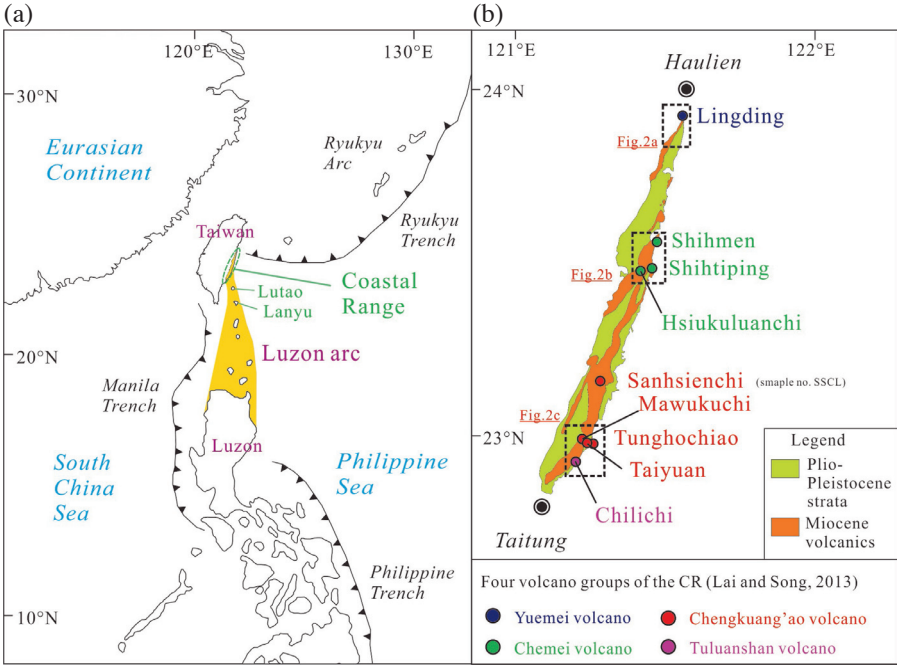

Fig. 1. Simplified tectonic map of the NLA and geological map of the CR. (a) The NLA includes the CR of Taiwan and two oceanic volcanic islands (i.e., Lutao and Lanyu volcanoes). (b) Volcanic sequences marked by different colors correspond to the four major volcanoes in the CR. Three rectangles represent the ranges of Figs. 2a - c.

rocks in this sequence yielded ages of 29.7 - 9.2 Ma using the K/Ar method (Ho 1969; Richard et al. 1986) and 16.4 - 8.3 Ma using zircon fission track dating (Yang et al. 1988, 1995). Recently, Shao et al. (2015) obtained the youngest grains of zircons yielding the mean $^{206}Pb/^{238}U$ date at ~9 Ma in the CM sequence from Chimei volcano, which represents the emplacement age of the magma. The Tuluanshan Formation include three subsequences; from the lower part to the upper part, these are named the Shihmen Volcanic Breccia (SM), Shihtiping Tuff (STP), and Kangkou Limestone (Yen 1967; Song and Lo 1988). The SM sequence is composed of mono- to heterolithologic volcanic breccias, some tuff breccias, and occasional lava flows. It was formed by a more violent eruption when a volcanic island grew above the volatile fragmentation depth (Song 1990). The STP sequence conformably overlies the SM sequence. It represents the top of these volcanic sequences and contains ignimbrite, white tuff, and peperite (Song and Lo 1988; Lai and Song 2013). Its impacted structure, plastic deformation, and welded structure indicate that the STP sequence was formed within a subaerial environment (Song 1990; Lai and Song 2013). The results of the $^{40}Ar/^{39}Ar$ dating of the ignimbrite in this sequence were reported by Lai et al. (2017), and include ages of ~7.2 Ma in Yuemei volcano, ~4.2 Ma in Chimei volcano, and ~6.2 Ma in Chengkuang'ao volcano. Other dating studies that used the K/Ar and $^{40}Ar/^{39}Ar$ methods yielded inconsistent or inaccurate ages due to sample weathering, low-temperature alteration, and the analysis of samples from unknown sequences (Lo et al. 1994; Lai et al. 2017).

Abundant geochemical data in the NLA have been reported by previous studies (Chen 1975; Lan 1982; Jacques 1987; Vidal et al. 1989; Chen et al. 1990; Defant et al. 1990; Song 1990; Yang 1992; Yang et al. 1992; McDermott et al. 1993; Fourcade et al. 1994; Marini et al. 2005; Lai et al. 2008, 2017; Shao et al. 2015). To summarize the magma genesis models from previous studies, magmas from the NLA underwent only source contamination (Chen et al. 1990; Defant et al. 1990; McDermott et al. 1993; Marini et al. 2005) or crustal contamination before they were erupted (Yang 1992; Fourcade et al. 1994; Shao et al. 2015; Lai et al. 2017). Recently, Shao et al. (2015) reported the magmatic ages of the bottom sequence in Chimei volcano and proposed that the inherited zircons originated from the old continental crust of the Cathaysia Block. Furthermore, Lai et al. (2017) reported that the effects of crustal contamination increased after 6 Ma, according to the whole-rock Sr-Nd isotopic data.

3. SAMPLES

Fourteen volcanic samples were analyzed during this study (Table 1). These samples were collected from the CM, SM, and STP sequences from the four major volcanoes of the CR (Figs. 1b and 2). At Yuemei volcano, we selected one sample (no. LD) from the SM sequence and another one (no. 130811-6) from the STP sequence at the Lindging section (Figs. 1b and 2a). Four samples were selected from Chimei volcano, one of which was from the Shihmen section (no. SM-1), which belongs to the SM sequence; the others were selected from the STP sequence at the Shihtiping section (no. STP-1, 130812-3, and STPW). In order to obtain complete data from whole volcanic sequences in this volcano, we also combined these data with the dating analyses of the CM sequence at the Hsiukulunchi section (no. CM-1, 6, 10, 17, 20, and 24) reported by Shao et al. (2015) (Figs. 1b and 2b). A total of seven samples were collected from Chengkuang'ao volcano (Figs. 1b and 2c). Two samples were selected from lava flows in the lower part of the SM sequence at the Mawukuchi (no. TH-1) and Sanhsienchi (no. SSCL) sections. Four samples were selected from the Taiyuan section, two of which were from the SM sequence (no. SM-2 and TYB) and two of which were from the STP sequence (no. STP-2 and TYW). The remaining sample was collected from the STP sequence in the Tunghochiao section (no. THCW). Only one sample was collected from Tuluanshan volcano, which was collected from the STP sequence (no. CLCW) at the Chilichi section (Figs. 1b and 2c). All fourteen samples were fresh, homogeneous and considered to be representative of the volcanic sequences to which they belonged. Zircons from all samples were analyzed for both their U-Pb ages and Hf isotope data, except for one sample from the SM sequence at the Lingding section (no. LD), which was not analyzed for its Hf isotopic data because its zircons were exhausted after being dated.

4. ANALYTICAL METHODS

Zircons were separated from all volcanic samples using conventional techniques, combining magnetic separation and heavy liquid methods. They were then mounted in epoxy and polished to expose the interiors of crystals for analysis. Cathodoluminescence (CL) images were taken at the Institute of Earth Sciences, Academia Sinica, Taipei, in order to examine the internal structures of individual zircons to select suitable positions for U-Pb dating and Lu-Hf isotope analyses.

In situ zircon U-Pb isotope dating analyses were performed using an Agilent 7500s inductively coupled plasma mass spectrometer (ICP-MS) attached to a New Wave UP213 laser ablation system at the Department of Geosciences, National Taiwan University. The laser repetition rate was 4 Hz, and the spot diameter was ~30 to 40 μm. Calibrations were performed by analyzing the GJ-1 zircon standard (608.5 ± 0.4 Ma, Jackson et al. 2004). Two other well-known zircon standards, 91500 (1065.4 ± 0.6 Ma, Wiedenbeck et al. 1995) and Mud Tank (732 ± 5 Ma, Black and Gulson 1978), as well as one new standard, Plešovice (337.1 ± 0.4 Ma, Sláma et al. 2008), were used for data quality control.

Table 1. Sample list of selected volcanic rocks in the Coastal Range.

Sample no.	Volcano	Outcrop section	Volcanic sequence	Lithofacies	Mean U-Pb age (Ma, 2σ)	Note
130811-6	Yuemei	Lingding	STP Formation	White bomb	-	This study
LD	Yuemei	Lingding	SM Formation	Black breccia	-	This study
STP-1	Chimei	Shihtiping	STP Formation	White bomb	-	This study
STPW	Chimei	Shihtiping	STP Formation	White bomb	4.6 ± 1.5 Ma (n = 3/80)	This study
130812-3	Chimei	Shihtiping	STP Formation	White bomb	4.2 ± 0.1 Ma (n = 16/17)	This study
SM-1	Chimei	Shihmei	SM Formation	Black breccia	-	This study
CM-1, 6, 10, 17, 20, 24	Chimei	Hsiukuluanchi	CM Formation	Lava flow	9.0 ± 0.3 (n = 10/50)	Shao et al. (2015)
TYW	Chengkuang'ao	Taiyuan	STP Formation	White bomb	7.8 ± 0.2 (n = 24/24)	This study
STP-2	Chengkuang'ao	Taiyuan	STP Formation	White bomb	8.0 ± 0.2 (n = 31/38)	This study
THCW	Chengkuang'ao	Tunghochiao	STP Formation	White bomb	6.5 ± 0.1 (n = 24/24)	This study
TYB	Chengkuang'ao	Taiyuan	SM Formation	Black breccia	8.0 ± 0.2 (n = 24/24)	This study
SM-2	Chengkuang'ao	Taiyuan	SM Formation	Black breccia	7.0 ± 0.2 (n = 31/32)	This study
TH-1	Chengkuang'ao	Mawukuchi	SM Formation	Lava flow	7.9 ± 0.2 (n = 25/25)	This study
SSCL	Chengkuang'ao	Sanhsienchi	SM Formation	Lava flow	9.2 ± 0.4 (n = 8/23)	This study
CLCW	Tuluanshan	Chilichi	STP Formation	White bomb	8.5 ± 0.2 (n = 23/23)	This study

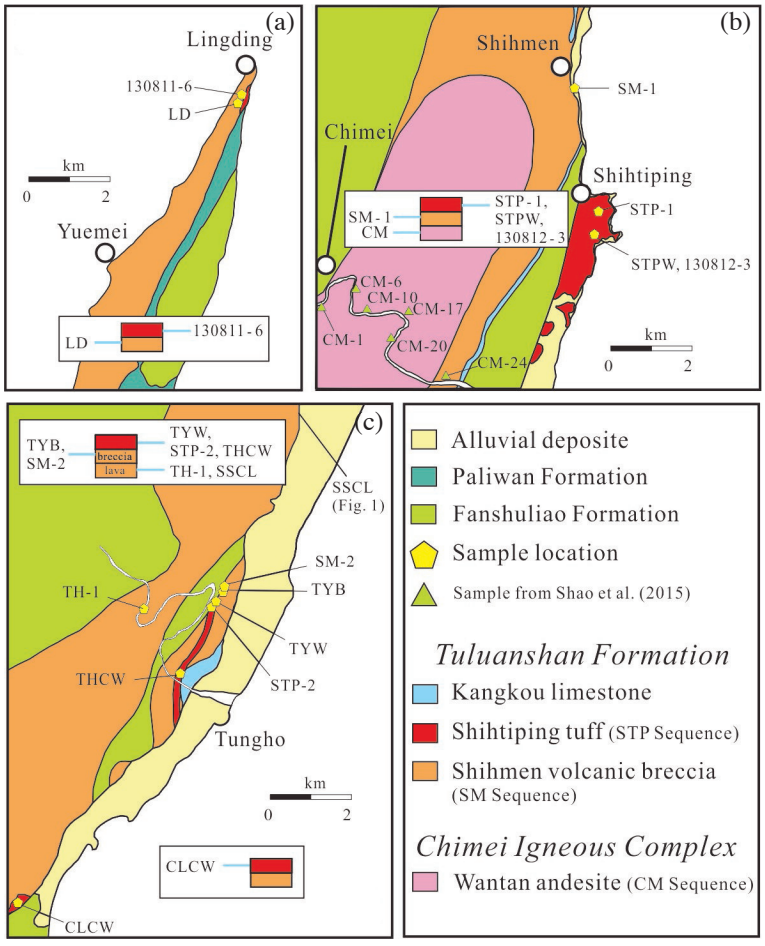

Fig. 2. Sample localities and volcanic sequences from four major volcanoes. (a) Yuemei volcano. (b) Chimei volcano. (c) Chengkuang'ao and Tuluanshan volcanoes.

The operating conditions and detailed analytical procedures of these LA-ICPMS analyses have been described by Chiu et al. (2009). U-Th-Pb isotopic ratios were calculated using the GLITTER 4.4 (GEMOC) software, and the relative standard deviations of the GJ-1 reference values were set at 2%. The presence of common lead was directly corrected using the common lead correction function proposed by Andersen (2002). The weighted mean U-Pb ages, concordia plots, probability curves, and histogram plots were constructed using Isoplot v. 3.70 (Ludwig 2009). Because modern-day ^{235}U comprises less than 1% of natural U, relatively little ^{207}Pb was produced during the Phanerozoic (cf. Ireland and Williams 2003). Consequently, $^{207}Pb/^{206}Pb$ ages are used only for inherited zircons that are older than 1000 Ma, and $^{206}Pb/^{238}U$ ages are used to indicate the crystallization ages of younger zircons.

In situ Lu-Hf isotopic analyses were performed using a Thermo Finnigan Neptune multicollector-ICPMS attached to a New Wave UP193FX laser ablation system at the Department of Geosciences, National Taiwan University. Lu-Hf isotopes were measured on the dated locations of individual zircons with a spot diameter of ~50 μm. Calibrations were performed using the Mud Tank zircon standard ($^{176}Hf/^{177}Hf$ = 0.282498 ± 0.000035, Lee et al. unpublished data). Detailed descriptions of these analytical techniques can be found in Wu et al. (2006). To avoid the isobaric interference between ^{176}Yb and ^{176}Hf, we discarded all analyses in which $^{176}Yb/^{177}Hf$ was > 0.2.

5. RESULTS

5.1 Zircon U-Pb Ages

The zircon U-Pb age results are listed in Table A1. The significant mean age results of concordia diagrams, histograms and zircon CL images of each sample are plotted in Figs. 3 - 7. Only a few zircons from the Chengkuang'ao volcano were analyzed for both their core and rim ages, because the zircons in the samples collected from Yuemei and Chimei volcanoes are generally too small to analyze repeatedly (i.e., they have diameters of < 100 μm). Moreover, although the zircons from the Chengkuang'ao and Tuluanshan volcanoes are large (with diameters of ~150 - 300 μm), no apparent age variations between their cores and rims were observed. Many inherited zircons were found in Yuemei and Chimei volcanoes, but few were found in Chengkuang'ao and Tuluanshan volcanoes. The histograms of all analyzed ages are shown in Fig. 8 with the order of volcanic sequences from top to bottom, i.e., Yuemei volcano: STP, SM (Figs. 8a and b), Chimei volcano: STP, SM, and CM (Figs. 8c - e), Chengkuang'ao volcano: STP, SM (breccia), SM (lava) (Figs. 8f - h), and Tuluanshan volcano: STP (Fig. 8i). Except for data from the CM sequence in Chimei

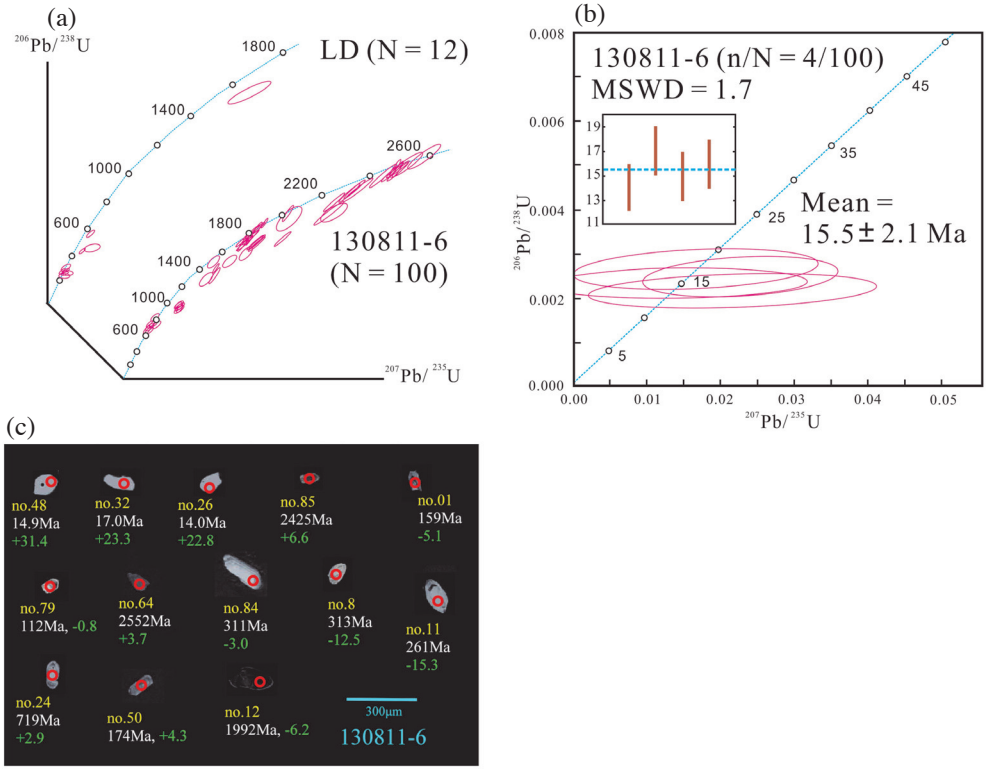

Fig. 3. (a) U-Pb concordia diragrams of sample no. LD from the SM sequence and no. 130811-6 from the STP sequence in Yuemei volcano. The numeric (N) denotes the number of zircon. (b) Weighted mean $^{206}Pb/^{238}U$ ages and (c) CL images of magmatic zircons from the STP sequence in Yuemei volcano.

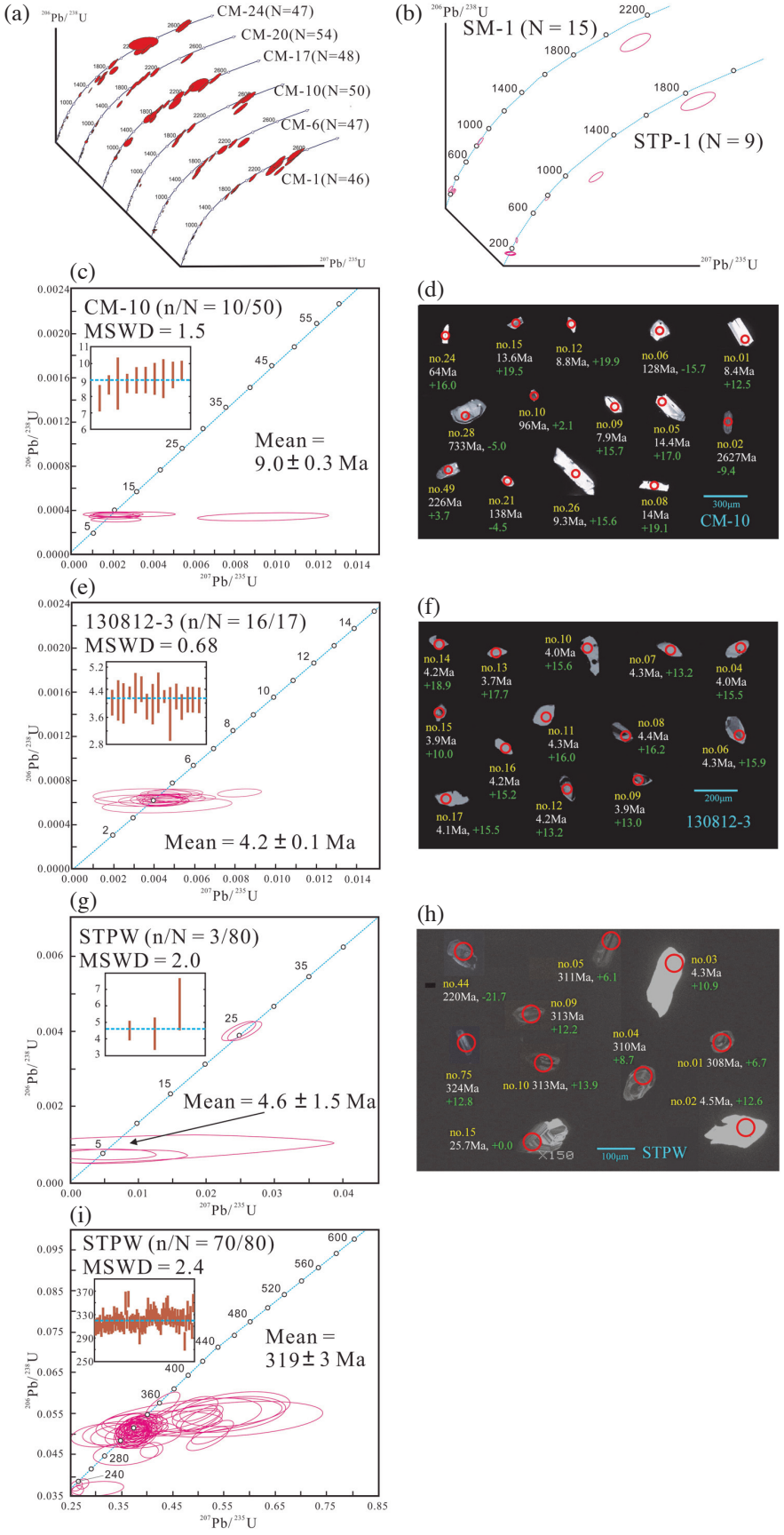

Fig. 4. U-Pb concordia diagrams and CL images of zircons from the CM, SM, and STP sequences in Chimei volcano. (a) Ages from the CM sequences were published by Shao et al. (2015). (b) Sample no. SM-1 and STP-1 from SM and STP sequences, respectively. (c) and (d) Sample no. CM-10 from CM sequence. (e) and (f) Sample no. 130812-3 from STP sequence. (g) to (i) Sample no. STPW from STP sequence.

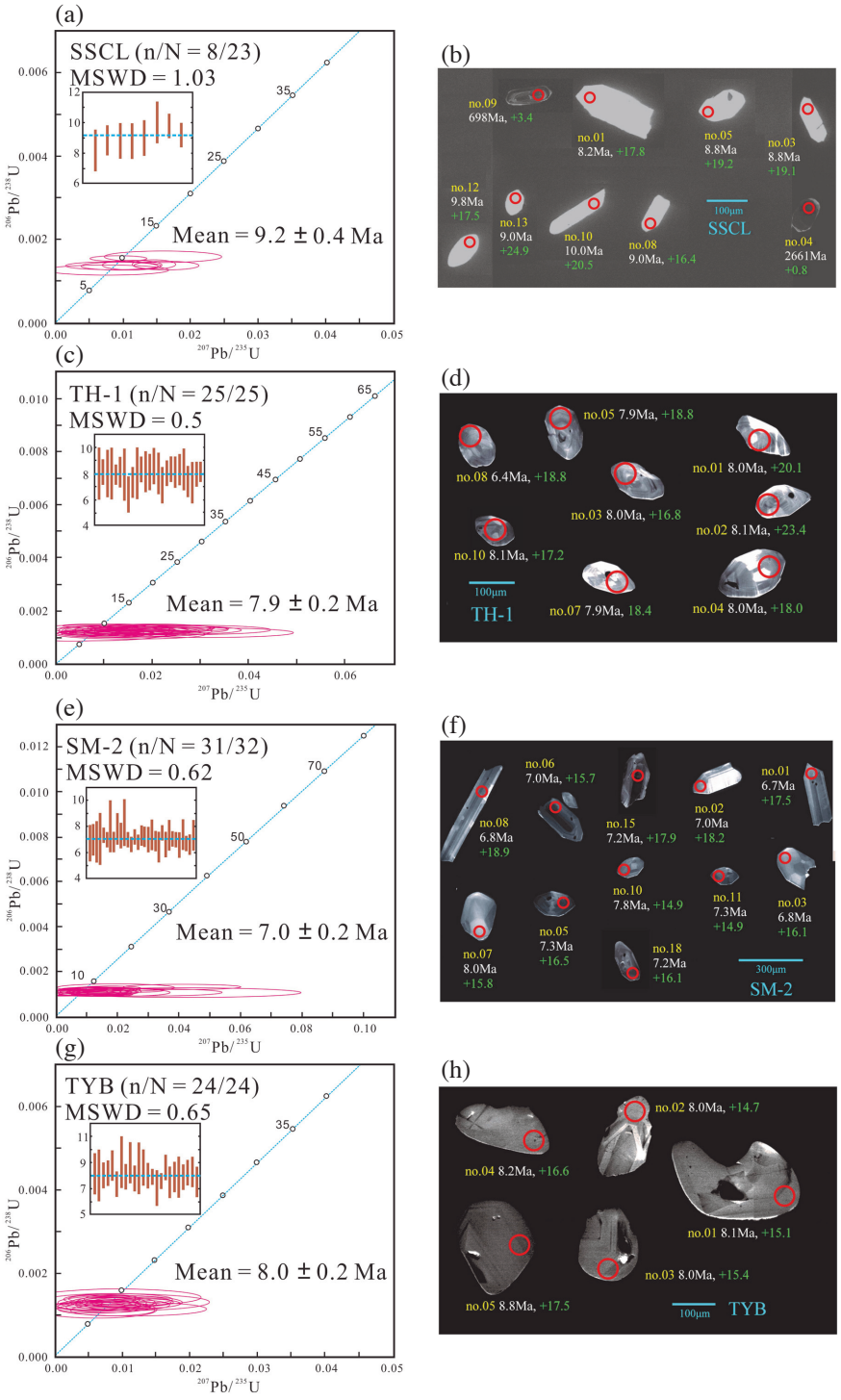

Fig. 5. U-Pb concordia diagrams and CL images of zircons from (a) (b) lava flows (Sample no. SSCL and TH-1) and (c) (d) volcanic breccias (Sample no. SM-2 and TYB) in the SM sequence of Chengkuang'ao volcano.

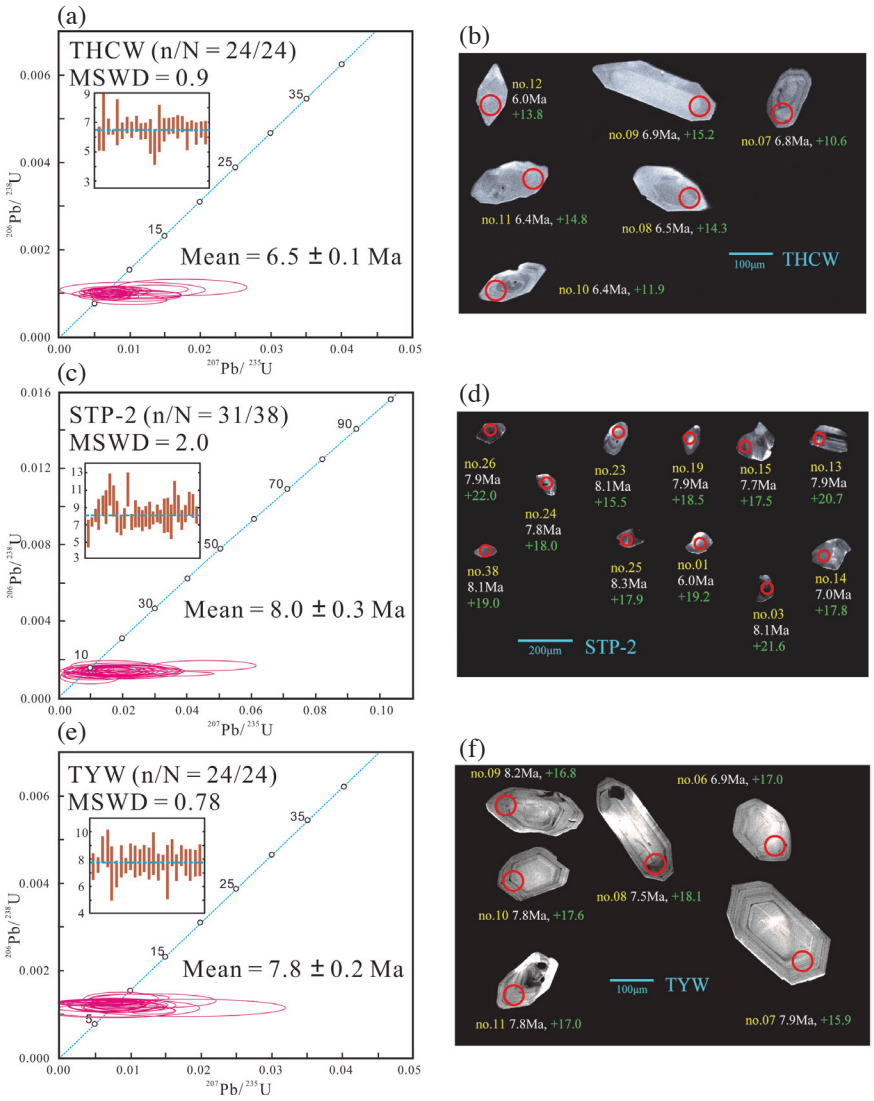

Fig. 6. U-Pb concordia diagrams and CL images of zircons from volcanic bombs in ignimbrite of the STP sequence in Chengkuang'ao volcano. (a) (b) Sample no. THCW, (c) (d) Sample no. STP-2, and (e) (f) Sample no. TYW.

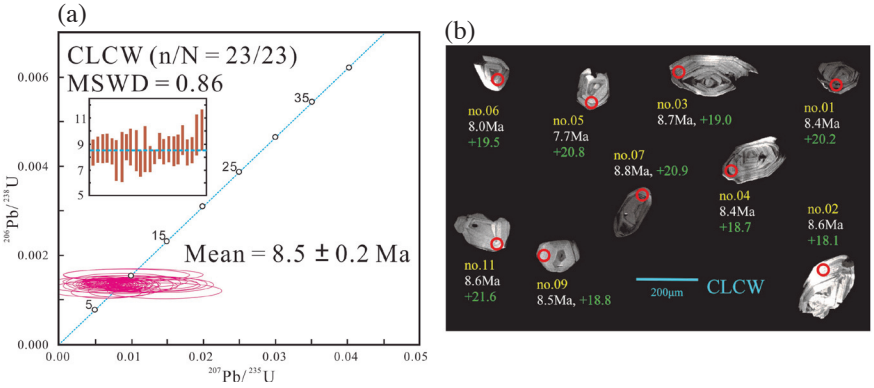

Fig. 7. (a) U-Pb concordia diagrams and (b) CL images of zircons from the STP sequence in Tuluanshan volcano.

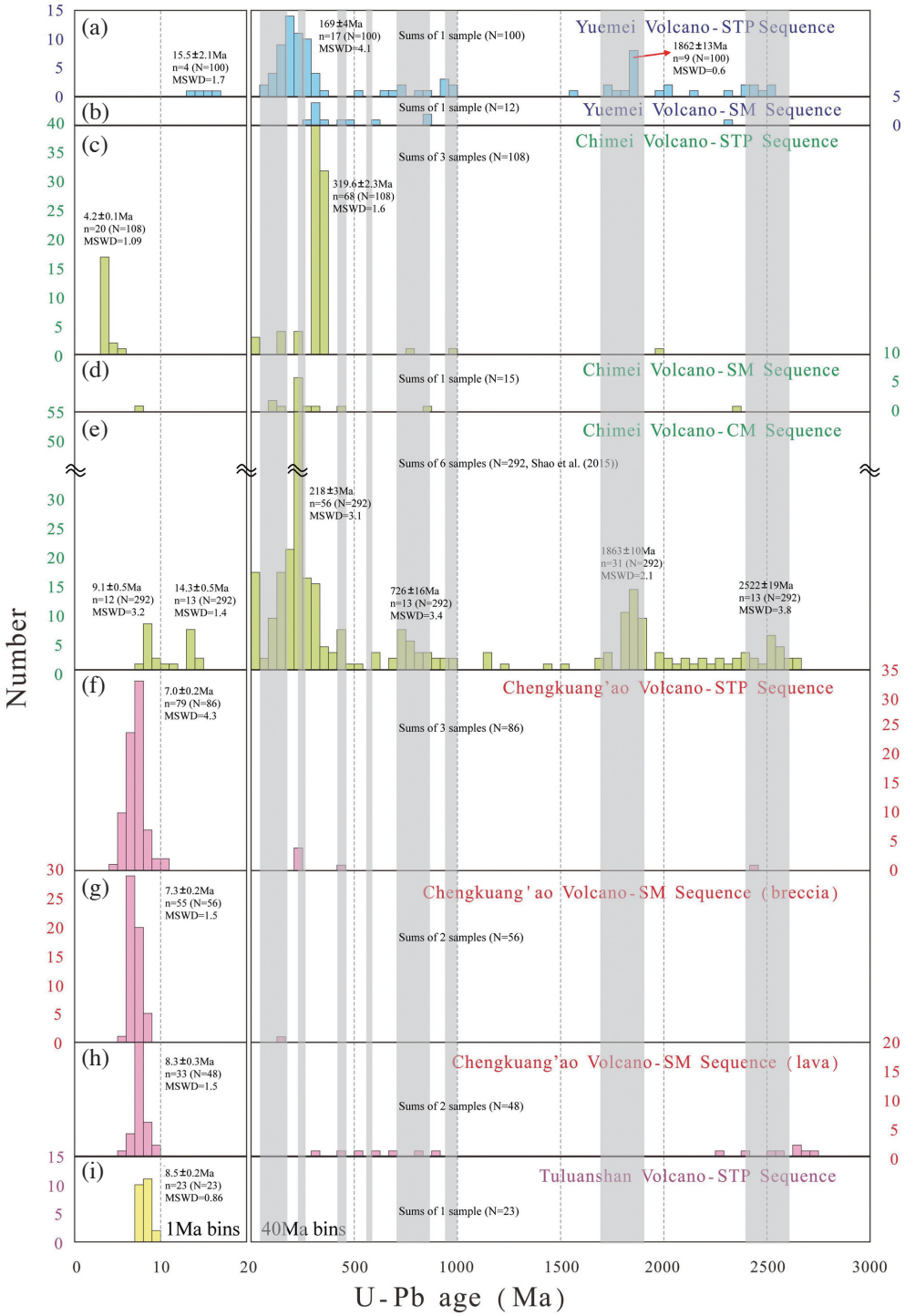

Fig. 8. Probabilistic histogram of age distributions for each volcanic sequence from the four major volcanoes in the CR. Note that the age intervals are different, with the boundary of 20 Ma. In each sequence, the total amount of zircons (N), number of rock samples, and peak ages are marked on the figure. (a) and (b) Yuemei volcano. (c) to (e) Chimei volcano. (f) to (h) Chenkuang'ao volcano. (i) Tuluanshan volcano. The gray areas show the Cathaysian-type ages (data from Wang et al. 2005, 2007; Chen et al. 2008; Li et al. 2014). Ages from the CM sequences in the Chimei volcano were published by Shao et al. (2015).

volcano, which were published by Shao et al. (2015), the other results were collected from fourteen samples and comprise a total of 448 individual zircon analyses.

5.1.1 Yuemei Volcano

5.1.1.1 SM Sequence

One volcanic breccia sample (no. LD, Fig. 3a) yielded only 12 zircon grains from the SM sequence. These zircons are irregular in shape, with lengths ranging from 60 - 80 μm, and they display oscillatory bands and cloudy-zoned CL image patterns (Fig. A1a). These zircons have relatively high U concentrations (155 - 2169 ppm), and their Th/U ratios (0.15 - 1.54) are higher than those of metamorphic zircons (Rubatto and Gebauer 2000) (Table A1). All of these zircons are inherited zircons and do not have Cenozoic ages. Except for one grain (LD-11), which yields an old age of 2308 Ma, all other zircons yielded ages ranging from 236 - 812 Ma (Fig. 8b).

5.1.1.2 STP Sequence

One volcanic bomb (no. 130811-6, Figs. 3a - c) was analyzed for its U-Pb ages on 102 spots from 100 zircon grains from the STP sequence. These zircons are irregular or rounded in shape, with diameters ranging from 50 - 100 μm. Their CL images display unzoned patterns, oscillatory bands, cloudy-zoned patterns, and resorbed cores (Fig. 3c). These zircons have heterogeneous U concentrations (25 - 2061 ppm) and yield Th/U ratios that are higher than 0.1 (Table A1), which are indicative of a magmatic origin (Rubatto and Gebauer 2000). Almost all of these zircons are inherited, except for four grains that record Miocene ages from a concordant cluster yielding a mean $^{206}Pb/^{238}U$ age of 15.5 ± 2.1 Ma (n = 4, MSWD = 1.7) (Figs. 3b and 8a). Besides, many ages are distributed from the Mesozoic to the Late Paleozoic (327 - 66 Ma), and others yield ages of Precambrian (2576 - 650 Ma) (Fig. 3a). Two age peaks are identified at 1862 ± 13 Ma (n = 9, MSWD = 0.6) and 169 ± 4 Ma (n = 17, MSWD = 4.1) (Fig. 8a).

5.1.2 Chimei Volcano

5.1.2.1 CM Sequence

The zircon U-Pb ages of volcanic rocks in this sequence was analyzed by Shao et al. (2015), and we use them in the discussion section.

5.1.2.2 SM Sequence

Only one volcanic breccia (no. SM-1, Fig. 4b) from the SM sequence was analyzed for its zircon U-Pb ages. A total of 15 zircon grains exhibit rounded to subrounded shapes and range in size from 50 - 80 μm. Many of these zircons show CL images with oscillatory bands and cloudy-zoned patterns (Fig. A1b). The U concentrations range from 196 - 753 ppm and exhibit Th/U ratios (0.2 - 1.89) that are characteristic of magmatic zircons (Table A1). Only one Miocene age was presented by grain SM1-03, which yielded a $^{206}Pb/^{238}U$ age of 7.9 ± 0.7 Ma. (Fig. 8d)

5.1.2.3 STP Sequence

Zircons from three volcanic bombs (no. STP-1, STPW, and 130812-3) collected from the STP sequence were analyzed for their U-Pb ages. These zircons are characterized by euhedral, prismatic shapes with aspect ratios ranging from 1:1 to 3:1. In STP-1 and 130812-3, zircons range in diameter from 100 - 150 μm, and their CL images exhibit unzoned patterns and oscillatory bands (Figs. A1c and 4f). Zircons from STPW are smaller in size (50 - 100 μm) and display oscillatory bands and cloudy-zoned CL image patterns (Fig. 4h).

In no. STP-1, only 9 zircon grains were separated; they did not yield significant ages (Fig. 4b). Their U concentrations are heterogeneous and range from 44 - 1519 ppm, and their Th/U ratios range from 0.11 - 1.85, thus indicating that they are magmatic zircons (Table A1).

A total of 80 spots were analyzed in sample no. STPW (Figs. 4g - i). All points, except for three (STPW-17, 44, and 47), yielded Th/U ratios of 0.17 - 1.85 and heterogeneous U concentrations ranging from 89 - 2669 ppm, which are indicative of magmatic zircons (Table A1). The dating results yield a Carboniferous age population at 319 ± 3 Ma (n = 70, MSWD = 2.4) (Fig. 4i), and only three grains yield Cenozoic ages, with a mean age of 4.6 ± 1.5 Ma (n = 3, MSWD = 2.0) (Fig. 4g).

Sample no. 130812-3 (Figs. 4e and f) yields U concentrations ranging from 127 - 935 ppm, with Th/U ratios of 0.31 - 1.47 (Table A1). A total of 17 spots were analyzed; 16 of these form a concordant cluster, yielding a mean $^{206}Pb/^{238}U$ age of 4.2 ± 0.1 Ma (n = 16, MSWD = 0.68).

Combining all the ages of these three samples indicates that two distinctive age peaks at 319.6 ± 2.3 Ma (n = 68, MSWD = 1.6) and 4.2 ± 0.1 Ma (n = 20, MSWD = 1.09) can be identified from the STP sequence in Chimei volcano (Fig. 8c).

5.1.3 Chengkuang'ao Volcano

5.1.3.1 Lava Flows in the SM Sequence

Zircon grains were separated from two lava flow samples (no. SSCL and TH-1, Figs. 5a - d) from the SM sequence for U-Pb dating. These zircons are dominated by euhedral shapes and range in size from 100 - 250 μm. Most zircons reveal unzoned patterns, oscillatory bands, and resorbed cores in CL images (Figs. 5b and d).

Sample no. SSCL records zircon U concentrations ranging from 38 - 2804 ppm and Th/U ratios of 0.24 - 1.85 (Table A1). A total of 8 analyses from 23 spots form a concordant cluster yielding a mean $^{206}Pb/^{238}U$ age of 9.2 ± 0.4 Ma (n = 8, MSWD = 1.03) (Fig. 5a).

Zircons of another sample no. TH-1 has low U concentrations (50 - 202 ppm) and Th/U ratios of 0.36 - 1.14 (Table A1). The analyses of 25 zircon grains form a concordant cluster yielding a mean $^{206}Pb/^{238}U$ age of 7.9 ± 0.2 Ma (n = 25, MSWD = 0.5) (Fig. 5c).

Combining the dating results of these two samples reveals that few inherited zircons can be found. Except for six concentrated ages ranging from 2726 - 2541 Ma, other inherited ages are variable. Moreover, an obvious age peak yields a mean age of 8.3 ± 0.3 Ma (n = 33, MSWD = 1.5) (Fig. 8h).

5.1.3.2 Volcanic Breccias in the SM Sequence

Zircons grains were separated from two volcanic breccias (no. TYB and SM-2, Figs. 5e - h) from the SM sequence for U-Pb age analyses. These zircons are characterized by euhedral, prismatic and rounded shapes with diameters ranging from 100 - 300 μm (Figs. 5f and h). The CL images of these zircons show unzoned patterns, oscillatory bands, cloudy-zoned patterns, and resorbed cores, with aspect ratios ranging from 1:1 to 4:1.

In sample no. TYB, a total of 24 zircon grains yield a mean age of 8.0 ± 0.2 Ma (n = 24, MSWD = 0.65) (Fig. 5g). These zircons exhibit very low U concentrations (16 - 113 ppm) and magmatic original Th/U ratios (0.27 - 0.91) (Table A1).

A total of 32 zircon U-Pb analyses were obtained from sample no. SM-2, and 31 of these yield a mean age of 7.0 ± 0.2 Ma (n = 31, MSWD = 0.62) (Fig. 5e). These zircons also record low U concentrations (34 - 345 ppm) and Th/U ratios ranging from 0.43 - 1.16 (Table A1).

Combining these two samples reveals that almost no inherited zircons are present in this sequence. On the other hand, the Cenozoic ages form a concordant cluster, yielding a mean $^{206}Pb/^{238}U$ age of 7.3 ± 0.2 Ma (n = 55, MSWD = 1.5) (Fig. 8g).

5.1.3.3 STP Sequence

Zircon grains from three volcanic bombs (no. THCW, STP-2, and TYW, Figs. 6a - f) from the STP sequence were analyzed for their U-Pb ages. Most of the zircons separated from these rock samples are euhedral and range in length from 100 - 300 μm. Their CL images show unzoned patterns, oscillatory bands and cloudy-zoned patterns, with aspect ratios ranging from 1:1 to 3:1 (Figs. 6b, d, and f).

Samples no. THCW records heterogeneous zircon U concentrations ranging from 47 - 1478 ppm and Th/U ratios ranging from 0.3 - 0.76 (Table A1). A total of 24 spots were analyzed and form a concordant cluster yielding a mean $^{206}Pb/^{238}U$ age of 6.5 ± 0.1 Ma (n = 24, MSWD = 0.9) (Fig. 6a).

In sample no. STP-2, a total of 38 zircons were analyzed for their U-Pb ages. Unlike the other two sample in this sequence, seven inherited zircons were present, yielding ages ranging from 2468 - 51 Ma. The magmatic zircons form a concordant cluster, yielding a mean $^{206}Pb/^{238}U$ age of 8.0 ± 0.3 Ma (n = 31, MSWD = 2.0) (Fig. 6c). These zircons exhibit low U concentrations (37 - 860 ppm) and Th/U ratios ranging from 0.27 - 0.94 (Table A1).

A total of 24 zircon U-Pb analyses were obtained from sample no. TYW and yield a mean age of 7.8 ± 0.2 Ma (n = 24, MSWD = 0.78) (Fig. 6e). Their U concentrations are relatively low (24 - 182 ppm), and their Th/U ratios ranging from 0.27 - 0.57 (Table A1).

Combining all the dates from these three samples reveals that a few inherited zircons can be found. Four of the inherited ages show uniform range from 225 - 245 Ma. Moreover, an obvious age peak yields a mean age of 7.0 ± 0.2 Ma (n = 79, MSWD = 4.3) (Fig. 8f).

5.1.4 Tuluanshan Volcano

A total of 23 zircon grains from only one volcanic breccia sample (no. CLCW) from the STP sequence were analyzed for their U-Pb ages (Fig. 7). No inherited zircons were found in this sample, and all 23 analyses form a concordant cluster yielding a mean $^{206}Pb/^{238}U$ age of 8.5 ± 0.2 Ma (n = 23, MSWD = 0.86) (Figs. 7a and 8i). The CL images show euhedral zircons with diameters ranging from 100 - 200 μm and oscillatory bands (Fig. 7b). These zircons record low U concentrations (19 - 110 ppm) and Th/U ratios ranging from 0.41 - 0.78 (Table A1).

5.2 Zircon Hf Isotopic Ratios

A total of 247 dated zircon grains from thirteen samples (no zircons remained after dating analyses from sample no. LD) in the CR were analyzed for their $^{176}Hf/^{177}Hf$ isotopic ratios. Moreover, we analyzed 117 and 89 zircon grains which were dated for their U-Pb ages by Shao et al. (2014) from the Lutao and Lanyu volcanic rocks, respectively. The results of these analyses are listed in Table A2, and their ε_{Hf} data are plotted in Fig. 9. The $^{176}Lu/^{177}Hf$ decay constant ($\lambda_{Lu\text{-}Hf} = 1.86 \times 10^{-11} y^{-1}$) was reported by Scherer et al. (2001). The initial $^{176}Hf/^{177}Hf$ isotopic ratios between the sample and the chondritic uniform reservoir (CHUR) are given as $\varepsilon_{Hf}(T)$ values (Patchett and Tatsumoto 1981). The relative parameters are: $(^{176}Lu/^{177}Hf)_{CHUR,0} = 0.0332 \pm 29$ (Blichert-Toft and Albarède 1997), $(^{176}Hf/^{177}Hf)_{CHUR,0} = 0.282772 \pm 29$ (Blichert-Toft and Albarède 1997), $(^{176}Lu/^{177}Hf)_{DM} = 0.0384$ (Griffin et al. 2000), and $(^{176}Hf/^{177}Hf)_{DM} = 0.28325$ (Nowell et al. 1998).

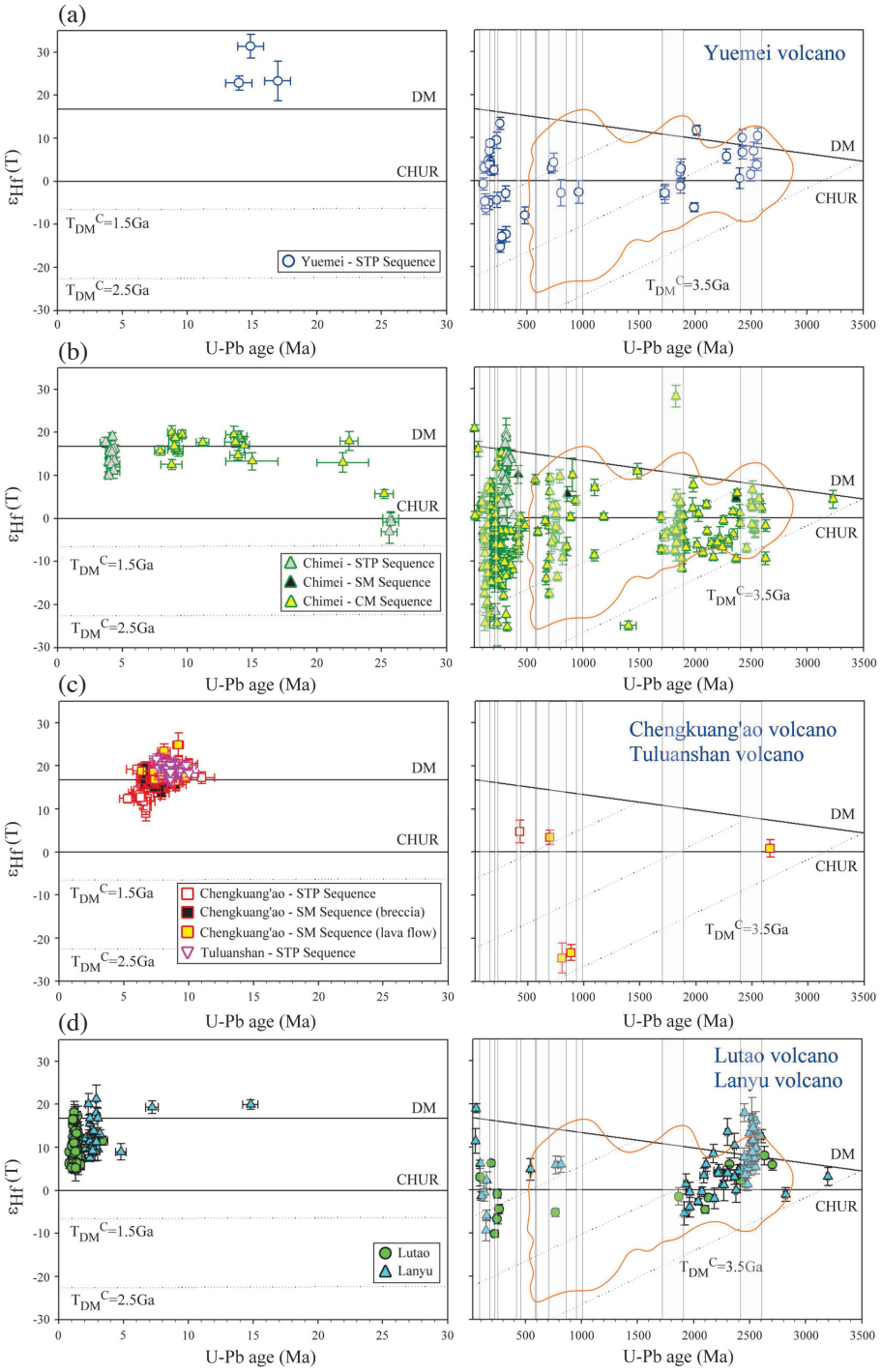

Fig. 9. Plot of zircon $\varepsilon_{Hf}(T)$ values versus crystallization ages from six volcanoes in the NLA. (a) Yuemei volcano, (b) Chimei volcano, (c) Chengkuang'ao and Tuluanshan volcanoes, (d) Lutao and Lanyu volcanoes. Data from the CM sequences in the Chimei volcano were published by Shao et al. (2015). Lutao and Lanyu zircon U-Pb ages were published by Shao et al. (2014), and their Hf isotopic analyses were performed in this study. Data from different volcanic sequences are marked with different symbols. The gray areas show the Cathaysian-type ages (data from Wang et al. 2005, 2007; Chen et al. 2008; Li et al. 2014). The orange areas show Hf isotopes of the Cathaysian-type zircons (data from Li et al. 2014).

T^{C}_{DM} refers to the zircon Hf crustal model ages, which are based on a depleted mantle (DM) source and the assumption that the host magma of the zircons has the average continental $^{176}Lu/^{177}Hf$ ratio of 0.015 (Griffin et al. 2002). All individual volcanic sequences in these four major volcanoes record significantly variable $\varepsilon_{Hf}(T)$ values that exceed the external analytical errors of the method (~3-ε units), which implies that the protolith magma in the NLA has a heterogeneous isotopic composition.

5.2.1 Yuemei Volcano

5.2.1.1 STP Sequence

A total of 43 Hf isotopic ratios were obtained from sample no. 130811-6 (Table A2). These zircons exhibit various Hf isotopic ratios, with $\varepsilon_{Hf}(T)$ values ranging from +31.4 to -15.3 (Fig. 9a). Three zircon grains with a Miocene age peak (15.5 ± 2.1 Ma) show high and positive $\varepsilon_{Hf}(T)$ values ranging from +31.4 to +22.8. The older zircons (169 ± 4 Ma) yield heterogeneous $\varepsilon_{Hf}(T)$ values ranging from +8.7 to -5.1, and those recording an older mean age of 1862 ± 13 Ma also exhibit variable $\varepsilon_{Hf}(T)$ values ranging from +11.7 to -6.2.

5.2.2 Chimei Volcano

5.2.2.1 CM Sequence

The zircon Hf isotopic data of volcanic rocks in this sequence was analyzed by Shao et al. (2015), and we use them in the discussion section.

5.2.2.2 SM Sequence

Only a few zircons from one sample (no. SM-1, n = 4) of the SM sequence were analyzed for their Hf isotopic compositions after being dated; they yielded $\varepsilon_{Hf}(T)$ values ranging from +10.1 to +3.5 (Fig. 9b and Table A2).

5.2.2.3 STP Sequence

In sample no. STP-1, only three spots were analyzed for their Hf isotopic compositions; they showed heterogeneous $\varepsilon_{Hf}(T)$ values ranging from -1.3 to -13.6 (Table A2). A total of 27 spots were analyzed for their Hf isotopic compositions in sample no. STPW. Two spots recording young ages (~4 Ma) yielded high $\varepsilon_{Hf}(T)$ values of +12.1 and +10.9. Another three spots exhibiting Oligocene ages (~25 Ma) yielded negative $\varepsilon_{Hf}(T)$ values ranging from 0 to -3.1. The other spots, recording Carboniferous ages (~319 Ma), yielded variable $\varepsilon_{Hf}(T)$ values ranging from +19.5 to +3.2 (Table A2). The youngest sample (no. 130812-3), which had an age of 4.2 ± 2.1 Ma, yielded positive $\varepsilon_{Hf}(T)$ values ranging from +18.9 to +10.0 (Table A2). Plot of zircon $\varepsilon_{Hf}(T)$ values versus U-Pb ages in this sequence can be found in Fig. 9b.

5.2.3 Chengkuang'ao Volcano

5.2.3.1 Lava Flows in the SM Sequence

Two lava flow samples from Chengkuang'ao volcano were analyzed for their Hf isotopic compositions (Table A2). Twelve spots from sample no. SSCL yielded $\varepsilon_{Hf}(T)$ values ranging from +24.9 to -24.6; however, zircons recording Late Miocene ages, ranging from 10.0 - 8.2 Ma, yielded a relative uniform and positive $\varepsilon_{Hf}(T)$ values (ranging from +24.9 to +16.4) (Fig. 9c). A total of 23 Hf isotopic analyses were obtained from another sample (no. TH-1) exhibiting zircon ages ranging from 8.6 - 6.4 Ma; they yielded similar $\varepsilon_{Hf}(T)$ values (ranging from +23.4 to +16.7) as the former sample (Fig. 9c).

5.2.3.2 Volcanic Breccias in the SM Sequence

Two volcanic breccia samples were analyzed for their Hf isotopic compositions (Fig. 9c and Table A2). A total of 24 Hf isotopic analyses were obtained from zircons in sample no. TYB (9.0 - 7.0 Ma). Their $\varepsilon_{Hf}(T)$ values are uniform and range from +20.2 to +15.1. Another sample no. SM-2 (8.0 - 6.7 Ma) were analyzed 20 Hf isotopic ratios. They also have uniform $\varepsilon_{Hf}(T)$ values ranging from +19.6 to +17.5.

5.2.3.3 STP Sequence

Zircons from three samples were analyzed for their Hf isotopic compositions on previous U-Pb age spots; all data are plotted and listed in Fig. 9c and Table A2. In sample no. TYW, 24 Hf isotopic analyses from zircons with ages ranging from 8.8 - 6.9 Ma yield uniform $\varepsilon_{Hf}(T)$ values (ranging from +20.0 to +15.4). Sample no. STP-2 yields 18 Hf isotopic analyses, which also show similar zircon ages (11.0 - 6.0 Ma) and uniform $\varepsilon_{Hf}(T)$ values (ranging from +22.0 to +15.5), except for one inherited zircon, which has an age of 430 Ma [$\varepsilon_{Hf}(T)$ value = +4.8]. The other sample no. THCW yields 24 Hf isotopic analyses of zircons with ages ranging from 7.0 - 5.3 Ma; their $\varepsilon_{Hf}(T)$ values range from +16.2 to +8.9.

5.2.4 Tuluanshan Volcano

5.2.4.1 STP Sequence

We only collected one sample from the STP sequence of Tuluanshan volcano, which yields a population mean age of 8.5 ± 0.2 Ma and uniform $\varepsilon_{Hf}(T)$ values ranging from +21.6 to +16.9 (Fig. 9c and Table A2).

5.2.5 Lutao Volcano

Shao et al. (2014) published the results of U-Pb dating of both volcanic rocks and sands at Lutao volcano. We analyzed the $^{176}Hf/^{177}Hf$ isotopic ratios of zircons based on these ages. The Hf isotopic ratios record variable $\varepsilon_{Hf}(T)$ values,

ranging from +17.8 to -4.5 in volcanic rocks and from +18.1 to -10.2 in sands (Fig. 9d and Table A2). The volcanic rocks yield a Quaternary age peak of 1.31 ± 0.03 Ma (Table 2) and positive $\varepsilon_{Hf}(T)$ values ranging from +17.8 to +5.2. The sands yield an age peak of 1.23 ± 0.03 Ma and positive $\varepsilon_{Hf}(T)$ values ranging from +18.1 to +4.9. The inherited zircons yield a range of ages, ranging from ca. 100 - 270 Ma, as well as $\varepsilon_{Hf}(T)$ values ranging from +6.2 to -10.2. They also yield an older range of crustal model ages, ranging from ca. 2700 - 1870 Ma, with $\varepsilon_{Hf}(T)$ values ranging from +8.0 to -4.5.

5.2.6 Lanyu Volcano

Shao et al. (2014) also performed U-Pb age dating in Lanyu volcano. We analyzed the $^{176}Hf/^{177}Hf$ isotopic ratios of zircons based on the dated positions of these samples. For all zircons, the $\varepsilon_{Hf}(T)$ values of volcanic rocks range from +20.0 to -9.4 and those of sands range from +21.3 to +3.0 (Fig. 9d and Table A2). Zircons recording a mean Quaternary age of 2.61 ± 0.13 Ma (Table 2) yield uniform and positive $\varepsilon_{Hf}(T)$ values ranging from +12.8 to +12.3 in the volcanic rocks, and those exhibiting a mean age of 2.69 ± 0.11 Ma yield positive $\varepsilon_{Hf}(T)$ values ranging from +21.3 to +7.5 in the sands. In general, of all the analyzed data, inherited zircons showing $\varepsilon_{Hf}(T)$ values ranging from +6.1 to -9.4 yield a range of ages, ranging from ca. 160 - 100 Ma; zircons recording $\varepsilon_{Hf}(T)$ values ranging from +17.9 to -5.5 yield an older range of crustal model ages, ranging from ca. 2600 - 1920 Ma.

Six lava flow samples (no. CM-1, 6, 10, 17, 20, and 24) yielded 292 irregular zircon grains ranging in size from 50 - 120 μm, which were analyzed here (Fig. 4a). The CL images show unzoned patterns, oscillatory bands, cloudy-zoned patterns, and resorbed cores (Fig. 4d, no. CM-10 for example). In general, these zircons exhibit U concentrations ranging from 15 - 8176 ppm and highly variable Th/U ratios (0.01 - 2.44). Of these six samples, no. CM-10 yields ten Cenozoic ages; they yield a youngest age of 9.0 ± 0.3 Ma (n = 10, MSWD = 1.5) (Fig. 4c). Combining all ages of the analyzed zircons in these six samples, the magmatic and inherited zircons has significant age populations with peaks at 2522 ± 19 Ma (n = 13, MSWD = 3.8), 1863 ± 10 Ma (n = 31, MSWD = 2.1), 726 ± 16 Ma (n = 13, MSWD = 3.4), 218 ± 3 Ma (n = 56, MSWD = 3.1), 14.3 ± 0.5 Ma (n = 13, MSWD = 1.4), and 9.1 ± 0.5 Ma (n = 12, MSWD = 3.2) (Fig. 8e) (Shao et al. 2015).

According to Shao et al. (2015), magmatic zircons yield highly variable $\varepsilon_{Hf}(T)$ values ranging from +20.9 to -30.7 (in addition to two grains with extreme values of +28.2 and -37.6) (Fig. 9b). The $\varepsilon_{Hf}(T)$ values of each population of mean ages are as follows: 2522 ± 19 Ma [in which $\varepsilon_{Hf}(T)$ values range from +6.5 to -7.0], 1863 ± 10 Ma [in which $\varepsilon_{Hf}(T)$ values range from +28.2 to -11.7], 726 ± 16 Ma [in which $\varepsilon_{Hf}(T)$ values range from +9.3 to -17.5], 218 ± 3 Ma [in which $\varepsilon_{Hf}(T)$ values range from +11.6 to -24.4], 24.1 ± 1.4 Ma [in which $\varepsilon_{Hf}(T)$ values range from +18.0 to +5.7], 14.3 ± 0.5 Ma [in which $\varepsilon_{Hf}(T)$ values range from +19.5 to +13.3], and 9.1 ± 0.5 Ma [in which $\varepsilon_{Hf}(T)$ values range from +19.9 to +12.5] (Shao et al. 2015).

6. DISCUSSION

6.1 Zircon U-Pb Ages and Hf Isotopes in the CM Sequence of the Chimei Volcano

The results of the zircon U-Pb dating and Hf isotopic data from the CM sequence of Chimei volcano have previously been reported by Shao et al. (2015).

6.2 Volcanic History of the CR

Our zircon U-Pb data can be used to identify the stages of volcanism in the CR. According to the U-Pb ages of individual volcanic sequences, the evolution of each volcano over time differed between these four major volcanic

Table 2. Ages of the volcanic sequences in volcanoes of the Northern Luzon Arc.

Volcano	Volcanic sequence	Lithofacies	Ages
Yuemei	STP Formation	White bomb	7.2 Ma (^{40}Ar-^{39}Ar; Lai et al. 2017)
Chimei	STP Formation	White bomb	4.2 Ma (^{40}Ar-^{39}Ar; Lai et al. 2017)
			4.2 Ma (This study)
	CM Formation	Lava flow	9.0 Ma (Zircon U-Pb; Shao et al. 2015)
Chengkuang'ao	STP Formation	White bomb	7.4 - 6.2 Ma (^{40}Ar-^{39}Ar; Lai et al. 2017)
			8.0 - 6.5 Ma (This study)
	SM Formation	Black breccia	8.0 - 7.0 Ma (This study)
	SM Formation	Lava flow	9.2 - 7.9 Ma (This study)
Tuluanshan	STP Formation	White bomb	8.5 Ma (This study)
Lanyu	Lava Flow, breccia and river/beach sands		2.6 Ma (Zircon U-Pb; Shao et al. 2014)
Lutao	Lava flow, breccia and river/beach sands		1.3 Ma (Zircon U-Pb; Shao et al. 2014)

islands. In addition, zircon $\varepsilon_{Hf}(T)$ values provided clues that could be used to trace the similarities and differences in the petrogenesis of each volcano.

In Yuemei volcano, the main body of the volcano has already sunk beneath the surface with subduction (Lai and Song 2013; Lai et al. 2017). Consequently, we only observed the SM and STP sequences in the distal volcanic facies of this volcano. Almost all of the zircons in these two sequences are inherited, which indicates that these magmas erupted quickly after they were formed and thus did not exist for long enough to form magmatic zircons. The youngest mean age peak in the STP sequence, which is composed of 4 dates, is 15.5 ± 2.1 Ma; however, this sequence may exhibit an unconformity with the sedimentary sequence of the Fanshuliao Formation, which contains planktic foraminifers with ages of 5.2 - 3.35 Ma (Huang et al. 1988). If so, this indicates that an age gap of ~10 Ma exists in the geological record. In addition, the K-Ar and $^{40}Ar/^{39}Ar$ ages of the volcanic breccias in the STP sequence in this volcano are 6.2 ± 0.6 Ma (Song 1990) and 7.2 ± 0.1 Ma (Lai et al. 2017), respectively (Table 2). Based on these results, the age of 15.5 Ma might not represent the age of the magmatic zircons in Yuemei volcano. These inherited zircons have high and positive $\varepsilon_{Hf}(T)$ values (ranging from +31.4 to +23.3, Fig. 9a), indicating that they may have been picked up from a DM source during the later ascent of magma.

In Chimei volcano, zircons in these volcanic sequences have Oligocene to Miocene U-Pb age peaks of 24.1 ± 1.4 Ma [$\varepsilon_{Hf}(T)$ values = +18.0 to +5.7], 14.3 ± 0.5 Ma [$\varepsilon_{Hf}(T)$ values = +19.5 to +13.3], and 9.1 ± 0.5 Ma [$\varepsilon_{Hf}(T)$ values = +19.9 to +12.5] in the CM sequence (Shao et al. 2015). Only one age data point of 7.9 ± 0.7 Ma was obtained from the SM sequence, and an age of 4.2 ± 0.1 Ma [$\varepsilon_{Hf}(T)$ values = +18.9 to +10.0] was obtained from the STP sequence (Fig. 9b and Table 2). Shao et al. (2015) proposed that the age of the oldest igneous exposure in the NLA is ~9 Ma, and they argued that the age of 14 Ma recorded in the CM sequence represents the initiation of the subduction of the South China Sea Plate. Although the previous dating results of this sequence have yielded zircon fission track ages ranging from 16.4 - 8.3 Ma (Yang et al. 1995) and whole-rock K-Ar ages ranging from 22.2 - 9.0 Ma (Ho 1969; Juang and Bellon 1984; Richard et al. 1986), these data are considered to be inaccurate, due to the occurrence of low-temperature alteration (Lo et al. 1994) or the inheritance of excess radiogenic Ar in minerals or whole-rock samples, which have probably caused these dating results to be older than their erupted ages (Yang et al. 1995). On the other hand, the $^{206}Pb/^{238}U$ age result of 4.2 ± 0.1 Ma obtained from the STP sequence is consistent with those of previous studies, such as those of whole-rock $^{40}Ar/^{39}Ar$ dating (4.2 ± 0.1 Ma, Lai et al. 2017), whole-rock K-Ar dating (4.4 ± 0.2 Ma, Richard et al. 1986), and zircon fission track dating (4.4 ± 0.6 Ma, Yang et al. 1995). In addition, the Kangkou Limestone, which overlaps the STP sequence, contains planktic foraminifers with ages of 5.2 - 3.75 Ma (Huang et al. 1988, 1995); these ages also match the time at which volcanism ended. We argue that this age, which was obtained from the STP sequence, represents the timing of the youngest period of magmatism in the Chimei volcano. Moreover, this age is also the youngest U-Pb age obtained from magmatic zircons in the four major volcanoes in the CR. Additionally, magmatic zircons in the STP sequence are larger than those in the older sequences in Chimei volcano; this indicates that this magma remained in the chamber for a long period of time after it was formed.

In Chengkuang'ao volcano, all of the Miocene zircon U-Pb age peaks in volcanic sequences occur within a short interval, from lava flow of the SM sequence [8.3 ± 0.3 Ma, $\varepsilon_{Hf}(T)$ values = +24.9 to +16.4], to volcanic breccia of the SM sequence [7.3 ± 0.2 Ma, $\varepsilon_{Hf}(T)$ values = +20.2 to +13.6] to the STP sequence [7.0 ± 0.2 Ma, $\varepsilon_{Hf}(T)$ values = +22.0 to +4.8] (Fig. 9c). These results imply that the volcanic sequences were rapidly emplaced on this volcanic island. In lava flow of the SM sequence, the oldest age of a single zircon grain is 9.2 ± 0.4 Ma, which indicates that the volcanism here became violent at the same time as it did at Chimei volcano. Previous studies of this sequence here have obtained an age of ~15.2 Ma (K-Ar dating; Richard et al. 1986), which may represent the timing of the initiation of subduction. Some further studies have reported whole-rock $^{40}Ar/^{39}Ar$ ages in the STP sequence of 7.4 ± 0.1, 6.2 ± 0.1 Ma (Table 2) (Lai et al. 2017), and 5.4 ± 0.5 Ma (Lo et al. 1994). These results demonstrate that the ages of the STP sequence in this volcano range from ~7.4 - 5.4 Ma and that it was then covered by the Tungho Limestone (containing planktic foraminifers with ages of 5.2 - 2.9 Ma, Huang et al. 1988, 1995).

In Tuluanshan volcano, only one sample from the STP sequence shows a U-Pb age peak of 8.5 ± 0.2 Ma (Table 2). This volcano is only exposed at the top of the volcanic sequence. Based on our data, the time at which its volcanism ceased may be ~8.5 Ma. Moreover, the few inherited zircons present in Chengkuang'ao and Tuluanshan volcanoes indicate that small degrees of crustal contamination occurred in these two volcanoes (Fig. 9c).

6.3 Implications for the Older Zircon Ages from the NLA

6.3.1 Cenozoic Zircons (30 - 15 Ma)

Shao et al. (2015) argued that the initiation of NLA magmatism began during the Middle Miocene [14.3 ± 0.5 Ma, with $\varepsilon_{Hf}(T)$ values from +19.5 to +13.3 in the CM sequence of Chimei volcano] (Fig. 9b). We also found some zircons with a similar age peak at 15.5 ± 2.1 Ma (n = 3), with very high and positive $\varepsilon_{Hf}(T)$ values ranging from +31.4 to +22.8, in the STP sequence of Yuemei volcano (Figs. 3b and 9a). Although most of the zircon ages in the Lanyu volcanic island are very young, we found one zircon with an age of 14.8

± 1.2 Ma and an $\varepsilon_{Hf}(T)$ value of +20.0 (Fig. 9d) (Shao et al. 2014). In our data, two other Oligocene age peaks are present in Chimei volcano: one is at 24.1 ± 1.4 Ma and records $\varepsilon_{Hf}(T)$ values ranging from +18.0 to +5.7 in the CM sequence, and the other is at 25.7 Ma and has $\varepsilon_{Hf}(T)$ values ranging from 0 to -3.0 in the STP sequence (Fig. 9b).

Previous studies have indicated that the South China Sea opened from 32 - 15 Ma (Taylor and Hayes 1983). Before the formation of the South China Sea Plate, another old plate, named the proto-South China Sea Plate, might have existed between the South China Block and Kalimantan at ca. 60 Ma (Parker and Gealey 1985; Lee and Lawver 1994). The proto-South China Sea Plate subducted toward the east beneath the Kalimantan and West Philippine Basin from 50 - 20 Ma (Williams et al. 1998; Hall 2002). Based on the aforementioned tectonic activities, the initiation of the subduction of the South China Sea Plate might be later than ~20 Ma.

We argue that the ages of 15.5 and 14.8 Ma can also refer to the earlier magmatism of the initiation of subduction of the South China Sea Plate, based on their depleted ε_{Hf} isotopic characteristics [$\varepsilon_{Hf}(T)$ values ranging from +31.4 to +22.8] and the fact that these magmas did not erupt extensively until their later eruptions at ~9 Ma. Zircons that record ages of 24 and 25 Ma in the CM sequence of Chimei volcano (24.1 ± 1.4 Ma) have higher $\varepsilon_{Hf}(T)$ values (from +18.0 to +5.7) and lower U concentrations (51 - 268 ppm) (Shao et al. 2015) than those from the STP sequence [25.7 Ma, $\varepsilon_{Hf}(T)$ values from 0 to -3.0, and U contents ranging from 572 - 2669 ppm] (Fig. 9b and Tables A1 and A2). However, we only obtained a total of six ages of 25 - 24 Ma from these zircons; thus, more evidence is required to understand the exact implications of these ages.

6.3.2 Xenocrystic Zircons of 320 Ma

In the STP sequence of Chimei volcano, we not only found the youngest magmatic zircons (4.2 ± 0.1 Ma, sample no. 130812-3) (Figs. 4e and 8c) but also found an age peak of 319.6 ± 2.3 Ma, with $\varepsilon_{Hf}(T)$ values ranging from +19.5 to +3.2 (sample no. STPW, Figs. 4i and 8c). This group is unique because these ages are abnormal in the Cathaysia Block. Only one previous study reported similar ages of inherited zircons (322 - 314 Ma, n = 13) from two sedimentary rocks recording Permian and Jurassic ages (Hu et al. 2012). However, the Carboniferous zircons in their data have negative $\varepsilon_{Hf}(T)$ values (from -5.1 to -18.4), which are obviously different than the positive values exhibited in our zircons. Determining where and how the magma from the Chimei volcano could obtain such inherited zircons with homogeneous ages and positive $\varepsilon_{Hf}(T)$ values requires more evidence.

6.3.3 Pre-Miocene Volcanism (> 30 Ma)

Shao et al. (2015) suggested that a micro-continent or a continental fragment split off from the Eurasian margin by the opening of the South China Sea, which then drifted and accreted to the western Philippine Sea Plate prior to the initiation of the subduction of the NLA. This micro-continent or continental fragment was referred to as part of the Cathaysia Block, which belonged to the South China Block in the eastern margin of the Eurasian Plate (Li et al. 2003). According to the zircon dating work performed by Li et al. (2014), a total of 4041 Precambrian detrital zircons from the Cathaysia Block have three major peak ages at ~2485 Ma (the Wutai orogeny, 2600 - 2400 Ma), ~1853 Ma (the Luliang orogeny, 1900 - 1700 Ma), and ~970 Ma (the Sibao orogeny, 1000 - 930 Ma), as well as four subordinate peaks at ~1426, ~1074, ~780 Ma (the Jinning orogeny, 850 - 700 Ma), and ~588 Ma (the gray columns in Figs. 8 and 9). In addition to exhibiting Precambrian ages, the Cathaysia Block also records Paleozoic to Mesozoic U-Pb ages, including peaks at 450 - 410 Ma (the Caledonian orogeny, Wang et al. 2007), 243 - 210 Ma (the Indosinian orogeny, Wang et al. 2005), and 180 - 65 Ma (the Yanshanian orogeny, Chen et al. 2008) (the gray columns in Figs. 8 and 9).

Inherited zircons dated to the Precambrian, Paleozoic and Mesozoic collected from several volcanoes in the NLA show similar age peaks as those detrital zircons from the Cathaysia Block, such as those from Yuemei volcano, Chimei volcano, and Lanyu volcano. Yuemei volcano records inherited ages, including those associated with the Wutai stage (2576 - 2399 Ma, ~8.9%), Luliang stage (1875 - 1729, ~10.7%), Jinning stage (848 - 719, ~6.3%), Indosinian stage (249 - 204 Ma, ~16.1%), and Yanshanian stage (182 - 66 Ma, ~25.9%) (Figs. 8a, b, and 9a). According to Shao et al. (2015), the inherited zircon age peaks in Chimei volcano are associated with the Wutai stage (2592 - 2395 Ma, ~3.9%), Luliang stage (1898 - 1697, ~8.2%), Jinning stage (847 - 648, ~4.8%), Caledonian stage (441 - 409, 1.9%), Indosinian stage (245 - 206 Ma, ~16.6%), and Yanshanian stage (182 - 64 Ma, ~11.6%) (Figs. 8c - e and 9b). Moreover, this characteristic can also be found in Lanyu volcano, which exhibits age peaks associated with the Wutai stage (2605 - 2401 Ma, ~24.4%), Luliang stage (1901 - 1841 Ma, ~3.0%), Jinning Stage (816 - 772 Ma, ~1.2%), and Yanshanian stage (171 - 61 Ma, ~11.6%) (Fig. 9d; data from Shao et al. 2014). In addition to these ages, our analyzed results in Yuemei and Lanyu volcanoes and those of another study performed in Chimei volcano (Shao et al. 2015) also indicate that the Cathaysian-type inherited zircons have variable zircon Hf isotopic ratios, in contrast to the magmatic zircons, which record high and positive $\varepsilon_{Hf}(T)$ values since the Miocene (Figs. 9b - d).

These Cathaysian-type inherited zircons could have been involved in NLA magmatism by one of two major mechanisms. The first possible way is that the sediments that were eroded from the Cathaysia Block and deposited in the South China Sea Plate were subducted with the subducting

slab into the subduction zone. However, when the NLA started to form on the Philippine Sea Plate during the Middle Miocene (~20 - 15 Ma), it was still located far away from the Cathaysia continental block, and it thus would have been hard to obtain detrital zircons from this region (Hall 2002). Thus, the subducted oceanic crust was covered by more pelagic sediments (Fourcade et al. 1994; Marini et al. 2005) than continental sediments (Defant et al. 1990; Marini et al. 2005). Additionally, according to our measured zircon Hf isotopic ratios and whole-rock Nd and Hf isotopic compositions (Lai et al. unpublished data), source contamination did not play an important role from 10 - 6 Ma (Fig. 10).

Another mechanism for the source of the Cathaysian-type inherited zircons was that magma traveled through a continental fragment prior to being erupted. Smyth et al. (2007) proposed that the Early Cenozoic East Java arc was underlain by a continental fragment of Gondwana, based on their similar inherited zircon ages. Similarly, Shao et al. (2015) suggested that a mirco-continent or a continental fragment of Cathaysia must have overlain the Luzon subduction zone and that old Cathaysian-type inherited zircons were picked up during the ascent of magma to the magma chamber. In addition, several previous studies reported that the North Palawan (Suggate et al. 2014) and Mindoro (Knittel et al. 2010) Continental Terranes were part of the continental margin of the South China Block, which rifted during the opening of South China Sea and were then accreted to the Philippine Sea Plate. According to the results of age and Hf isotopic analyses, we argue the Cathaysian accreted micro-continent or continental fragment was not a unique feature of the NLA in Chimei volcano, but also existed in some volcanoes around this subduction area.

6.4 Implications for the Petrogenesis of the NLA

In general, crustal materials can contaminate magmas in one of two main ways: one, source contamination, in which sediments eroded from the continental crust are subducted

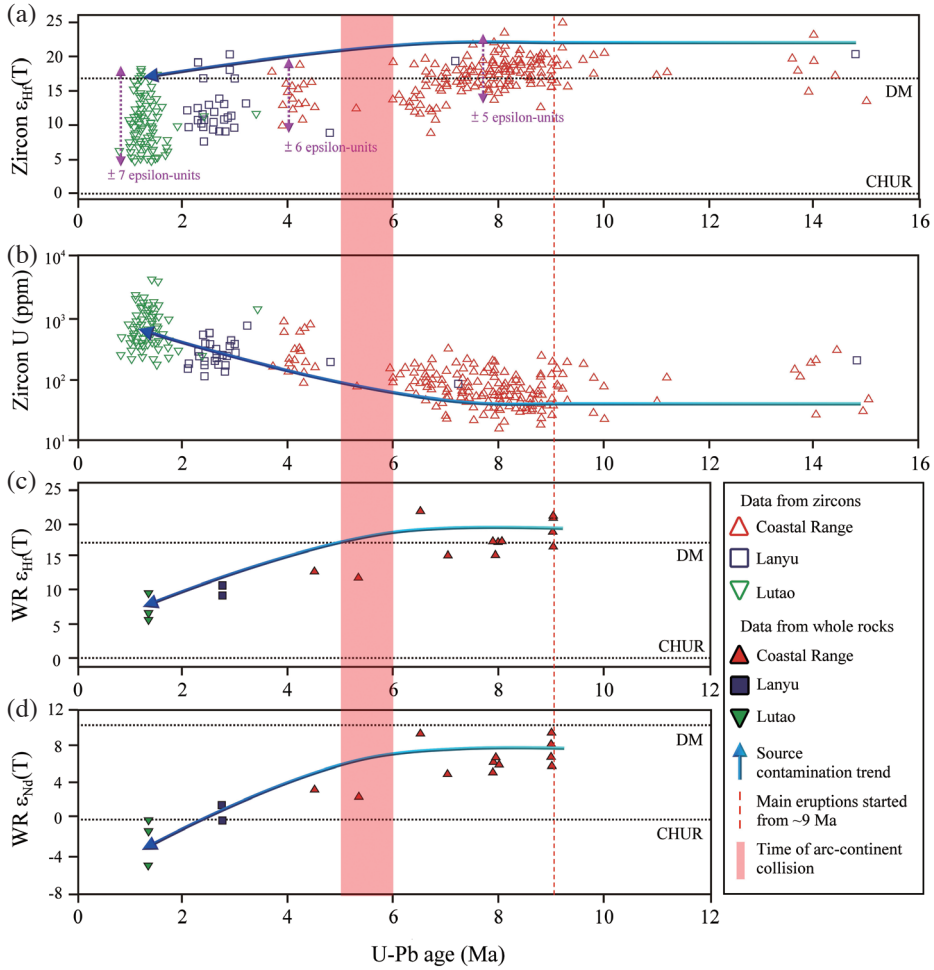

Fig. 10. (a) and (b) Plot of zircon ε_{Hf}(T) values and uranium concentration versus crystallization age after 16 Ma. The dotted pink and blue arrows represent the degree of source contamination, which increases after 6 Ma. (c) and (d) Plots of whole-rock ε_{Hf}(T) and ε_{Nd}(T) values (Lai et al. unpublished data) versus their mean U-Pb ages. The trend of source contamination can also be observed in the whole-rock patterns. Data from the CM sequences in the Chimei volcano were published by Shao et al. (2015).

into the mantle wedge and infect the magma source; and two, crustal contamination, which occurs when magma rises throughout the overlying continental crust and reacts with crustal materials. Based on our data, we argue that magmas in the NLA went through both source and crustal contamination, but to different degrees, prior to being erupted.

6.4.1 Evidence of Crustal Contamination

Numerous previous studies have considered crustal contamination when discussing the petrogenesis of the NLA, based on the observed variations in trace elements (Defant et al. 1990), the petrography of xenoliths and minerals (Yang 1992), inherited zircons (Shao et al. 2015), and a primary $^{143}Nd/^{144}Nd$ and $^{87}Sr/^{86}Sr$ mixing model (Lai et al. 2017). In our study, high proportions of inherited zircons were found in Yuemei, Chimei, and Lanyu volcanoes. These inherited zircons may not have been supplied from the subduction of crustal sediments, because the subduction zone was still located far from the Eurasian continent at 15 - 9 Ma (Lee and Lawver 1995; Hall 2002). Moreover, temperatures under intra-oceanic subduction zones can reach higher than 1000°C (Blatt et al. 2006), and the closure temperature of the Pb-U system in zircon is ~900°C (Lee et al. 1997); thus, few zircons could still record inherited Hf isotope ratios after being subducted with the downgoing slab. Our dating results indicate that the ages of the inherited zircons overlap with those of the Cathaysia Block, as discussed above. Based on the aforementioned lines of discussion, we suggest that these inherited zircons were collected from the overlying micro-continent or continental fragment by the ascending magma. Consequently, crustal contamination is an important process in the petrogenesis of the NLA.

6.4.2 Evidence of Source Contamination

Previous studies have suggested that source contamination is the main mechanism of the petrogenesis of the NLA (Chen et al. 1990; McDermott et al. 1993; Fourcade et al. 1994; Marini et al. 2005) and have provided several mixing models between a DM component and another enriched component. Our zircon $\varepsilon_{Hf}(T)$ values have a decreasing trend of depleted-mantle involvement through time in each volcano in the NLA (Fig. 10a). Magma sources exhibit the characteristics of a DM component, such as an intra-oceanic arc, i.e., the highest $\varepsilon_{Hf}(T)$ values recorded in Chimei, Chengkuang'ao, Lanyu, and Lutao after 9 Ma are +19.9, +24.9, +21.3, and +18.1, respectively (Table A2). The zircon $\varepsilon_{Hf}(T)$ values of the depleted component are homogeneous before 6 Ma and decrease smoothly after 6 Ma, which is also the time when the arc-continent collision began (Teng 1990). Similar decreasing curves can also be found on the diagrams of whole-rock $\varepsilon_{Hf}(T)$ and $\varepsilon_{Nd}(T)$ values versus age (Figs. 10c and d). Moreover, the U contents of these dated zircons show smoothly increasing trends after 6 Ma (Fig. 10b). Because uranium is an incompatible element, it is enriched in magmas with higher degrees of partial melting, such as those of the continental crust. For this reason, when crustal materials eroded from continental crust are subducted with the subducting slab into the magma source, its U concentrations will increase.

Further evidence can be found based on the variations in zircon Hf isotopic data from each volcano in the NLA. The zircon $\varepsilon_{Hf}(T)$ values in the NLA show high and positive from ~15 - 8 Ma (+25 to +15; ±5 ε-unit variation), and became lower from ~6 - 4.2 Ma (+20 to +8; ±6 ε-units), and the lowest from ~1.3 Ma (+19 to +5; ±7 ε-units) (Fig. 10a). These results can be interpreted as evidence of the binary mixing of magmas between a DM source and the increasing continental crust materials that was subducted into the magma source (Lai et al. 2017).

These results indicate that source contamination occurred in the NLA and may have been due to the addition of crustal materials to the magma source. The fact that the degree of source contamination obviously increases after 6 Ma might be the result of more crustal materials being involved in the subduction zone when the NLA started colliding the Eurasian continental margin.

7. CONCLUDING REMARKS

The results of the U-Pb dating and Hf isotopic analysis of zircons from volcanic rocks from six volcanoes of the NLA display various age spectra, implying that their magmatic and tectonic histories are as follows. The 15 - 14 Ma peak ages in the CR represent the magmatism caused by the initiation of the subduction of the South China Sea Plate. The main magmatism of the NLA began ca. 9 Ma and ceased ca. 4 Ma in the CR. The magmatism of the NLA erupted after Miocene and showed high and positive $\varepsilon_{Hf}(T)$ values. The inherited zircons from Yuemei, Chimei, and Lanyu volcanoes indicate that the magmas in these volcanoes interacted with old zircons from fragments of Cathaysia and thus represent crustal contamination. Our results indicate that these old micro-continents or continental fragments commonly existed around the Luzon Arc. Both crustal and source contamination can be recognized based on the $\varepsilon_{Hf}(T)$ values and U concentrations of zircons, as well as the Hf and Nd isotopic compositions of whole-rock samples. The degree of source contamination increases after 6 Ma, which might be the result of arc-continent collision causing the tectonic environment to become more compressive, thus extending the retention time of magmas in chambers; or due to the increasing amount of crustal materials involved in the magma source when the NLA started colliding the Eurasian continental margin.

Acknowledgements We thank Profs. B.-M. Jahn, C.-H. Chen, T.-F. Yang, S.-R. Song, and Y.-H. Lee for their fruitful discussions and constructive comments on the analyzed data; we also thank Dr. T.-T. Lo and Ms. W.-Y. Hsia for their help with many minor matters. This study was supported by the MOST 105-2116-M-003-007 and 106-2116-M-003-006 grants.

REFERENCES

Andersen, T., 2002: Correction of common lead in U-Pb analyses that do not report ^{204}Pb. *Chem. Geol.*, **192**, 59-79, doi: 10.1016/s0009-2541(02)00195-x. [Link]

Black, L. P. and B. L. Gulson, 1978: The age of the Mud Tank carbonatite, Strangways Range, Northern Territory. *J. Aust. Geol. Geophys.*, **3**, 227-232.

Blatt, H., R. Tracy, and B. Owens, 2006: Petrology: Igneous, Sedimentary, and Metamorphic, W. H. Freeman, 530 pp.

Blichert-Toft, J. and F. Albarède, 1997: The Lu-Hf isotope geochemistry of chondrites and the evolution of the mantle-crust system. *Earth Planet. Sci. Lett.*, **148**, 243-258, doi: 10.1016/s0012-821x(97)00040-x. [Link]

Chen, C.-H., Y.-N. Shieh, T. Lee, C.-H. Chen, and S. A. Mertzman, 1990: Nd-Sr-O isotopic evidence for source contamination and an unusual mantle component under Luzon Arc. *Geochim. Cosmochim. Acta*, **54**, 2473-2483, doi: 10.1016/0016-7037(90)90234-c. [Link]

Chen, C.-H., C.-Y. Lee, H.-Y. Lu, and P.-S. Hsieh, 2008: Generation of Late Cretaceous silicic rocks in SE China: Age, major element and numerical simulation constraints. *J. Asian Earth Sci.*, **31**, 479-498, doi: 10.1016/j.jseaes.2007.08.002. [Link]

Chen, J.-C., 1975: Geochemistry of andesites from the Coastal Range, Eastern Taiwan. *Proc. Geol. Soc. China*, **18**, 73-88.

Chen, W. S., 1997: Lithofacies analyses of the arc-related sequence in Coastal Range, eastern Taiwan. *J. Geol. Soc. China*, **40**, 313-338.

Chiu, H.-Y., S.-L. Chung, F.-Y. Wu, D. Liu, Y.-H. Liang, I.-J. Lin, Y. Iizuka, L.-W. Xie, Y. Wang, and M.-F. Chu, 2009: Zircon U-Pb and Hf isotopic constraints from eastern Transhimalayan batholiths on the precollisional magmatic and tectonic evolution in southern Tibet. *Tectonophysics*, **477**, 3-19, doi: 10.1016/j.tecto.2009.02.034. [Link]

Defant, M. J., R. Maury, J.-L. Joron, M. D. Feigenson, J. Leterrier, H. Bellon, D. Jacques, and M. Richard, 1990: The geochemistry and tectonic setting of the northern section of the Luzon arc (The Philippines and Taiwan). *Tectonophysics*, **183**, 187-205, doi: 10.1016/0040-1951(90)90416-6. [Link]

Fourcade, S., R. Maury, M. J. Defant, and F. McDermott, 1994: Mantle metasomatic enrichment versus arc crust contamination in the Philippines: Oxygen isotope study of Batan ultramafic nodules and northern Luzon arc lavas. *Chem. Geol.*, **114**, 199-215, doi: 10.1016/0009-2541(94)90053-1. [Link]

Griffin, W. L., N. J. Pearson, E. Belousova, S. E. Jackson, E. van Achterbergh, S. Y. O'Reilly, and S. R. Shee, 2000: The Hf isotope composition of cratonic mantle: LAM-MC-ICPMS analysis of zircon megacrysts in kimberlites. *Geochim. Cosmochim. Acta*, **64**, 133-147, doi: 10.1016/s0016-7037(99)00343-9. [Link]

Griffin, W. L., X. Wang, S. E. Jackson, N. J. Pearson, S. Y. O'Reilly, X. Xu, and X. Zhou, 2002: Zircon chemistry and magma mixing, SE China: in-situ analysis of Hf isotopes, Tonglu and Pingtan igneous complexes. *Lithos*, **61**, 237-269, doi: 10.1016/s0024-4937(02)00082-8. [Link]

Hall, R., 2002: Cenozoic geological and plate tectonic evolution of SE Asia and the SW Pacific: Computer-based reconstructions, model and animations. *J. Asian Earth Sci.*, **20**, 353-431, doi: 10.1016/s1367-9120(01)00069-4. [Link]

Ho, C. S., 1969: Geological significance of potassium-argon ages of the Chimei igneous complex in eastern Taiwan. *Bull. Geol. Surv. Taiwan*, **20**, 63-74.

Hsu, T. L., 1956: Geology of the Coastal Range, eastern Taiwan. *Bull. Geol. Surv. Taiwan*, **8**, 39-63.

Hu, X., Z. Huang, J. Wang, J. Yu, K. Xu, L. Jansa, and W. Hu, 2012: Geology of the Fuding inlier in southeastern China: Implication for late Paleozoic Cathaysian paleogeography. *Gondwana Research*, **22**, 507-518, doi: 10.1016/j.gr.2011.09.016. [Link]

Huang, C. Y., P. B. Yuan, and L. S. Teng, 1988: Paleontology of the Kangkou Limestone in the middle Coastal Range, eastern Taiwan. *Acta Geol. Taiwan.*, **26**, 133-160.

Huang, C. Y., P. B. Yuan, S.-R. Song, C.-W. Lin, C. Wang, M.-T. Chen, C.-T. Shyu, and B. Karp, 1995: Tectonics of short-lived intra-arc basins in the arc-continent collision terrane of the Coastal Range, eastern Taiwan. *Tectonics*, **14**, 19-38, doi: 10.1029/94tc02452. [Link]

Ireland, T. R. and I. S. Williams, 2003: Considerations in zircon geochronology by SIMS. *Rev. Mineral. Geochem.*, **53**, 215-241, doi: 10.2113/0530215. [Link]

Jackson, S. E., N. J. Pearson, W. L. Griffin, and E. A. Belousova, 2004: The application of laser ablation-inductively coupled plasma-mass spectrometry to in situ U-Pb zircon geochronology. *Chem. Geol.*, **211**, 47-69, doi: 10.1016/j.chemgeo.2004.06.017. [Link]

Jacques, D., 1987: Géologie et pétrologie de l'Archipel Babuyan et des Monts Tabungon et Cagua Nord Luzon, Philippines: Implications magmatologiques et géodynamiques. Ph.D. Thesis, Universite de Bretagne occidentale, Brest.

Juang, W. S. and H. Bellon, 1984: The potassium-argon dating of andesites from Taiwan. *Proc. Geol. Soc. China*, **27**, 86-100.

Knittel, U., C.-H. Hung, T. F. Yang, and Y. Iizuka, 2010: Permian arc magmatism in Mindoro, the Philippines: An early Indosinian event in the Palawan Continental Terrane. *Tectonophysics*, **493**, 113-117, doi: 10.1016/j.tecto.2010.07.007. [Link]

Lai, Y.-M. and S.-R. Song, 2013: The volcanoes of an oceanic arc from origin to destruction: A case from the northern Luzon Arc. *J. Asian Earth Sci.*, **74**, 97-112, doi: 10.1016/j.jseaes.2013.03.021. [Link]

Lai, Y.-M., S.-R. Song, and Y. Iizuka, 2008: Magma mingling in the Tungho area, Coastal Range of eastern Taiwan. *J. Volcanol. Geotherm. Res.*, **178**, 608-623, doi: 10.1016/j.jvolgeores.2008.05.020. [Link]

Lai, Y.-M., S.-R. Song, C.-H. Lo, T.-H. Lin, M.-F. Chu, and S.-L. Chung, 2017: Age, geochemical and isotopic variations in volcanic rocks from the Coastal Range of Taiwan: Implications for magma generation in the Northern Luzon Arc. *Lithos*, **272-273**, 92-115, doi: 10.1016/j.lithos.2016.11.012. [Link]

Lan, C. Y., 1982: Mineralogy, petrology and hydrothermal alteration of Chimei igneous complex. MRSO Report 193, Hualien, Taiwan.

Lee, J. K. W., I. S. Williams, and D. J. Ellis, 1997: Pb, U and Th diffusion in natural zircon. *Nature*, **390**, 159-162, doi: 10.1038/36554. [Link]

Lee, T.-Y. and L. A. Lawver, 1994: Cenozoic plate reconstruction of the South China Sea region. *Tectonophysics*, **235**, 149-180, doi: 10.1016/0040-1951(94)90022-1. [Link]

Lee, T.-Y. and L. A. Lawver, 1995: Cenozoic plate reconstruction of Southeast Asia. *Tectonophysics*, **251**, 85-138, doi: 10.1016/0040-1951(95)00023-2. [Link]

Li, X.-H., Z.-X. Li, and W.-X. Li, 2014: Detrital zircon U-Pb age and Hf isotope constrains on the generation and reworking of Precambrian continental crust in the Cathaysia Block, South China: A synthesis. *Gondwana Research*, **25**, 1202-1215, doi: 10.1016/j.gr.2014.01.003. [Link]

Li, Z. X., X. H. Li, P. D. Kinny, J. Wang, S. Zhang, and H. Zhou, 2003: Geochronology of Neoproterozoic syn-rift magmatism in the Yangtze Craton, South China and correlations with other continents: Evidence for a mantle superplume that broke up Rodinia. *Precambrian Res.*, **122**, 85-109, doi: 10.1016/s0301-9268(02)00208-5. [Link]

Lo, C.-H., T. C. Onstott, C.-H. Chen, and T. Lee, 1994: An assessment of $^{40}Ar/^{39}Ar$ dating for the whole-rock volcanic samples from the Luzon Arc near Taiwan. *Chem. Geol.*, **114**, 157-178, doi: 10.1016/0009-2541(94)90049-3. [Link]

Ludwig, K. R., 2009: Isoplot v. 3.71: A Geochronological Toolkit for Microsoft Excel: Berkeley, California, Berkeley Geochronology Center Special Publication.

Marini, J.-C., C. Chauvel, and R. C. Maury, 2005: Hf isotope compositions of northern Luzon arc lavas suggest involvement of pelagic sediments in their source. *Contrib. Mineral. Petrol.*, **149**, 216-232, doi: 10.1007/s00410-004-0645-4. [Link]

McDermott, F., M. J. Defant, C. J. Hawkesworth, R. C. Maury, and J. L. Joron, 1993: Isotope and trace element evidence for three component mixing in the genesis of the North Luzon arc lavas (Philippines). *Contrib. Mineral. Petrol.*, **113**, 9-23, doi: 10.1007/bf00320828. [Link]

Nowell, G. M., P. D. Kempton, S. R. Noble, J. G. Fitton, A. D. Saunders, J. J. Mahoney, and R. N. Taylor, 1998: High precision Hf isotope measurements of MORB and OIB by thermal ionisation mass spectrometry: Insights into the depleted mantle. *Chem. Geol.*, **149**, 211-233, doi: 10.1016/s0009-2541(98)00036-9. [Link]

Parker, E. S. and W. K. Gealey, 1985: Plate tectonic evolution of the western Pacific-Indian Ocean region. *Energy*, **10**, 249-261, doi: 10.1016/0360-5442(85)90045-3. [Link]

Patchett, P. J. and M. Tatsumoto, 1981: Lu/Hf in chondrites and definition of a chondritic hafnium growth curve. Lunar and Planetary Science Conference, Vol. 12, 822-824.

Richard, M., H. Bellon, R. Maury, E. Barrier, and J. Wen-Shing, 1986: Miocene to recent calc-alkalic volcanism in eastern Taiwan: K-Ar ages and petrography. *Tectonophysics*, **125**, 87-102, doi: 10.1016/0040-1951(86)90008-9. [Link]

Rubatto, D. and D. Gebauer, 2000: Use of cathodoluminescence for U-Pb zircon dating by ion microprobe: Some examples from the Western Alps. In: Pagel, M., V. Barbin, P. Blanc, and D. Ohnenstetter (Eds.), Cathodoluminescence in Geosciences, Springer, Berlin, Heidelberg, 373-400, doi: 10.1007/978-3-662-04086-7_15. [Link]

Scherer, E., C. Münker, and K. Mezger, 2001: Calibration of the lutetium-hafnium clock. *Science*, **293**, 683-687, doi: 10.1126/science.1061372. [Link]

Shao, W.-Y., S.-L. Chung, and W.-S. Chen, 2014: Zircon U-Pb age determination of volcanic eruptions in Lutao and Lanyu in the Northern Luzon magmatic arc. *Terr. Atmos. Ocean. Sci.*, **25**, 149-187, doi: 10.3319/TAO.2013.11.06.01(TT). [Link]

Shao, W.-Y., S.-L. Chung, W.-S. Chen, H.-Y. Lee, and L.-W. Xie, 2015: Old continental zircons from a young oceanic arc, eastern Taiwan: Implications for Luzon subduction initiation and Asian accretionary orogeny. *Geology*, **43**, 479-482, doi: 10.1130/g36499.1. [Link]

Sláma, J., J. Košler, D. J. Condon, J. L. Crowley, A. Gerdes,

J. M. Hanchar, M. S. A. Horstwood, G. A. Morris, L. Nasdala, N. Norberg, U. Schaltegger, B. Schoene, M. N. Tubrett, and M. J. Whitehouse, 2008: Plešovice zircon — A new natural reference material for U-Pb and Hf isotopic microanalysis. *Chem. Geol.*, **249**, 1-35, doi: 10.1016/j.chemgeo.2007.11.005. [Link]

Smyth, H. R., P. J. Hamilton, R. Hall, and P. D. Kinny, 2007: The deep crust beneath island arcs: Inherited zircons reveal a Gondwana continental fragment beneath East Java, Indonesia. *Earth Planet. Sci. Lett.*, **258**, 269-282, doi: 10.1016/j.epsl.2007.03.044. [Link]

Song, S.-R., 1990: A Study of the Volcanic Rocks in the Central Coastal Range of Eastern Taiwan and the Evolution of Volcanic Island Arc of the Northern Luzon Arc. Ph.D. Thesis, Institute of Geology, National Taiwan University, 251 pp. (in Chinese)

Song, S.-R. and H.-J. Lo, 1988: Volcanic geology of Fengpin-Takangkou area, coastal range of Taiwan. *Acta Geol. Taiwan.*, **26**, 223-235.

Song, S.-R. and H.-J. Lo, 2002: Lithofacies of volcanic rocks in the central Coastal Range, eastern Taiwan: implications for island arc evolution. *J. Southeast Asian Earth Sci.*, **21**, 23-38, doi: 10.1016/s1367-9120(02)00003-2. [Link]

Suggate, S. M., M. A. Cottam, R. Hall, I. Sevastjanova, M. A. Forster, L. T. White, R. A. Armstrong, A. Carter, and E. Mojares, 2014: South China continental margin signature for sandstones and granites from Palawan, Philippines. *Gondwana Research*, **26**, 699-718, doi: 10.1016/j.gr.2013.07.006. [Link]

Taylor, B. and D. E. Hayes, 1983: Origin and history of the South China Sea basin. In: Hayes, D. E. (Ed.), The Tectonic and Geologic Evolution of Southeast Asian Seas and Islands: Part 2, American Geophysical Union, Washington, D. C., 23-56, doi: 10.1029/GM027p0023. [Link]

Teng, L. S., 1990: Geotectonic evolution of late Cenozoic arc-continent collision in Taiwan. *Tectonophysics*, **183**, 57-76, doi: 10.1016/0040-1951(90)90188-e. [Link]

Vidal, P., C. Dupuy, R. Maury, and M. Richard, 1989: Mantle metasomatism above subduction zones: Trace-element and radiogenic isotope characteristics of peridotite xenoliths from Batan Island (Philippines). *Geology*, **17**, 1115-1118, doi: 10.1130/0091-7613(1989)017<1115:MMASZT>2.3.CO;2. [Link]

Wang, Y., 1966: Some geologic observations in the Coastal Range, eastern Taiwan. *Proc. Geol. Soc. China*, **9**, 86-93.

Wang, Y., Y. Zhang, W. Fan, and T. Peng, 2005: Structural signatures and $^{40}Ar/^{39}Ar$ geochronology of the Indosinian Xuefengshan tectonic belt, South China Block. *J. Struct. Geol.*, **27**, 985-998, doi: 10.1016/j.jsg.2005.04.004. [Link]

Wang, Y., W. Fan, M. Sun, X. Liang, Y. Zhang, and T. Peng, 2007: Geochronological, geochemical and geothermal constraints on petrogenesis of the Indosinian peraluminous granites in the South China Block: A case study in the Hunan Province. *Lithos*, **96**, 475-502, doi: 10.1016/j.lithos.2006.11.010. [Link]

Wiedenbeck, M., P. Allé, F. Corfu, W. L. Griffin, M. Meier, F. Oberli, A. V. Quadt, J. C. Roddick, and W. Spiegel, 1995: Three natural zircon standards for U-Th-Pb, Lu-Hf, trace element and REE analyses. *Geostand. Geoanal. Res.*, **19**, 1-23, doi: 10.1111/j.1751-908x.1995.tb00147.x. [Link]

Williams, P. R., C. R. Johnston, R. A. Almond, and W. H. Simamora, 1988: Late Cretaceous to Early Tertiary structural elements of West Kalimantan. *Tectonophysics*, **148**, 279-297, doi: 10.1016/0040-1951(88)90135-7. [Link]

Wu, F.-Y., Y.-H. Yang, L.-W. Xie, J.-H. Yang, and P. Xu, 2006: Hf isotopic compositions of the standard zircons and baddeleyites used in U-Pb geochronology. *Chem. Geol.*, **234**, 105-126, doi: 10.1016/j.chemgeo.2006.05.003. [Link]

Yang, T. F., 1992: Magma evolution of the North Luzon arc and its tectonic implication. Ph.D. Thesis, Department of Geology, National Taiwan University, 458 pp. (in Chinese)

Yang, T. F., T. K. Liu, and C. H. Chen, 1988: Thermal event records of the Chimei igneous complex: constraint on the ages of magma activities and the structural implication based on fission track dating. *Acta Geol. Taiwan.*, **26**, 237-246.

Yang, T. F., C.-H. Chen, and T. Lee, 1992: Fission-track dating of Lutao volcanics: Implications of partial annealing and eruption history. *J. Geol. Soc. China*, **35**, 19-34.

Yang, T. F., J. Tien, C.-H. Chen, T. Lee, and R. S. Punongbayan, 1995: Fission-track dating of volcanics in the northern part of the Taiwan-Luzon Arc: Eruption ages and evidence for crustal contamination. *J. Southeast Asian Earth Sci.*, **11**, 81-93, doi: 10.1016/0743-9547(94)00041-c. [Link]

Yen, T. P., 1967: Structural analysis of the Tananao Schist of Taiwan. *Bull. Geol. Surv. Taiwan*, **18**, 1-110.

APPENDIX A.

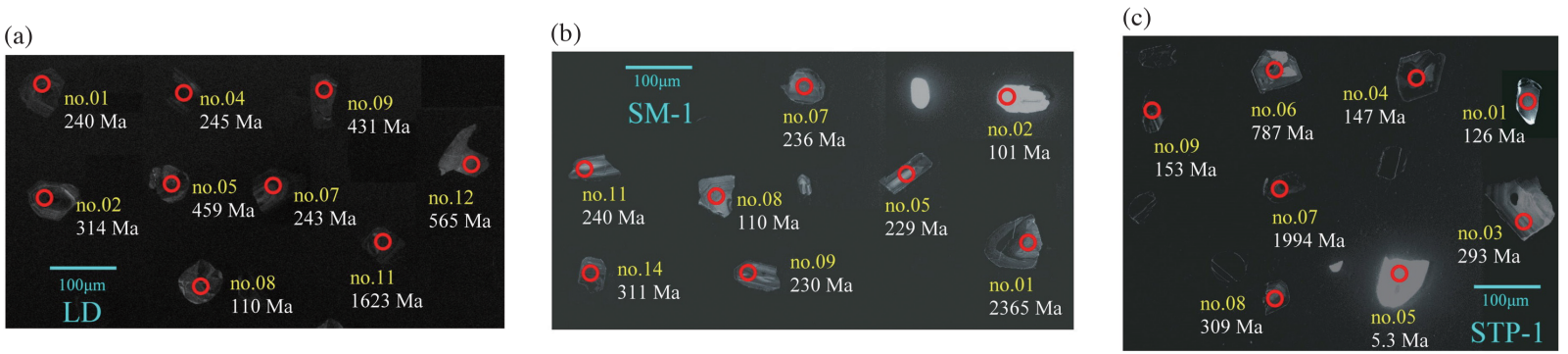

Fig. A1. CL images of zircons from the CR. (a) Sample no. LD from the STP sequence in Yuemei volcano. (b) Sample no. SM-1 from the SM sequence in Chimei volcano. (c) Sample no. STP-1 from the STP sequence in Chimei volcano.

Table A1. Zircon U-Pb isotopic data of Coastal Range samples.

Spot	U (ppm)	Th/U	U-Th-Pb ratios								Ages (Ma)							
			$^{207}Pb/^{235}U$	±1 s	$^{206}Pb/^{238}U$	±1 s	$^{207}Pb/^{206}Pb$	±1 s	$^{208}Pb/^{232}Th$	±1 s	$^{206}Pb/^{238}U$	±1 s	$^{207}Pb/^{206}Pb$	±1 s	$^{207}Pb/^{235}U$	±1 s	$^{208}Pb/^{232}Th$	±1 s
Yuemei volcano-Shihmen Formation																		
LD-01	920	1.06	0.30910	0.00850	0.03793	0.00092	0.05911	0.00071	0.01114	0.00032	**240**	**6**	571	24	273	7	224	6
LD-02	376	0.59	0.35789	0.03323	0.04985	0.00137	0.05206	0.00366	0.01566	0.00034	**314**	**8**	288	143	311	25	314	7
LD-03	1119	0.56	1.22767	0.02950	0.13378	0.00307	0.06656	0.00070	0.04147	0.00114	**809**	**17**	824	24	813	13	821	22
LD-04	2169	1.54	0.36837	0.04365	0.03879	0.00111	0.06887	0.00661	0.01179	0.00025	**245**	**7**	895	199	318	32	237	5
LD-05	493	0.94	0.91978	0.06971	0.07386	0.00197	0.09032	0.00489	0.02180	0.00051	**459**	**12**	1432	108	662	37	436	10
LD-06	987	0.52	1.23390	0.02985	0.13429	0.00308	0.06665	0.00071	0.04058	0.00112	**812**	**18**	827	22	816	14	804	22
LD-07	388	0.76	0.27031	0.00682	0.03844	0.00086	0.05101	0.00056	0.01250	0.00034	**243**	**5**	241	27	243	5	251	7
LD-08	1730	0.48	0.35084	0.00846	0.03731	0.00079	0.06821	0.00072	0.01585	0.00058	**236**	**5**	875	22	305	6	318	12
LD-09	1025	0.32	0.70819	0.01900	0.06919	0.00168	0.07424	0.00087	0.01728	0.00057	**431**	**10**	1048	24	544	11	346	11
LD-10	533	0.42	0.27524	0.00768	0.03843	0.00091	0.05195	0.00064	0.01308	0.00043	**243**	**6**	283	27	247	6	263	9
LD-11	561	0.15	5.79218	0.14291	0.28631	0.00658	0.14673	0.00158	0.08318	0.00266	1623	33	**2308**	**19**	1945	21	1615	50
LD-12	155	0.91	0.87493	0.02589	0.09164	0.00224	0.06924	0.00091	0.02832	0.00100	**565**	**13**	906	27	638	14	564	20
Yuemei volcano-Shihtiping Formation																		
20130811-06-01	1089	0.45	0.16965	0.00434	0.02501	0.00061	0.04921	0.00055	0.00755	0.00018	**159**	**4**	158	28	159	4	152	4
20130811-06-02	1792	0.34	0.17820	0.00464	0.02590	0.00065	0.04992	0.00057	0.00765	0.00018	**165**	**4**	191	27	167	4	154	4
20130811-06-03	373	0.55	8.26171	0.20382	0.39272	0.00954	0.15259	0.00167	0.10677	0.00245	2135	44	**2375**	**18**	2260	22	2050	45
20130811-06-04	409	0.58	0.18881	0.01234	0.02362	0.00060	0.05796	0.00251	0.00733	0.00016	**151**	**4**	528	92	176	11	148	3
20130811-06-05	2061	1.45	0.13005	0.00355	0.01825	0.00042	0.05167	0.00062	0.00262	0.00009	**117**	**3**	271	29	124	3	53	2
20130811-06-06	154	0.33	0.27307	0.00995	0.03880	0.00105	0.05104	0.00086	0.01046	0.00033	**245**	**7**	243	40	245	8	210	7
20130811-06-07	1603	0.39	6.20561	0.15514	0.31156	0.00760	0.14447	0.00160	0.07889	0.00195	1748	37	**2281**	**20**	2005	22	1535	37

Table A1. (Continued)

Spot	U (ppm)	Th/U	U-Th-Pb ratios								Ages (Ma)							
			$^{207}Pb/^{235}U$	±1 s	$^{206}Pb/^{238}U$	±1 s	$^{207}Pb/^{206}Pb$	±1 s	$^{208}Pb/^{232}Th$	±1 s	$^{206}Pb/^{238}U$	±1 s	$^{207}Pb/^{206}Pb$	±1 s	$^{207}Pb/^{235}U$	±1 s	$^{208}Pb/^{232}Th$	±1 s
20130811-06-08	223	0.65	0.37440	0.01017	0.04983	0.00122	0.05450	0.00065	0.01476	0.00037	**313**	**7**	392	27	323	8	296	7
20130811-06-09	139	0.57	10.9243	0.27307	0.47693	0.01158	0.16614	0.00183	0.12490	0.00311	2514	51	**2519**	**18**	2517	23	2379	56
20130811-06-10	474	0.88	0.16883	0.00462	0.02351	0.00058	0.05209	0.00062	0.00702	0.00018	**150**	**4**	289	26	158	4	141	4
20130811-06-11	116	0.94	0.31798	0.00957	0.04124	0.00103	0.05593	0.00074	0.01225	0.00032	**261**	**6**	450	29	280	7	246	6
20130811-06-12	1073	0.16	5.12855	0.12860	0.30376	0.00736	0.12246	0.00135	0.09145	0.00238	1710	36	**1992**	**20**	1841	21	1769	44
20130811-06-13	168	0.48	0.31617	0.01161	0.04112	0.00112	0.05576	0.00095	0.01157	0.00041	**260**	**7**	443	39	279	9	233	8
20130811-06-14	275	0.53	9.13663	0.25263	0.42244	0.01094	0.15686	0.00190	0.11026	0.00364	2272	50	**2422**	**21**	2352	25	2114	66
20130811-06-15	146	0.61	4.83603	0.12335	0.30719	0.00745	0.11419	0.00128	0.08881	0.00247	1727	37	**1867**	**19**	1791	21	1720	46
20130811-06-16	709	0.12	4.70959	0.12677	0.30287	0.00793	0.11277	0.00134	0.07805	0.00208	1706	39	**1845**	**22**	1769	23	1519	39
20130811-06-17	238	0.91	0.13494	0.00426	0.01818	0.00046	0.05383	0.00076	0.00558	0.00014	**116**	**3**	364	33	129	4	112	3
20130811-06-18	89	0.63	11.7015	0.28969	0.49378	0.01145	0.17188	0.00186	0.12456	0.00354	2587	49	**2576**	**18**	2581	23	2373	64
20130811-06-19	406	0.54	0.19849	0.00539	0.02855	0.00070	0.05043	0.00060	0.00875	0.00021	**181**	**4**	215	25	184	5	176	4
20130811-06-20	324	0.14	5.32137	0.13264	0.33752	0.00823	0.11435	0.00126	0.09192	0.00219	1875	40	**1870**	**19**	1872	21	1777	41
20130811-06-21	704	0.40	8.93479	0.22105	0.41888	0.01013	0.15470	0.00169	0.11804	0.00286	2255	46	**2399**	**18**	2331	23	2255	52
20130811-06-22	74	0.50	4.82798	0.14834	0.28344	0.00790	0.12355	0.00165	0.06038	0.00211	1609	40	**2008**	**24**	1790	26	1185	40
20130811-06-23	58	1.14	1.20610	0.03512	0.13282	0.00339	0.06586	0.00084	0.03878	0.00102	**804**	**19**	802	25	803	16	769	20
20130811-06-24	107	1.11	1.20488	0.03211	0.11791	0.00293	0.07411	0.00086	0.03665	0.00092	**719**	**17**	1044	25	803	15	728	18
20130811-06-25	329	1.54	0.06999	0.00230	0.01022	0.00026	0.04969	0.00074	0.00303	0.00008	**66**	**2**	181	37	69	2	61	2
20130811-06-26	25	0.28	0.02181	0.00800	0.00216	0.00016	0.07327	0.02212	0.00137	0.00021	***14.0***	***1.0***	1021	673	22	8	28	4
20130811-06-27	589	0.48	3.26187	0.13711	0.22302	0.00570	0.10608	0.00242	0.06473	0.00159	1298	30	**1733**	**40**	1472	33	1268	30
20130811-06-28	461	0.21	1.57525	0.04009	0.15889	0.00388	0.07190	0.00081	0.04450	0.00121	**951**	**22**	983	23	960	16	880	23
20130811-06-29	267	1.59	0.17523	0.00517	0.02535	0.00064	0.05013	0.00065	0.00751	0.00021	**161**	**4**	201	31	164	4	151	4
20130811-06-30	363	0.35	5.17432	0.13216	0.30288	0.00750	0.12391	0.00140	0.08303	0.00228	1706	37	**2013**	**19**	1848	22	1612	43
20130811-06-31	438	0.51	1.62370	0.04129	0.16437	0.00411	0.07165	0.00081	0.04774	0.00112	**981**	**23**	976	23	979	16	943	22
20130811-06-32	35	0.45	0.01669	0.00682	0.00267	0.00019	0.04535	0.01569	0.00074	0.00013	***17.0***	***1.0***	-2	496	17	7	15	3
20130811-06-33	220	1.16	0.27273	0.00835	0.03656	0.00095	0.05411	0.00073	0.01127	0.00029	**231**	**6**	376	27	245	7	227	6
20130811-06-34	460	0.26	0.90733	0.04465	0.10617	0.00304	0.06198	0.00166	0.03267	0.00090	**650**	**18**	673	54	656	24	650	18
20130811-06-35	273	0.58	0.28937	0.00865	0.04057	0.00106	0.05173	0.00068	0.01155	0.00030	**256**	**7**	273	30	258	7	232	6
20130811-06-36	213	0.57	0.26321	0.00746	0.03624	0.00090	0.05268	0.00065	0.01132	0.00028	**229**	**6**	315	27	237	6	228	6
20130811-06-37	213	0.37	0.29171	0.00912	0.04107	0.00107	0.05151	0.00071	0.01248	0.00036	**259**	**7**	264	31	260	7	251	7
20130811-06-38	621	0.68	0.42395	0.01173	0.04948	0.00126	0.06215	0.00075	0.01483	0.00043	**311**	**8**	679	26	359	8	298	9
20130811-06-39	1005	0.55	2.18732	0.05885	0.15822	0.00412	0.10026	0.00119	0.01966	0.00056	**947**	**23**	1629	22	1177	19	394	11
20130811-06-40	160	0.68	11.0573	0.27849	0.47110	0.01162	0.17024	0.00190	0.12167	0.00300	2488	51	**2560**	**20**	2528	23	2321	54
20130811-06-41	702	0.37	0.17447	0.00500	0.02486	0.00063	0.05090	0.00064	0.00760	0.00022	**158**	**4**	236	31	163	4	153	4
20130811-06-42	370	0.50	0.40339	0.01199	0.05200	0.00136	0.05626	0.00073	0.01490	0.00046	**327**	**8**	463	27	344	9	299	9
20130811-06-43	282	0.61	0.19290	0.00554	0.02640	0.00066	0.05300	0.00067	0.00804	0.00022	**168**	**4**	329	29	179	5	162	4
20130811-06-44	790	1.61	0.09562	0.00341	0.01309	0.00035	0.05298	0.00087	0.00333	0.00013	**84**	**2**	328	40	93	3	67	3
20130811-06-45	686	0.30	0.16896	0.00457	0.02425	0.00060	0.05054	0.00060	0.00749	0.00021	**154**	**4**	220	27	159	4	151	4
20130811-06-46	474	0.45	0.18441	0.00488	0.02673	0.00065	0.05003	0.00058	0.00802	0.00019	**170**	**4**	196	26	172	4	161	4

Table A1. (Continued)

Spot	U (ppm)	Th/U	U-Th-Pb ratios								Ages (Ma)							
			$^{207}Pb/^{235}U$	±1 s	$^{206}Pb/^{238}U$	±1 s	$^{207}Pb/^{206}Pb$	±1 s	$^{208}Pb/^{232}Th$	±1 s	$^{206}Pb/^{238}U$	±1 s	$^{207}Pb/^{206}Pb$	±1 s	$^{207}Pb/^{235}U$	±1 s	$^{208}Pb/^{232}Th$	±1 s
20130811-06-47	263	0.28	10.1808	0.25542	0.45022	0.01109	0.16401	0.00182	0.11768	0.00288	2396	49	**2497**	**20**	2451	23	2249	52
20130811-06-48	28	0.32	0.01481	0.00697	0.00231	0.00015	0.04652	0.01922	0.00105	0.00015	***14.9***	***1.0***	25	665	15	7	21	3
20130811-06-49	260	1.02	3.57653	0.09036	0.24503	0.00603	0.10587	0.00118	0.06673	0.00160	1413	31	**1729**	**20**	1544	20	1306	30
20130811-06-50	638	0.45	0.19837	0.00531	0.02740	0.00067	0.05251	0.00061	0.00823	0.00020	**174**	**4**	308	28	184	4	166	4
20130811-06-51	191	0.71	5.16273	0.12662	0.32658	0.00783	0.11466	0.00125	0.08875	0.00208	1822	38	**1875**	**21**	1846	21	1719	39
20130811-06-52	767	0.36	0.27510	0.01502	0.03217	0.00081	0.06202	0.00227	0.00990	0.00023	**204**	**5**	675	76	247	12	199	5
20130811-06-53	421	0.24	1.62040	0.04005	0.16121	0.00385	0.07291	0.00079	0.04639	0.00116	**963**	**21**	1011	22	978	16	917	22
20130811-06-54	509	0.17	2.15243	0.05534	0.15751	0.00376	0.09912	0.00111	0.04150	0.00130	**943**	**21**	1608	20	1166	18	822	25
20130811-06-55	116	0.22	10.7909	0.29333	0.46971	0.01096	0.16664	0.00198	0.11990	0.00539	2482	48	**2524**	**19**	2505	25	2289	97
20130811-06-56	542	0.34	0.63489	0.01597	0.07794	0.00187	0.05908	0.00065	0.02296	0.00058	**484**	**11**	570	26	499	10	459	11
20130811-06-57	783	0.52	0.19723	0.00522	0.02750	0.00067	0.05202	0.00060	0.00833	0.00022	**175**	**4**	286	27	183	4	168	4
20130811-06-58	735	0.01	3.59888	0.09335	0.23338	0.00577	0.11185	0.00127	0.06504	0.00202	1352	30	**1830**	**20**	1549	21	1274	38
20130811-06-59	2054	1.39	0.09555	0.00253	0.01114	0.00027	0.06221	0.00072	0.00107	0.00003	**71**	**2**	681	24	93	2	22	1
20130811-06-60	225	0.29	4.12931	0.11165	0.26203	0.00613	0.11431	0.00135	0.07489	0.00329	1500	31	**1869**	**20**	1660	22	1460	62
20130811-06-61	547	0.60	0.18142	0.00478	0.02618	0.00063	0.05027	0.00058	0.00776	0.00018	**167**	**4**	207	28	169	4	156	4
20130811-06-62	406	2.33	0.26834	0.00716	0.03645	0.00086	0.05340	0.00062	0.01164	0.00029	**231**	**5**	346	27	241	6	234	6
20130811-06-63	458	0.76	0.29784	0.00923	0.03945	0.00097	0.05476	0.00076	0.01196	0.00039	**249**	**6**	402	32	265	7	240	8
20130811-06-64	68	0.34	10.9827	0.27120	0.47016	0.01130	0.16943	0.00185	0.12250	0.00289	2484	50	**2552**	**17**	2522	23	2336	52
20130811-06-65	331	0.30	4.77341	0.12458	0.30516	0.00764	0.11346	0.00130	0.07670	0.00200	1717	38	**1856**	**21**	1780	22	1494	38
20130811-06-66	609	0.19	4.63754	0.11380	0.30888	0.00740	0.10890	0.00118	0.08255	0.00195	1735	36	**1781**	**19**	1756	20	1603	36
20130811-06-67	1335	0.33	0.16254	0.00430	0.02255	0.00055	0.05227	0.00060	0.00666	0.00017	**144**	**3**	297	27	153	4	134	3
20130811-06-68	329	0.21	8.18206	0.22186	0.36945	0.00829	0.16062	0.00196	0.10290	0.00232	2027	39	**2462**	**20**	2251	25	1980	42
20130811-06-69	367	0.17	5.11457	0.13252	0.32444	0.00806	0.11434	0.00130	0.08384	0.00228	1811	39	**1870**	**19**	1839	22	1627	43
20130811-06-70	110	0.37	0.02275	0.00539	0.00249	0.00018	0.06639	0.01160	0.00099	0.00012	***16.0***	***1.0***	819	392	23	5	20	2
20130811-06-71	536	0.52	0.18420	0.00492	0.02583	0.00063	0.05171	0.00060	0.00765	0.00019	**164**	**4**	273	25	172	4	154	4
20130811-06-72	745	0.68	0.19990	0.00533	0.02619	0.00064	0.05536	0.00064	0.00756	0.00019	**167**	**4**	427	26	185	5	152	4
20130811-06-73	1194	1.25	0.23365	0.00599	0.03248	0.00078	0.05218	0.00059	0.00977	0.00025	**206**	**5**	293	27	213	5	197	5
20130811-06-74	459	0.38	0.18676	0.00510	0.02705	0.00065	0.05007	0.00060	0.00803	0.00022	**172**	**4**	198	28	174	4	162	4
20130811-06-75	436	0.82	0.35762	0.00940	0.04600	0.00111	0.05639	0.00065	0.01383	0.00037	**290**	**7**	468	25	310	7	278	7
20130811-06-76	160	0.56	0.31880	0.01009	0.04390	0.00112	0.05267	0.00074	0.01260	0.00032	**277**	**7**	315	34	281	8	253	6
20130811-06-77	490	0.22	1.38294	0.03563	0.14063	0.00349	0.07133	0.00081	0.03088	0.00076	**848**	**20**	967	24	882	15	615	15
20130811-06-78	689	0.44	0.19927	0.00565	0.02825	0.00071	0.05117	0.00063	0.00829	0.00021	**180**	**4**	248	28	185	5	167	4
20130811-06-79	473	3.33	0.12165	0.00367	0.01747	0.00044	0.05050	0.00067	0.00502	0.00012	**112**	**3**	218	30	117	3	101	2
20130811-06-80	336	0.61	1.09909	0.02914	0.12162	0.00304	0.06555	0.00076	0.03308	0.00083	**740**	**17**	792	28	753	14	658	16
20130811-06-81	1363	0.33	0.17815	0.00469	0.02416	0.00060	0.05347	0.00062	0.00710	0.00017	**154**	**4**	349	24	166	4	143	3
20130811-06-82	418	0.65	5.17024	0.12733	0.32749	0.00787	0.11451	0.00125	0.08778	0.00210	1826	38	**1872**	**19**	1848	21	1701	39
20130811-06-83	69	0.05	0.23648	0.01789	0.03275	0.00104	0.05237	0.00266	0.01028	0.00037	**208**	**6**	302	114	216	15	207	7
20130811-06-84	237	0.55	0.35804	0.00978	0.04938	0.00120	0.05259	0.00063	0.01471	0.00038	**311**	**7**	311	27	311	7	295	8
20130811-06-85	578	0.30	7.96624	0.20778	0.36769	0.00919	0.15715	0.00180	0.09016	0.00253	2019	43	**2425**	**21**	2227	24	1745	47

Table A1. (Continued)

Spot	U (ppm)	Th/U	U-Th-Pb ratios								Ages (Ma)							
			$^{207}Pb/^{235}U$	±1 s	$^{206}Pb/^{238}U$	±1 s	$^{207}Pb/^{206}Pb$	±1 s	$^{208}Pb/^{232}Th$	±1 s	$^{206}Pb/^{238}U$	±1 s	$^{207}Pb/^{206}Pb$	±1 s	$^{207}Pb/^{235}U$	±1 s	$^{208}Pb/^{232}Th$	±1 s
20130811-06-86	1001	0.17	4.86333	0.12660	0.22106	0.00550	0.15957	0.00183	0.03198	0.00094	1287	29	2451	20	1796	22	636	18
20130811-06-87	186	0.57	0.23118	0.00779	0.03368	0.00082	0.04979	0.00079	0.00992	0.00035	**214**	**5**	185	36	211	6	200	7
20130811-06-88	260	0.25	0.30034	0.01577	0.03917	0.00097	0.05560	0.00184	0.01221	0.00027	**248**	**6**	437	68	267	12	245	5
20130811-06-89	593	0.54	1.16539	0.03205	0.12446	0.00315	0.06792	0.00082	0.03296	0.00106	**756**	**18**	866	26	784	15	655	21
20130811-06-90	247	0.54	3.53068	0.10768	0.26258	0.00684	0.09755	0.00130	0.04755	0.00191	1503	35	**1578**	**24**	1534	24	939	37
20130811-06-91	428	0.23	6.45632	0.21255	0.35464	0.00970	0.13204	0.00179	0.10069	0.00274	1957	46	**2125**	**23**	2040	29	1939	50
20130811-06-92	622	0.47	5.66882	0.21428	0.26955	0.00715	0.15253	0.00270	0.07545	0.00194	1539	36	2374	31	1927	33	1470	36
20130811-06-93	383	0.42	0.27884	0.00810	0.03737	0.00092	0.05412	0.00069	0.01135	0.00032	**237**	**6**	376	26	250	6	228	6
20130811-06-94	458	0.61	0.21391	0.00675	0.02777	0.00072	0.05588	0.00078	0.00824	0.00023	**177**	**5**	448	31	197	6	166	5
20130811-06-95	535	0.81	0.24729	0.00656	0.03486	0.00085	0.05145	0.00060	0.01014	0.00025	**221**	**5**	261	25	224	5	204	5
20130811-06-96	664	1.37	0.17488	0.00521	0.02104	0.00054	0.06029	0.00079	0.00605	0.00017	**134**	**3**	614	29	164	5	122	3
20130811-06-97	56	1.11	0.31184	0.01215	0.04356	0.00114	0.05192	0.00100	0.01251	0.00033	**275**	**7**	282	43	276	9	251	7
20130811-06-98	309	0.62	0.33709	0.00942	0.04281	0.00107	0.05711	0.00070	0.01259	0.00032	**270**	**7**	496	29	295	7	253	6
20130811-06-99	744	0.63	0.27713	0.00795	0.03754	0.00096	0.05355	0.00067	0.01086	0.00031	**238**	**6**	352	28	248	6	218	6
20130811-06-100	657	0.62	0.25736	0.00844	0.02863	0.00075	0.06519	0.00096	0.00901	0.00036	**182**	**5**	780	30	233	7	181	7
20130811-06-101	352	0.79	0.23836	0.00748	0.03293	0.00085	0.05251	0.00073	0.00918	0.00028	**209**	**5**	308	32	217	6	185	6
20130811-06-102	285	1.82	0.13551	0.00422	0.01937	0.00049	0.05076	0.00070	0.00575	0.00016	**124**	**3**	230	31	129	4	116	3
Mean $^{206}Pb/^{238}U$ age = 15.5 ± 2.1 Ma (n = 4, MSWD = 1.7, N = 100)																		

Table A2. Zircon Hf isotopic data of the Northern Luzon Arc.

Spot	Inferred age (Ma)	±2 s	Hf isotopes													
			$^{176}Hf/^{177}Hf$	±2 s	$^{176}Lu/^{177}Hf$	±2 s	$^{176}Yb/^{177}Hf$	±2 s	$^{176}Hf/^{177}Hf$ (T)	$^{176}Hf/^{177}Hf$ CHUR(T)	$\varepsilon_{Hf}(0)$	$\varepsilon_{Hf}(T)$	±2 s	T_{DM} (Ma)	T_{DM}^{C} (Ma)	
Yuemei volcano-Shihtiping Formation																
20130811-06-01	159	8	0.282532	0.000046	0.001306	0.000056	0.055532	0.002200	0.282528	0.282673	-8.5	-5.1	1.6	1027	1535	
20130811-06-05	117	6	0.282790	0.000038	0.002156	0.000140	0.075665	0.004200	0.282785	0.282699	0.6	3.0	1.3	676	982	
20130811-06-07	2281	40	0.281596	0.000046	0.002515	0.000028	0.095659	0.002000	0.281487	0.281328	-41.6	5.7	1.6	2414	2484	
20130811-06-08	313	14	0.282232	0.000050	0.001096	0.000016	0.032973	0.000800	0.282226	0.282577	-19.1	-12.5	1.8	1442	2113	
20130811-06-11	261	12	0.282186	0.000038	0.001728	0.000035	0.059099	0.002200	0.282178	0.282610	-20.7	-15.3	1.3	1532	2253	
20130811-06-12	1992	40	0.281370	0.000029	0.000807	0.000011	0.033000	0.000880	0.281339	0.281514	-49.6	-6.2	1.0	2614	2991	
20130811-06-13	260	14	0.282991	0.000040	0.001081	0.000019	0.045376	0.000810	0.282986	0.282610	7.7	13.3	1.4	370	436	
20130811-06-14	2422	42	0.281557	0.000055	0.000884	0.000033	0.028851	0.000920	0.281516	0.281236	-43.0	9.9	2.0	2364	2329	
20130811-06-15	1867	38	0.281668	0.000064	0.000433	0.000037	0.017234	0.000930	0.281653	0.281594	-39.0	2.1	2.3	2187	2385	
20130811-06-19	181	8	0.282726	0.000029	0.001049	0.000014	0.042339	0.000620	0.282722	0.282660	-1.6	2.2	1.0	746	1083	
20130811-06-20	1870	38	0.281624	0.000046	0.001903	0.000095	0.072750	0.002600	0.281556	0.281592	-40.6	-1.3	1.6	2335	2595	
20130811-06-21	2399	36	0.281340	0.000067	0.001611	0.000054	0.056476	0.001900	0.281266	0.281251	-50.6	0.5	2.4	2711	2890	
20130811-06-23	804	38	0.282220	0.000087	0.001951	0.000064	0.063871	0.001100	0.282190	0.282270	-19.5	-2.8	3.1	1493	1877	
20130811-06-24	719	34	0.282436	0.000035	0.002222	0.000075	0.087347	0.001100	0.282406	0.282323	-11.9	2.9	1.2	1192	1450	

Table A2. (Continued)

Spot	Inferred age (Ma)	±2 s	Hf isotopes													
			$^{176}Hf/^{177}Hf$	±2 s	$^{176}Lu/^{177}Hf$	±2 s	$^{176}Yb/^{177}Hf$	±2 s	$^{176}Hf/^{177}Hf$ (T)	$^{176}Hf/^{177}Hf$ CHUR(T)	$\varepsilon_{Hf}(0)$	$\varepsilon_{Hf}(T)$	±2 s	T_{DM} (Ma)	T_{DM}^{C} (Ma)
20130811-06-26	14.0	2.0	0.283409	0.000046	0.001326	0.000034	0.033338	0.000490	0.283409	0.282763	22.5	22.8	1.6	-230	-373
20130811-06-27	1733	80	0.281630	0.000062	0.001043	0.000038	0.046097	0.003000	0.281596	0.281680	-40.4	-3.0	2.2	2274	2596
20130811-06-29	161	8	0.282819	0.000054	0.002371	0.000094	0.089367	0.003400	0.282812	0.282672	1.7	4.9	1.9	637	894
20130811-06-30	2013	38	0.281883	0.000033	0.001363	0.000072	0.048266	0.000930	0.281831	0.281501	-31.4	11.7	1.2	1941	1900
20130811-06-32	17.0	2.0	0.283421	0.000130	0.001025	0.000051	0.033547	0.001700	0.283421	0.282761	23.0	23.3	4.6	-246	-402
20130811-06-36	229	12	0.282906	0.000054	0.002318	0.000130	0.075761	0.002600	0.282896	0.282630	4.7	9.4	1.9	508	660
20130811-06-40	2560	40	0.281467	0.000052	0.000568	0.000014	0.020853	0.001200	0.281439	0.281147	-46.2	10.4	1.8	2467	2409
20130811-06-41	158	8	0.282810	0.000069	0.001231	0.000013	0.033982	0.000420	0.282806	0.282674	1.3	4.7	2.4	630	908
20130811-06-47	2497	40	0.281248	0.000044	0.000399	0.000007	0.017931	0.000290	0.281229	0.281188	-53.9	1.5	1.6	2750	2908
20130811-06-48	14.9	2.0	0.283650	0.000077	0.001143	0.000025	0.031396	0.000890	0.283650	0.282763	31.0	31.4	2.7	-578	-929
20130811-06-49	1729	40	0.281637	0.000044	0.001015	0.000030	0.042613	0.000380	0.281604	0.281683	-40.1	-2.8	1.6	2263	2581
20130811-06-50	174	8	0.282795	0.000061	0.003031	0.000160	0.098568	0.004300	0.282785	0.282664	0.8	4.3	2.2	685	946
20130811-06-51	1875	42	0.281697	0.000061	0.000795	0.000045	0.031218	0.000660	0.281669	0.281589	-38.0	2.8	2.2	2168	2345
20130811-06-53	963	42	0.282110	0.000075	0.000813	0.000034	0.031632	0.000850	0.282095	0.282170	-23.4	-2.6	2.7	1600	1987
20130811-06-55	2524	38	0.281404	0.000058	0.000827	0.000130	0.048378	0.007300	0.281364	0.281170	-48.4	6.9	2.1	2569	2596
20130811-06-56	484	22	0.282250	0.000056	0.000718	0.000030	0.024472	0.000610	0.282243	0.282471	-18.5	-8.0	2.0	1403	1964
20130811-06-61	167	8	0.282781	0.000051	0.001919	0.000220	0.063055	0.006000	0.282775	0.282668	0.3	3.8	1.8	684	973
20130811-06-62	231	10	0.282515	0.000051	0.003003	0.000110	0.107097	0.002200	0.282502	0.282629	-9.1	-4.5	1.8	1101	1547
20130811-06-64	2552	34	0.281303	0.000041	0.000938	0.000007	0.038454	0.000930	0.281257	0.281152	-51.9	3.7	1.5	2714	2811
20130811-06-71	164	8	0.282871	0.000069	0.001028	0.000032	0.032438	0.000600	0.282868	0.282670	3.5	7.0	2.4	540	765
20130811-06-74	172	8	0.282915	0.000021	0.001019	0.000018	0.036406	0.001100	0.282912	0.282665	5.1	8.7	0.7	478	661
20130811-06-79	112	6	0.282692	0.000039	0.005282	0.000060	0.192593	0.005700	0.282681	0.282703	-2.8	-0.8	1.4	895	1220
20130811-06-80	740	34	0.282468	0.000059	0.002718	0.000051	0.087486	0.001500	0.282430	0.282310	-10.8	4.3	2.1	1161	1382
20130811-06-83	208	12	0.282715	0.000029	0.000278	0.000011	0.008703	0.000360	0.282714	0.282643	-2.0	2.5	1.0	746	1085
20130811-06-84	311	14	0.282506	0.000049	0.001961	0.000039	0.067805	0.001200	0.282495	0.282579	-9.4	-3.0	1.7	1083	1513
20130811-06-85	2425	42	0.281471	0.000045	0.001089	0.000056	0.034222	0.001300	0.281421	0.281234	-46.0	6.6	1.6	2495	2536
20130811-06-96	134	6	0.282516	0.000041	0.003634	0.000092	0.122485	0.000960	0.282507	0.282689	-9.1	-6.4	1.5	1119	1598
20130811-06-97	275	14	0.282246	0.000046	0.002280	0.000120	0.073218	0.002600	0.282234	0.282601	-18.6	-13.0	1.6	1468	2117
20130811-06-102	124	6	0.282564	0.000048	0.001918	0.000028	0.073047	0.002100	0.282560	0.282695	-7.4	-4.8	1.7	998	1486
Chimei volcano-Shihmen Formation															
SM1-01	2365	60	0.281435	0.000026	0.000707	0.000029	0.034743	0.000783	0.281404	0.281273	-47.3	4.6	0.9	2518	2612
SM1-02	101	6	0.283138	0.000045	0.005048	0.000097	0.263335	0.005002	0.283129	0.282709	13.0	14.8	1.6	179	212
SM1-04	420	18	0.282816	0.000058	0.002613	0.000027	0.129321	0.002212	0.282795	0.282511	1.5	10.1	2.0	646	766
SM1-06	861	36	0.282429	0.000049	0.002430	0.000015	0.107215	0.000894	0.282390	0.282234	-12.1	5.5	1.7	1208	1395
SM1-08	110	6	0.282808	0.000070	0.002949	0.000058	0.139083	0.002914	0.282802	0.282704	1.3	3.5	2.5	664	950
Chimei volcano-Shihtiping Formation															
STP1-03	293	14	0.282561	0.000051	0.001501	0.000036	0.077920	0.001808	0.282553	0.282590	-7.5	-1.3	1.8	991	1394
STP1-04	147	10	0.282299	0.000078	0.001346	0.000057	0.062097	0.003232	0.282296	0.282681	-16.7	-13.6	2.8	1357	2062
STP1-06	787	34	0.282246	0.000081	0.003257	0.000060	0.134701	0.003279	0.282198	0.282281	-18.6	-2.9	2.9	1509	1871
Chimei volcano-Shihtiping Formation															
STPW-01	308	14	0.282778	0.000061	0.001396	0.000076	0.049095	0.003476	0.282770	0.282581	0.2	6.7	2.2	678	894

Table A2. (Continued)

Spot	Inferred age (Ma)	±2 s	Hf isotopes												
			$^{176}Hf/^{177}Hf$	±2 s	$^{176}Lu/^{177}Hf$	±2 s	$^{176}Yb/^{177}Hf$	±2 s	$^{176}Hf/^{177}Hf$ (T)	$^{176}Hf/^{177}Hf$ CHUR(T)	$\varepsilon_{Hf}(0)$	$\varepsilon_{Hf}(T)$	±2 s	T_{DM} (Ma)	T_{DM}^{C} (Ma)
STPW-02	4.5	0.6	0.283126	0.000044	0.000946	0.000015	0.043570	0.000754	0.283126	0.282769	12.5	12.6	1.5	177	281
STPW-03	4.3	1.0	0.283077	0.000046	0.001623	0.000055	0.071464	0.003834	0.283077	0.282769	10.8	10.9	1.6	251	392
STPW-04	310	14	0.282839	0.000066	0.002379	0.000044	0.087398	0.002256	0.282826	0.282579	2.4	8.7	2.4	607	767
STPW-05	311	14	0.282769	0.000071	0.002920	0.000039	0.110484	0.002235	0.282752	0.282579	-0.1	6.1	2.5	722	934
STPW-07	304	16	0.283090	0.000059	0.004105	0.000193	0.182053	0.008182	0.283066	0.282583	11.2	17.1	2.1	250	225
STPW-09	313	14	0.282945	0.000055	0.003818	0.000057	0.143605	0.003150	0.282922	0.282577	6.1	12.2	1.9	471	546
STPW-10	313	14	0.282994	0.000108	0.003948	0.000082	0.150855	0.004324	0.282971	0.282577	7.8	13.9	3.8	397	436
STPW-12	310	14	0.282962	0.000058	0.003529	0.000064	0.133411	0.002358	0.282941	0.282579	6.7	12.8	2.1	441	505
STPW-13	316	14	0.282936	0.000066	0.002463	0.000037	0.089707	0.001331	0.282922	0.282576	5.8	12.3	2.3	465	545
STPW-14	311	14	0.282922	0.000042	0.001512	0.000052	0.060701	0.001065	0.282913	0.282579	5.3	11.8	1.5	474	568
STPW-15	25.7	1.2	0.282755	0.000046	0.001414	0.000044	0.064244	0.000826	0.282755	0.282756	-0.6	0.0	1.6	712	1110
STPW-28	356	14	0.282960	0.000065	0.004327	0.000101	0.150390	0.004763	0.282931	0.282551	6.7	13.5	2.3	453	498
STPW-29	25.6	1.2	0.282668	0.000076	0.001322	0.000023	0.050604	0.001274	0.282667	0.282756	-3.7	-3.1	2.7	834	1307
STPW-30	314	12	0.282794	0.000116	0.003010	0.000060	0.094923	0.002072	0.282777	0.282577	0.8	7.1	4.1	685	876
STPW-32	317	14	0.282955	0.000072	0.002222	0.000023	0.073317	0.001254	0.282941	0.282575	6.5	13.0	2.6	436	500
STPW-34	314	14	0.283122	0.000080	0.002612	0.000037	0.090384	0.002199	0.283107	0.282577	12.4	18.8	2.8	191	126
STPW-36	323	16	0.282780	0.000075	0.002785	0.000055	0.093650	0.002163	0.282763	0.282571	0.3	6.8	2.6	702	900
STPW-37	319	14	0.282981	0.000081	0.004880	0.000060	0.166879	0.002775	0.282952	0.282574	7.4	13.4	2.9	428	475
STPW-44	220	10	0.282024	0.000050	0.000094	0.000003	0.003782	0.000114	0.282023	0.282635	-26.5	-21.7	1.8	1688	2623
STPW-45	323	16	0.283075	0.000101	0.006455	0.000050	0.223607	0.001232	0.283036	0.282571	10.7	16.4	3.6	293	282
STPW-46	339	20	0.282760	0.000097	0.004269	0.000095	0.133365	0.002126	0.282733	0.282561	-0.4	6.1	3.4	763	958
STPW-53	25.7	1.2	0.282732	0.000062	0.001766	0.000024	0.062144	0.001553	0.282731	0.282756	-1.4	-0.9	2.2	752	1162
STPW-57	325	16	0.282680	0.000118	0.003307	0.000060	0.105046	0.001552	0.282659	0.282570	-3.3	3.2	4.2	864	1133
STPW-59	316	14	0.283143	0.000104	0.002886	0.000075	0.097458	0.003451	0.283126	0.282576	13.1	19.5	3.7	162	82
STPW-70	326	14	0.282950	0.000042	0.003789	0.000051	0.129006	0.001993	0.282927	0.282569	6.3	12.6	1.5	462	528
STPW-75	324	14	0.282940	0.000048	0.001311	0.000042	0.053979	0.000600	0.282932	0.282571	5.9	12.8	1.7	446	517
STPW-77	284	16	0.282898	0.000064	0.002634	0.000150	0.102241	0.003932	0.282884	0.282595	4.5	10.2	2.3	524	651
Chimei volcano-Shihtiping Formation															
20130812-03-02	4.0	0.4	0.283189	0.000026	0.001343	0.000130	0.041735	0.003900	0.283189	0.282770	14.7	14.8	0.9	88	137
20130812-03-03	4.1	0.6	0.283160	0.000026	0.002068	0.000070	0.068036	0.002400	0.283160	0.282769	13.7	13.8	0.9	133	203
20130812-03-04	4.0	0.6	0.283209	0.000023	0.001886	0.000061	0.067549	0.002000	0.283209	0.282770	15.5	15.5	0.8	60	92
20130812-03-06	4.3	0.2	0.283218	0.000025	0.001515	0.000120	0.053980	0.005200	0.283218	0.282769	15.8	15.9	0.9	46	71
20130812-03-07	4.3	0.6	0.283143	0.000022	0.002389	0.000065	0.084988	0.004100	0.283143	0.282769	13.1	13.2	0.8	159	242
20130812-03-08	4.4	0.4	0.283228	0.000024	0.002424	0.000023	0.081995	0.001100	0.283228	0.282769	16.1	16.2	0.8	33	48
20130812-03-09	3.9	0.4	0.283136	0.000026	0.001771	0.000042	0.059159	0.002700	0.283136	0.282770	12.9	13.0	0.9	166	258
20130812-03-10	4.0	0.6	0.283212	0.000019	0.001405	0.000061	0.047277	0.003400	0.283212	0.282770	15.6	15.6	0.7	55	85
20130812-03-11	4.3	0.6	0.283221	0.000026	0.002310	0.000200	0.072533	0.004900	0.283221	0.282769	15.9	16.0	0.9	43	64
20130812-03-12	4.2	0.2	0.283143	0.000022	0.002196	0.000084	0.073762	0.004500	0.283143	0.282769	13.1	13.2	0.8	158	242
20130812-03-13	3.7	0.8	0.283269	0.000034	0.002467	0.000050	0.079705	0.001400	0.283269	0.282770	17.6	17.7	1.2	-28	-45
20130812-03-14	4.2	0.4	0.283305	0.000029	0.002285	0.000120	0.078004	0.005600	0.283305	0.282769	18.8	18.9	1.0	-82	-128
20130812-03-15	3.9	0.4	0.283052	0.000025	0.001376	0.000019	0.044043	0.001500	0.283052	0.282770	9.9	10.0	0.9	286	450

Table A2. (Continued)

Spot	Inferred age (Ma)	±2 s	Hf isotopes												
			$^{176}Hf/^{177}Hf$	±2 s	$^{176}Lu/^{177}Hf$	±2 s	$^{176}Yb/^{177}Hf$	±2 s	$^{176}Hf/^{177}Hf$ (T)	$^{176}Hf/^{177}Hf$ CHUR(T)	$\varepsilon_{Hf}(0)$	$\varepsilon_{Hf}(T)$	±2 s	T_{DM} (Ma)	T_{DM}^{C} (Ma)
20130812-03-16	4.2	0.4	0.283199	0.000031	0.001673	0.000025	0.064539	0.000590	0.283199	0.282769	15.1	15.2	1.1	74	114
20130812-03-17	4.1	0.4	0.283209	0.000034	0.001900	0.000012	0.062593	0.001500	0.283209	0.282769	15.5	15.5	1.2	60	92
20130812-03-18	4.1	0.4	0.283118	0.000022	0.002424	0.000130	0.081178	0.005200	0.283118	0.282769	12.2	12.3	0.8	196	299
Chengkuang'ao volcano-lava flow in Shihmen Formation															
SSCL-01	8.2	1.4	0.283269	0.000042	0.001820	0.000013	0.092266	0.000978	0.283269	0.282767	17.6	17.8	1.5	-28	-49
SSCL-02	8.8	1.0	0.283248	0.000066	0.004511	0.000087	0.184383	0.003301	0.283247	0.282767	16.8	17.0	2.3	4	2
SSCL-03	8.8	1.2	0.283308	0.000038	0.002344	0.000011	0.121680	0.000727	0.283307	0.282767	18.9	19.1	1.3	-86	-137
SSCL-04	2661	38	0.281169	0.000058	0.001267	0.000023	0.051285	0.000702	0.281105	0.281081	-56.7	0.8	2.0	2920	3072
SSCL-05	8.8	1.2	0.283311	0.000031	0.001414	0.000011	0.071176	0.000874	0.283311	0.282767	19.1	19.2	1.1	-88	-145
SSCL-06	807	34	0.281605	0.000099	0.002113	0.000039	0.076094	0.001944	0.281573	0.282268	-41.3	-24.6	3.5	2375	3239
SSCL-08	9.0	1.2	0.283231	0.000060	0.003206	0.000138	0.125074	0.003653	0.283230	0.282766	16.2	16.4	2.1	29	39
SSCL-09	698	30	0.282461	0.000046	0.002149	0.000104	0.092529	0.004257	0.282433	0.282337	-11.0	3.4	1.6	1153	1403
SSCL-10	10.0	1.4	0.283345	0.000034	0.001293	0.000022	0.065811	0.002237	0.283345	0.282766	20.3	20.5	1.2	-138	-224
SSCL-12	9.8	0.8	0.283261	0.000040	0.001237	0.000050	0.055461	0.000958	0.283260	0.282766	17.3	17.5	1.4	-15	-30
SSCL-13	9.2	0.8	0.283471	0.000077	0.002290	0.000061	0.074489	0.002349	0.283470	0.282766	24.7	24.9	2.7	-328	-511
SSCL-17	886	40	0.281588	0.000051	0.001733	0.000043	0.076477	0.002293	0.281559	0.282218	-41.9	-23.3	1.8	2374	3218
SSCL-21	322	16	0.281638	0.000068	0.001758	0.000058	0.073044	0.003022	0.281627	0.282572	-40.1	-33.4	2.4	2306	3429
Chengkuang'ao volcano-lava flow in Shihmen Formation															
TH1-01	8.0	2.0	0.283337	0.000043	0.002900	0.000024	0.115363	0.000680	0.283336	0.282767	20.0	20.1	1.5	-131	-203
TH1-02	8.1	1.0	0.283429	0.000045	0.002291	0.000105	0.099985	0.003772	0.283429	0.282767	23.3	23.4	1.6	-267	-416
TH1-03	8.0	1.8	0.283242	0.000030	0.001539	0.000061	0.074103	0.001481	0.283242	0.282767	16.6	16.8	1.1	12	14
TH1-04	8.0	2.0	0.283276	0.000025	0.001334	0.000012	0.074294	0.000832	0.283275	0.282767	17.8	18.0	0.9	-37	-63
TH1-05	7.9	0.8	0.283299	0.000024	0.001665	0.000060	0.084794	0.001726	0.283299	0.282767	18.6	18.8	0.9	-72	-117
TH1-07	7.9	2.0	0.283287	0.000043	0.000812	0.000019	0.045252	0.001181	0.283287	0.282767	18.2	18.4	1.5	-53	-90
TH1-08	6.4	1.4	0.283300	0.000051	0.001474	0.000034	0.059321	0.000906	0.283299	0.282768	18.7	18.8	1.8	-72	-117
TH1-09	7.3	1.2	0.283239	0.000038	0.001920	0.000064	0.084664	0.001345	0.283239	0.282767	16.5	16.7	1.4	16	20
TH1-10	8.0	2.0	0.283255	0.000029	0.001480	0.000042	0.075407	0.001265	0.283254	0.282767	17.1	17.2	1.0	-7	-15
TH1-11	8.3	1.0	0.283274	0.000024	0.001743	0.000009	0.095903	0.001168	0.283274	0.282767	17.8	17.9	0.9	-35	-60
TH1-12	8.1	1.6	0.283278	0.000038	0.001642	0.000069	0.069810	0.002270	0.283278	0.282767	17.9	18.1	1.3	-40	-68
TH1-13	8.1	1.4	0.283262	0.000023	0.001262	0.000008	0.062217	0.000232	0.283262	0.282767	17.3	17.5	0.8	-17	-32
TH1-14	8.6	1.4	0.283280	0.000024	0.001126	0.000034	0.054325	0.000953	0.283280	0.282767	18.0	18.1	0.9	-43	-73
TH1-15	8.0	1.6	0.283248	0.000022	0.001408	0.000026	0.071062	0.001602	0.283248	0.282767	16.8	17.0	0.8	3	0
TH1-17	8.0	1.0	0.283270	0.000026	0.001493	0.000042	0.071979	0.001344	0.283270	0.282767	17.6	17.8	0.9	-29	-51
TH1-18	8.3	1.0	0.283307	0.000024	0.001900	0.000029	0.094323	0.001433	0.283307	0.282767	18.9	19.1	0.9	-84	-136
TH1-19	8.1	1.2	0.283315	0.000037	0.002776	0.000030	0.113161	0.001671	0.283314	0.282767	19.2	19.3	1.3	-97	-152
TH1-20	8.3	1.2	0.283290	0.000025	0.001413	0.000015	0.068137	0.000792	0.283290	0.282767	18.3	18.5	0.9	-58	-96
TH1-21	8.3	1.6	0.283295	0.000027	0.001378	0.000017	0.064907	0.000438	0.283295	0.282767	18.5	18.7	1.0	-65	-108
TH1-22	7.4	1.2	0.283242	0.000034	0.001410	0.000050	0.059240	0.001524	0.283242	0.282767	16.6	16.8	1.2	12	14
TH1-23	7.3	1.6	0.283298	0.000021	0.001274	0.000024	0.059290	0.001359	0.283297	0.282767	18.6	18.7	0.7	-69	-113
TH1-24	7.9	1.0	0.283262	0.000020	0.001556	0.000043	0.076377	0.001672	0.283262	0.282767	17.3	17.5	0.7	-18	-32
TH1-25	8.1	0.8	0.283344	0.000018	0.001364	0.000017	0.067944	0.001401	0.283344	0.282767	20.2	20.4	0.7	-136	-221

Table A2. (Continued)

Spot	Inferred age (Ma)	±2 s	Hf isotopes												
			$^{176}Hf/^{177}Hf$	±2 s	$^{176}Lu/^{177}Hf$	±2 s	$^{176}Yb/^{177}Hf$	±2 s	$^{176}Hf/^{177}Hf$ (T)	$^{176}Hf/^{177}Hf$ CHUR(T)	$\varepsilon_{Hf}(0)$	$\varepsilon_{Hf}(T)$	±2 s	T_{DM} (Ma)	T_{DM}^{C} (Ma)
Chengkuang'ao volcano-volcanic breccia in Shihmen Formation															
TYB-01	8.1	1.6	0.283195	0.000026	0.001287	0.000020	0.062676	0.000895	0.283195	0.282767	15.0	15.1	0.9	79	120
TYB-02	8.0	2.0	0.283183	0.000031	0.000881	0.000033	0.044152	0.001540	0.283183	0.282767	14.5	14.7	1.1	95	148
TYB-03	8.0	1.0	0.283203	0.000039	0.001821	0.000012	0.090980	0.000515	0.283203	0.282767	15.2	15.4	1.4	69	103
TYB-04	8.2	1.0	0.283237	0.000032	0.001611	0.000008	0.081159	0.000379	0.283237	0.282767	16.4	16.6	1.1	19	25
TYB-05	8.8	1.2	0.283261	0.000031	0.000941	0.000004	0.044668	0.000127	0.283261	0.282767	17.3	17.5	1.1	-16	-31
TYB-06	7.3	1.0	0.283281	0.000030	0.001920	0.000009	0.097088	0.000888	0.283281	0.282767	18.0	18.2	1.0	-46	-76
TYB-07	9.0	2.0	0.283276	0.000039	0.000943	0.000005	0.050120	0.000299	0.283276	0.282766	17.8	18.0	1.4	-37	-65
TYB-08	7.9	1.0	0.283258	0.000030	0.001500	0.000020	0.075604	0.000408	0.283258	0.282767	17.2	17.3	1.1	-11	-23
TYB-09	9.0	1.6	0.283207	0.000039	0.001496	0.000017	0.078195	0.000155	0.283207	0.282766	15.4	15.6	1.4	62	93
TYB-10	7.8	1.0	0.283193	0.000037	0.000870	0.000007	0.041107	0.000625	0.283193	0.282767	14.9	15.1	1.3	81	125
TYB-11	8.6	2.0	0.283220	0.000036	0.001260	0.000020	0.061174	0.000550	0.283220	0.282767	15.8	16.0	1.3	44	64
TYB-12	8.6	1.4	0.283310	0.000039	0.000941	0.000002	0.048820	0.000271	0.283310	0.282767	19.0	19.2	1.4	-86	-142
TYB-13	8.0	1.0	0.283183	0.000050	0.002263	0.000123	0.100873	0.003157	0.283182	0.282767	14.5	14.7	1.8	100	150
TYB-14	7.9	0.6	0.283339	0.000039	0.002844	0.000033	0.161626	0.001002	0.283338	0.282767	20.0	20.2	1.4	-134	-207
TYB-15	7.0	1.4	0.283260	0.000033	0.000904	0.000012	0.049717	0.000424	0.283260	0.282768	17.3	17.4	1.2	-14	-27
TYB-16	7.6	0.6	0.283226	0.000034	0.001842	0.000011	0.097287	0.001427	0.283225	0.282767	16.0	16.2	1.2	36	52
TYB-17	8.6	1.0	0.283237	0.000054	0.001382	0.000023	0.070288	0.001309	0.283237	0.282767	16.4	16.6	1.9	19	25
TYB-18	7.5	1.2	0.283291	0.000053	0.001197	0.000009	0.058232	0.000474	0.283290	0.282767	18.3	18.5	1.9	-58	-97
TYB-19	7.9	1.2	0.283153	0.000040	0.001510	0.000042	0.063605	0.001189	0.283152	0.282767	13.5	13.6	1.4	141	218
TYB-20	7.9	1.6	0.283313	0.000045	0.001597	0.000010	0.088645	0.000323	0.283313	0.282767	19.1	19.3	1.6	-92	-150
TYB-21	7.9	1.0	0.283247	0.000039	0.001035	0.000009	0.052769	0.000579	0.283246	0.282767	16.8	16.9	1.4	5	3
TYB-22	8.2	1.0	0.283206	0.000037	0.001718	0.000021	0.085447	0.000462	0.283206	0.282767	15.3	15.5	1.3	64	96
TYB-23	8.3	1.2	0.283209	0.000047	0.000636	0.000009	0.031267	0.000787	0.283209	0.282767	15.5	15.6	1.6	58	88
TYB-24	7.5	1.2	0.283203	0.000048	0.002095	0.000049	0.081991	0.002049	0.283203	0.282767	15.3	15.4	1.7	69	102
Chengkuang'ao volcano-volcanic breccia in Shihmen Formation															
SM2-01	6.7	1.4	0.283264	0.000024	0.001094	0.000034	0.053028	0.001446	0.283263	0.282768	17.4	17.5	0.8	-20	-35
SM2-02	7.0	1.2	0.283281	0.000031	0.001691	0.000073	0.077115	0.001901	0.283281	0.282768	18.0	18.2	1.1	-46	-75
SM2-03	6.8	1.6	0.283224	0.000024	0.001397	0.000003	0.071269	0.000196	0.283224	0.282768	16.0	16.1	0.9	37	55
SM2-05	7.3	0.6	0.283233	0.000025	0.002300	0.000022	0.123732	0.001898	0.283233	0.282767	16.3	16.5	0.9	25	34
SM2-06	7.0	0.6	0.283211	0.000028	0.003078	0.000051	0.166090	0.001802	0.283210	0.282768	15.5	15.7	1.0	60	86
SM2-07	8.0	2.0	0.283215	0.000025	0.000835	0.000037	0.036638	0.000937	0.283215	0.282767	15.7	15.8	0.9	50	76
SM2-08	6.8	0.8	0.283303	0.000052	0.002019	0.000052	0.095562	0.002305	0.283303	0.282768	18.8	18.9	1.8	-78	-125
SM2-10	7.8	1.2	0.283188	0.000060	0.002738	0.000073	0.109487	0.004065	0.283187	0.282767	14.7	14.9	2.1	93	138
SM2-11	7.3	1.0	0.283189	0.000030	0.001672	0.000032	0.074011	0.000657	0.283189	0.282767	14.7	14.9	1.1	89	135
SM2-13	7.0	0.6	0.283273	0.000031	0.002923	0.000083	0.134101	0.001745	0.283273	0.282768	17.7	17.9	1.1	-35	-57
SM2-14	6.6	0.6	0.283210	0.000020	0.001596	0.000006	0.076459	0.000672	0.283210	0.282768	15.5	15.6	0.7	57	87
SM2-15	7.2	0.6	0.283275	0.000030	0.002384	0.000041	0.101195	0.002681	0.283274	0.282768	17.8	17.9	1.0	-36	-60
SM2-17	7.3	0.8	0.283213	0.000020	0.002291	0.000023	0.106680	0.000887	0.283213	0.282767	15.6	15.7	0.7	55	80
SM2-18	7.2	0.8	0.283223	0.000023	0.002936	0.000073	0.135111	0.001424	0.283223	0.282768	16.0	16.1	0.8	40	57
SM2-19	7.0	1.0	0.283216	0.000019	0.001609	0.000005	0.071953	0.000267	0.283216	0.282768	15.7	15.8	0.7	49	74

Table A2. (Continued)

Spot	Inferred age (Ma)	±2 s	Hf isotopes												
			$^{176}Hf/^{177}Hf$	±2 s	$^{176}Lu/^{177}Hf$	±2 s	$^{176}Yb/^{177}Hf$	±2 s	$^{176}Hf/^{177}Hf$ (T)	$^{176}Hf/^{177}Hf$ CHUR(T)	$\varepsilon_{Hf}(0)$	$\varepsilon_{Hf}(T)$	±2 s	T_{DM} (Ma)	T_{DM}^{C} (Ma)
SM2-24	6.6	1.0	0.283241	0.000045	0.003936	0.000132	0.152055	0.003994	0.283241	0.282768	16.6	16.7	1.6	14	17
SM2-28	6.6	1.0	0.283323	0.000037	0.002408	0.000079	0.103429	0.002535	0.283323	0.282768	19.5	19.6	1.3	-109	-172
SM2-29	7.4	1.2	0.283230	0.000023	0.001816	0.000015	0.081728	0.001289	0.283230	0.282767	16.2	16.3	0.8	30	42
SM2-31	6.6	0.8	0.283271	0.000021	0.002130	0.000016	0.106779	0.001426	0.283270	0.282768	17.6	17.8	0.8	-31	-51
SM2-32	7.3	1.2	0.283239	0.000024	0.001846	0.000018	0.091807	0.000347	0.283239	0.282767	16.5	16.7	0.8	16	20
Chengkuang'ao volcano-Shihtiping Formation															
TYW-01	7.4	1.0	0.283334	0.000035	0.001568	0.000017	0.077440	0.000698	0.283334	0.282767	19.9	20.0	1.2	-122	-197
TYW-02	7.5	0.6	0.283263	0.000040	0.001570	0.000011	0.079501	0.000545	0.283263	0.282767	17.4	17.5	1.4	-19	-34
TYW-03	8.7	1.0	0.283320	0.000032	0.002104	0.000044	0.106320	0.002143	0.283320	0.282767	19.4	19.6	1.1	-103	-165
TYW-04	8.8	1.4	0.283218	0.000028	0.001290	0.000035	0.063799	0.001707	0.283218	0.282767	15.8	16.0	1.0	46	68
TYW-05	7.0	2.0	0.283211	0.000032	0.001220	0.000013	0.055068	0.000450	0.283211	0.282768	15.5	15.7	1.1	56	85
TYW-06	6.9	1.0	0.283249	0.000030	0.001336	0.000005	0.063156	0.000250	0.283248	0.282768	16.9	17.0	1.1	2	-1
TYW-07	7.9	1.2	0.283216	0.000031	0.000595	0.000007	0.029253	0.000528	0.283216	0.282767	15.7	15.9	1.1	49	74
TYW-08	7.5	0.6	0.283280	0.000034	0.002178	0.000047	0.112126	0.003071	0.283280	0.282767	18.0	18.1	1.2	-44	-73
TYW-09	8.2	1.0	0.283242	0.000030	0.001373	0.000010	0.067914	0.000367	0.283242	0.282767	16.6	16.8	1.1	11	13
TYW-10	7.8	1.2	0.283266	0.000037	0.001277	0.000043	0.061736	0.001868	0.283265	0.282767	17.5	17.6	1.3	-22	-40
TYW-11	7.8	1.0	0.283248	0.000030	0.001071	0.000019	0.054153	0.000724	0.283248	0.282767	16.8	17.0	1.1	3	0
TYW-12	8.1	1.0	0.283287	0.000034	0.001152	0.000015	0.055780	0.001273	0.283286	0.282767	18.2	18.4	1.2	-53	-89
TYW-13	7.7	1.2	0.283269	0.000041	0.001317	0.000006	0.065626	0.000780	0.283269	0.282767	17.6	17.7	1.4	-27	-48
TYW-14	8.4	1.6	0.283265	0.000048	0.000847	0.000003	0.040324	0.000163	0.283265	0.282767	17.4	17.6	1.7	-21	-40
TYW-15	7.4	1.0	0.283245	0.000032	0.001481	0.000021	0.068946	0.001298	0.283245	0.282767	16.7	16.9	1.1	7	7
TYW-16	7.7	0.6	0.283262	0.000034	0.002261	0.000015	0.106777	0.000370	0.283262	0.282767	17.3	17.5	1.2	-18	-32
TYW-17	7.0	2.0	0.283233	0.000026	0.000791	0.000014	0.034767	0.000608	0.283233	0.282768	16.3	16.4	0.9	24	35
TYW-18	8.4	1.0	0.283297	0.000027	0.001906	0.000012	0.085237	0.000372	0.283297	0.282767	18.6	18.7	1.0	-69	-113
TYW-19	7.4	1.0	0.283202	0.000031	0.000857	0.000005	0.036797	0.000190	0.283202	0.282767	15.2	15.4	1.1	69	106
TYW-20	8.2	0.8	0.283227	0.000022	0.001490	0.000037	0.063002	0.001406	0.283226	0.282767	16.1	16.3	0.8	34	49
TYW-21	7.8	1.0	0.283216	0.000032	0.001442	0.000023	0.059921	0.001076	0.283215	0.282767	15.7	15.9	1.1	50	74
TYW-22	7.6	1.2	0.283288	0.000038	0.001238	0.000025	0.052150	0.000720	0.283288	0.282767	18.2	18.4	1.4	-55	-91
TYW-23	7.7	1.0	0.283216	0.000053	0.001871	0.000086	0.069263	0.002455	0.283216	0.282767	15.7	15.9	1.9	50	73
TYW-24	7.9	1.2	0.283241	0.000029	0.000863	0.000002	0.036637	0.000214	0.283241	0.282767	16.6	16.8	1.0	13	16
Chengkuang'ao volcano-Shihtiping Formation															
THCW-01	5.9	0.8	0.283132	0.000031	0.001357	0.000010	0.066132	0.000445	0.283132	0.282768	12.7	12.9	1.1	171	267
THCW-02	7.0	2.0	0.283226	0.000037	0.001573	0.000017	0.082762	0.001065	0.283226	0.282768	16.1	16.2	1.3	34	50
THCW-03	6.7	0.6	0.283107	0.000031	0.001260	0.000006	0.061994	0.000169	0.283107	0.282768	11.8	12.0	1.1	206	323
THCW-04	6.3	0.2	0.283149	0.000039	0.002334	0.000047	0.102398	0.000783	0.283149	0.282768	13.3	13.5	1.4	149	227
THCW-05	7.0	1.6	0.283130	0.000032	0.000821	0.000014	0.039056	0.000444	0.283130	0.282768	12.7	12.8	1.1	171	270
THCW-06	6.4	0.6	0.283160	0.000022	0.001678	0.000013	0.079648	0.000691	0.283160	0.282768	13.7	13.8	0.8	132	203
THCW-07	6.8	0.6	0.283069	0.000027	0.001123	0.000021	0.047681	0.000248	0.283068	0.282768	10.5	10.6	0.9	260	410
THCW-08	6.5	0.6	0.283172	0.000028	0.001403	0.000028	0.069912	0.002020	0.283172	0.282768	14.1	14.3	1.0	113	174
THCW-09	6.9	0.6	0.283197	0.000024	0.001566	0.000018	0.078432	0.001336	0.283197	0.282768	15.0	15.2	0.9	77	117
THCW-10	6.4	0.6	0.283104	0.000049	0.001914	0.000044	0.074467	0.000889	0.283104	0.282768	11.7	11.9	1.7	214	330

Table A2. (Continued)

Spot	Inferred age (Ma)	±2 s	Hf isotopes												
			$^{176}Hf/^{177}Hf$	±2 s	$^{176}Lu/^{177}Hf$	±2 s	$^{176}Yb/^{177}Hf$	±2 s	$^{176}Hf/^{177}Hf$ (T)	$^{176}Hf/^{177}Hf$ CHUR(T)	$\varepsilon_{Hf}(0)$	$\varepsilon_{Hf}(T)$	±2 s	T_{DM} (Ma)	T_{DM}^{C} (Ma)
THCW-11	6.4	0.6	0.283188	0.000031	0.001345	0.000008	0.057188	0.000705	0.283188	0.282768	14.7	14.8	1.1	89	138
THCW-12	6.0	1.2	0.283158	0.000024	0.001284	0.000015	0.056435	0.000887	0.283158	0.282768	13.7	13.8	0.8	132	206
THCW-13	5.3	1.2	0.283120	0.000029	0.001093	0.000020	0.044958	0.000388	0.283120	0.282769	12.3	12.4	1.0	186	294
THCW-14	6.6	1.6	0.283099	0.000046	0.001228	0.000039	0.043313	0.001434	0.283099	0.282768	11.6	11.7	1.6	217	341
THCW-15	6.5	0.8	0.283132	0.000025	0.001259	0.000016	0.053618	0.000352	0.283132	0.282768	12.7	12.9	0.9	169	265
THCW-16	6.7	0.6	0.283020	0.000050	0.001185	0.000038	0.043565	0.001969	0.283020	0.282768	8.8	8.9	1.8	330	521
THCW-17	6.8	0.6	0.283117	0.000029	0.001134	0.000023	0.047583	0.001067	0.283117	0.282768	12.2	12.3	1.0	191	300
THCW-18	6.7	0.8	0.283101	0.000022	0.001086	0.000010	0.041689	0.000285	0.283100	0.282768	11.6	11.8	0.8	214	337
THCW-19	6.9	0.6	0.283192	0.000027	0.001113	0.000010	0.048564	0.000867	0.283192	0.282768	14.9	15.0	1.0	83	128
THCW-20	6.1	1.0	0.283173	0.000021	0.001094	0.000018	0.046127	0.000966	0.283172	0.282768	14.2	14.3	0.7	111	173
THCW-21	6.7	0.4	0.283058	0.000044	0.001529	0.000056	0.054861	0.001431	0.283057	0.282768	10.1	10.2	1.6	279	435
THCW-22	6.2	0.8	0.283141	0.000048	0.001672	0.000035	0.061224	0.001359	0.283141	0.282768	13.1	13.2	1.7	158	245
THCW-23	6.5	0.6	0.283098	0.000053	0.002002	0.000064	0.075394	0.002097	0.283097	0.282768	11.5	11.6	1.9	224	345
THCW-24	6.3	0.8	0.283127	0.000050	0.001261	0.000044	0.049051	0.001206	0.283127	0.282768	12.6	12.7	1.8	177	277
Chengkuang'ao volcano-Shihtiping Formation															
STP2-01	6.0	1.6	0.283311	0.000023	0.001130	0.000045	0.058076	0.002990	0.283311	0.282768	19.1	19.2	0.8	-87	-143
STP2-02	7.4	0.6	0.283262	0.000065	0.002861	0.000025	0.109269	0.001539	0.283261	0.282767	17.3	17.5	2.3	-18	-31
STP2-03	8.1	0.8	0.283377	0.000026	0.002302	0.000016	0.129006	0.001064	0.283377	0.282767	21.4	21.6	0.9	-189	-296
STP2-04	8.2	1.8	0.283276	0.000022	0.001308	0.000009	0.068302	0.000356	0.283275	0.282767	17.8	18.0	0.8	-37	-63
STP2-05	9.2	1.2	0.283368	0.000030	0.001551	0.000044	0.074506	0.000585	0.283368	0.282766	21.1	21.3	1.1	-172	-276
STP2-06	9.0	2.0	0.283308	0.000028	0.000815	0.000031	0.039838	0.001014	0.283308	0.282766	19.0	19.2	1.0	-83	-139
STP2-07	430	18	0.282657	0.000073	0.002319	0.000068	0.119911	0.001475	0.282639	0.282504	-4.1	4.8	2.6	873	1112
STP2-13	7.9	1.8	0.283353	0.000053	0.001300	0.000047	0.051357	0.002213	0.283353	0.282767	20.6	20.7	1.9	-150	-242
STP2-14	7.0	1.2	0.283272	0.000031	0.002184	0.000100	0.101431	0.002387	0.283272	0.282768	17.7	17.8	1.1	-33	-55
STP2-15	7.7	1.2	0.283262	0.000024	0.001592	0.000002	0.083736	0.000472	0.283262	0.282767	17.3	17.5	0.8	-17	-31
STP2-16	11.0	2.0	0.283253	0.000038	0.001651	0.000038	0.069056	0.001649	0.283253	0.282765	17.0	17.3	1.3	-5	-14
STP2-19	7.9	1.2	0.283291	0.000055	0.002768	0.000104	0.116943	0.002627	0.283291	0.282767	18.4	18.5	1.9	-62	-99
STP2-23	8.1	1.6	0.283204	0.000028	0.001379	0.000049	0.065141	0.001419	0.283204	0.282767	15.3	15.5	1.0	66	99
STP2-24	7.8	0.8	0.283276	0.000072	0.001487	0.000079	0.058207	0.003481	0.283276	0.282767	17.8	18.0	2.5	-38	-65
STP2-25	8.3	1.0	0.283274	0.000034	0.002925	0.000106	0.134123	0.002557	0.283274	0.282767	17.8	17.9	1.2	-36	-60
STP2-26	7.9	0.8	0.283391	0.000028	0.001630	0.000098	0.082010	0.005653	0.283390	0.282767	21.9	22.0	1.0	-205	-327
STP2-37	9.1	1.4	0.283316	0.000055	0.002259	0.000056	0.098083	0.001242	0.283316	0.282766	19.2	19.4	1.9	-98	-156
STP2-38	8.1	1.0	0.283304	0.000025	0.001655	0.000021	0.078062	0.001483	0.283303	0.282767	18.8	19.0	0.9	-78	-127
Tuluanshan volcano-Shihtiping Formation															
CLCW-01	8.4	1.0	0.283339	0.000026	0.001088	0.000016	0.054481	0.000929	0.283339	0.282767	20.1	20.2	0.9	-128	-209
CLCW-02	8.6	1.0	0.283280	0.000040	0.001439	0.000007	0.073010	0.000307	0.283279	0.282767	17.9	18.1	1.4	-43	-73
CLCW-03	8.7	1.2	0.283304	0.000043	0.001580	0.000006	0.079397	0.000344	0.283304	0.282767	18.8	19.0	1.5	-79	-129
CLCW-04	8.7	1.2	0.283294	0.000027	0.001465	0.000010	0.073011	0.000362	0.283294	0.282767	18.5	18.7	1.0	-64	-107
CLCW-05	8.4	1.0	0.283355	0.000032	0.000829	0.000002	0.041281	0.000412	0.283355	0.282767	20.6	20.8	1.1	-150	-246
CLCW-06	7.7	1.6	0.283317	0.000033	0.001018	0.000005	0.049550	0.000357	0.283317	0.282767	19.3	19.5	1.2	-97	-159
CLCW-07	8.0	2.0	0.283359	0.000029	0.001337	0.000019	0.065868	0.000642	0.283359	0.282767	20.8	20.9	1.0	-158	-255

Table A2. (Continued)

Spot	Inferred age (Ma)	±2 s	Hf isotopes													
			$^{176}Hf/^{177}Hf$	±2 s	$^{176}Lu/^{177}Hf$	±2 s	$^{176}Yb/^{177}Hf$	±2 s	$^{176}Hf/^{177}Hf$ (T)	$^{176}Hf/^{177}Hf$ CHUR(T)	$\varepsilon_{Hf}(0)$	$\varepsilon_{Hf}(T)$	±2 s	T_{DM} (Ma)	T_{DM}^{C} (Ma)
CLCW-08	8.8	1.0	0.283339	0.000032	0.001354	0.000020	0.065711	0.000686	0.283339	0.282767	20.0	20.2	1.1	-129	-209
CLCW-09	8.8	1.4	0.283298	0.000031	0.000894	0.000006	0.044011	0.000243	0.283298	0.282767	18.6	18.8	1.1	-69	-116
CLCW-10	8.5	1.6	0.283248	0.000030	0.000901	0.000002	0.044574	0.000358	0.283248	0.282767	16.9	17.0	1.1	2	-2
CLCW-11	7.5	1.0	0.283378	0.000031	0.000905	0.000013	0.043581	0.000479	0.283378	0.282767	21.4	21.6	1.1	-184	-299
CLCW-12	8.6	1.8	0.283245	0.000048	0.001499	0.000009	0.072867	0.000218	0.283245	0.282767	16.7	16.9	1.7	7	7
CLCW-13	7.9	1.0	0.283341	0.000074	0.001937	0.000024	0.094739	0.001485	0.283341	0.282767	20.1	20.3	2.6	-134	-213
CLCW-14	8.0	0.6	0.283324	0.000039	0.001111	0.000007	0.052714	0.000287	0.283324	0.282767	19.5	19.7	1.4	-107	-175
CLCW-15	8.9	1.0	0.283339	0.000039	0.001197	0.000003	0.059852	0.000641	0.283339	0.282766	20.1	20.2	1.4	-128	-209
CLCW-16	8.4	1.0	0.283306	0.000044	0.001446	0.000015	0.072656	0.000993	0.283306	0.282767	18.9	19.1	1.6	-82	-134
CLCW-17	8.6	1.0	0.283249	0.000043	0.001230	0.000018	0.059747	0.000268	0.283249	0.282767	16.9	17.1	1.5	1	-3
CLCW-18	8.4	1.2	0.283313	0.000048	0.000966	0.000009	0.043838	0.000296	0.283313	0.282767	19.1	19.3	1.7	-91	-150
CLCW-19C	8.6	1.2	0.283337	0.000040	0.001142	0.000015	0.051030	0.000664	0.283337	0.282767	20.0	20.2	1.4	-125	-204
CLCW-20	9.3	1.2	0.283294	0.000043	0.001396	0.000004	0.064527	0.000569	0.283294	0.282766	18.5	18.7	1.5	-64	-106
CLCW-22	8.6	1.0	0.283291	0.000035	0.001570	0.000007	0.070274	0.000321	0.283291	0.282767	18.3	18.5	1.2	-59	-98
CLCW-23	9.8	1.6	0.283336	0.000029	0.000943	0.000020	0.042398	0.000872	0.283335	0.282766	19.9	20.1	1.0	-122	-202
CLCW-24	10.0	1.6	0.283283	0.000027	0.000893	0.000002	0.037965	0.000125	0.283283	0.282766	18.1	18.3	1.0	-47	-81
Lutao-Huoshaoshan andesite															
LTA01-06	1.1	0.4	0.283211	0.000084	0.002406	0.000079	0.093175	0.003476	0.283211	0.282771	15.5	15.6	3.0	57	88
LTA01-21	1.3	0.4	0.283160	0.000035	0.001679	0.000090	0.074439	0.002617	0.283160	0.282771	13.7	13.8	1.2	131	204
LTA01-24	1.5	0.4	0.282918	0.000046	0.001552	0.000043	0.066232	0.000833	0.282918	0.282771	5.2	5.2	1.6	480	755
LTA01-26	1.2	0.2	0.283183	0.000029	0.001695	0.000014	0.071810	0.000554	0.283183	0.282771	14.5	14.6	1.0	97	152
LTA01-27	1.1	0.2	0.283022	0.000033	0.001252	0.000019	0.059079	0.001556	0.283022	0.282771	8.8	8.9	1.2	328	519
LTA01-36	1.2	0.2	0.283045	0.000041	0.001693	0.000060	0.078457	0.001360	0.283045	0.282771	9.6	9.7	1.4	299	468
Lutao-Ameishan volcanic breccia															
LTA02-10	1.4	0.4	0.283210	0.000080	0.001570	0.000033	0.053851	0.001187	0.283210	0.282771	15.5	15.5	2.8	58	90
LTA02-14	1.7	0.2	0.282991	0.000025	0.001421	0.000042	0.067881	0.001241	0.282991	0.282771	7.7	7.8	0.9	374	591
LTA02-15	1.5	0.2	0.283161	0.000060	0.003636	0.000162	0.161364	0.007086	0.283161	0.282771	13.8	13.8	2.1	136	202
LTA02-16	1.3	0.2	0.283006	0.000052	0.004763	0.000124	0.221013	0.003878	0.283006	0.282771	8.3	8.3	1.9	387	556
LTA02-19	1.4	0.2	0.283057	0.000036	0.002963	0.000055	0.159171	0.001070	0.283056	0.282771	10.1	10.1	1.3	292	441
LTA02-20	2456	38	0.281328	0.000045	0.001517	0.000026	0.066751	0.000965	0.281257	0.281214	-51.1	1.5	1.6	2721	2873
LTA02-21	2.4	0.2	0.283084	0.000053	0.003295	0.000102	0.144199	0.002797	0.283084	0.282771	11.0	11.1	1.9	253	378
LTA02-22	1.4	0.2	0.283051	0.000034	0.001953	0.000055	0.104876	0.003373	0.283051	0.282771	9.9	9.9	1.2	292	454
LTA02-23	2134	42	0.281403	0.000021	0.000753	0.000016	0.045461	0.000690	0.281373	0.281423	-48.4	-1.8	0.8	2565	2827
LTA02-24	1.4	0.2	0.283056	0.000033	0.005356	0.000009	0.284469	0.000832	0.283056	0.282771	10.0	10.1	1.2	314	442
Lutao-Ameishan volcanic breccia															
LTA03-01	2103	48	0.281352	0.000026	0.000942	0.000041	0.050170	0.001052	0.281315	0.281443	-50.2	-4.5	0.9	2647	2974
LTA03-06	1.7	0.2	0.283058	0.000071	0.005042	0.000038	0.216301	0.002228	0.283058	0.282771	10.1	10.2	2.5	307	437
LTA03-10	1867	38	0.281579	0.000057	0.000787	0.000004	0.036190	0.000307	0.281551	0.281594	-42.2	-1.5	2.0	2328	2608
LTA03-13	96	4	0.282799	0.000057	0.002114	0.000025	0.099869	0.001329	0.282795	0.282712	1.0	2.9	2.0	661	973
LTA03-17	1.2	0.4	0.282982	0.000032	0.000763	0.000011	0.037762	0.000694	0.282982	0.282771	7.4	7.5	1.1	380	610
LTA03-18	1.7	0.4	0.282931	0.000024	0.001209	0.000008	0.064183	0.001116	0.282931	0.282771	5.6	5.7	0.9	458	726

Table A2. (Continued)

Spot	Inferred age (Ma)	±2 s	Hf isotopes												
			$^{176}Hf/^{177}Hf$	±2 s	$^{176}Lu/^{177}Hf$	±2 s	$^{176}Yb/^{177}Hf$	±2 s	$^{176}Hf/^{177}Hf$ (T)	$^{176}Hf/^{177}Hf$ CHUR(T)	$\varepsilon_{Hf}(0)$	$\varepsilon_{Hf}(T)$	±2 s	T_{DM} (Ma)	T_{DM}^{C} (Ma)
LTA03-19	1.4	0.2	0.282984	0.000034	0.001108	0.000016	0.060764	0.001074	0.282984	0.282771	7.5	7.5	1.2	381	606
Lutao-Kungkuan andesite															
LTA04-07	1.4	0.2	0.283043	0.000033	0.002994	0.000089	0.116412	0.002728	0.283043	0.282771	9.6	9.6	1.2	313	472
LTA04-08	1.0	0.4	0.282981	0.000038	0.000737	0.000014	0.026713	0.000474	0.282981	0.282771	7.4	7.4	1.4	381	613
LTA04-10	1.4	0.2	0.283110	0.000066	0.005177	0.000106	0.205051	0.003472	0.283110	0.282771	12.0	12.0	2.3	225	319
LTA04-11	1.2	0.2	0.283160	0.000045	0.003510	0.000058	0.136562	0.002733	0.283160	0.282771	13.7	13.7	1.6	138	205
LTA04-13	1.4	0.2	0.283132	0.000049	0.004671	0.000171	0.189012	0.003844	0.283132	0.282771	12.7	12.8	1.7	187	269
LTA04-14	1.2	0.2	0.283041	0.000034	0.003123	0.000125	0.128077	0.003261	0.283041	0.282771	9.5	9.5	1.2	317	477
LTA04-16	1.2	0.2	0.283233	0.000078	0.004216	0.000058	0.157943	0.003015	0.283233	0.282771	16.3	16.3	2.8	27	39
LTA04-17	1.3	0.2	0.283142	0.000034	0.004521	0.000168	0.187778	0.004944	0.283142	0.282771	13.1	13.1	1.2	171	247
LTA04-19	1.2	0.2	0.283053	0.000039	0.003196	0.000109	0.135003	0.002850	0.283053	0.282771	9.9	9.9	1.4	299	450
LTA04-20	1.4	0.2	0.282981	0.000020	0.000854	0.000029	0.035382	0.001247	0.282981	0.282771	7.4	7.4	0.7	382	612
LTA04-22	1.2	0.2	0.283039	0.000031	0.003342	0.000135	0.139130	0.003415	0.283039	0.282771	9.5	9.5	1.1	321	480
LTA04-23	1.7	0.2	0.282951	0.000044	0.002596	0.000111	0.098992	0.003152	0.282951	0.282771	6.3	6.4	1.6	446	681
LTA04-24	1.2	0.2	0.283071	0.000027	0.002945	0.000089	0.128610	0.001755	0.283070	0.282771	10.6	10.6	1.0	270	409
LTA04-25	1.1	0.2	0.283009	0.000026	0.001824	0.000015	0.083138	0.000952	0.283009	0.282771	8.4	8.4	0.9	351	548
LTA04-26	1.2	0.2	0.283032	0.000020	0.002737	0.000012	0.124018	0.000647	0.283032	0.282771	9.2	9.2	0.7	327	498
LTA04-27	1.1	0.2	0.283122	0.000041	0.003429	0.000134	0.140655	0.003224	0.283122	0.282771	12.4	12.4	1.4	196	292
LTA04-28	1.2	0.2	0.283055	0.000022	0.002167	0.000008	0.113159	0.001179	0.283055	0.282771	10.0	10.0	0.8	288	445
LTA04-29	1.2	0.2	0.282969	0.000029	0.001249	0.000040	0.066136	0.002026	0.282969	0.282771	7.0	7.0	1.0	403	639
LTA04-30	1.2	0.2	0.283022	0.000028	0.002316	0.000023	0.114898	0.001070	0.283022	0.282771	8.8	8.9	1.0	337	519
Lutao-Kungkuan andesite															
LTA05-03	1.2	0.2	0.283136	0.000058	0.004683	0.000026	0.174515	0.002184	0.283136	0.282771	12.9	12.9	2.1	180	259
LTA05-07	1.3	0.2	0.283023	0.000037	0.002160	0.000068	0.091365	0.001426	0.283023	0.282771	8.9	8.9	1.3	334	516
LTA05-17	1.3	0.2	0.282956	0.000022	0.001146	0.000015	0.057417	0.000854	0.282956	0.282771	6.5	6.5	0.8	421	669
LTA05-22	1.3	0.2	0.283238	0.000084	0.004123	0.000034	0.160297	0.002450	0.283238	0.282771	16.5	16.5	3.0	19	27
LTA05-34	1.5	0.2	0.283261	0.000065	0.004540	0.000059	0.168367	0.001824	0.283260	0.282771	17.3	17.3	2.3	-17	-25
LTA05-35	1.6	0.2	0.283128	0.000072	0.004301	0.000035	0.155847	0.001635	0.283128	0.282771	12.6	12.6	2.5	192	279
LTA05-38	1.3	0.2	0.282962	0.000025	0.001372	0.000003	0.066154	0.000458	0.282962	0.282771	6.7	6.8	0.9	415	655
LTA05-39	1.2	0.2	0.283065	0.000038	0.001123	0.000037	0.043229	0.001092	0.283065	0.282771	10.4	10.4	1.3	266	422
LTA05-40	1.4	0.2	0.283048	0.000026	0.001945	0.000030	0.097430	0.001677	0.283048	0.282771	9.8	9.8	0.9	296	460
LTA05-41	1.2	0.2	0.283005	0.000031	0.002680	0.000015	0.129079	0.001369	0.283005	0.282771	8.2	8.3	1.1	366	558
LTA05-42	1.7	0.4	0.282940	0.000028	0.000768	0.000002	0.033705	0.000317	0.282940	0.282771	6.0	6.0	1.0	439	705
LTA05-43	1.5	0.2	0.283087	0.000032	0.004097	0.000019	0.221690	0.002373	0.283086	0.282771	11.1	11.2	1.1	255	373
Lutao-Kungkuan andesite															
LTA06-04	1.4	0.2	0.283022	0.000027	0.000958	0.000028	0.042368	0.000937	0.283022	0.282771	8.8	8.9	1.0	325	519
LTA06-05	1.1	0.2	0.283201	0.000054	0.005057	0.000168	0.205311	0.006944	0.283201	0.282771	15.2	15.2	1.9	78	111
LTA06-06	1.2	0.2	0.283054	0.000028	0.002198	0.000035	0.100746	0.001521	0.283054	0.282771	10.0	10.0	1.0	289	446
LTA06-08	1.3	0.2	0.283172	0.000027	0.003274	0.000022	0.164466	0.001453	0.283172	0.282771	14.1	14.2	1.0	119	178
LTA06-09	1.4	0.2	0.283186	0.000078	0.004138	0.000095	0.166151	0.003515	0.283186	0.282771	14.6	14.7	2.8	101	147
LTA06-20	1.2	0.2	0.283173	0.000054	0.003009	0.000046	0.114671	0.001456	0.283173	0.282771	14.2	14.2	1.9	117	176

Table A2. (Continued)

Spot	Inferred age (Ma)	±2 s	Hf isotopes												
			$^{176}Hf/^{177}Hf$	±2 s	$^{176}Lu/^{177}Hf$	±2 s	$^{176}Yb/^{177}Hf$	±2 s	$^{176}Hf/^{177}Hf$ (T)	$^{176}Hf/^{177}Hf$ CHUR(T)	$\varepsilon_{Hf}(0)$	$\varepsilon_{Hf}(T)$	±2 s	T_{DM} (Ma)	T_{DM}^{C} (Ma)
LTA06-21	1.2	0.2	0.283240	0.000034	0.004138	0.000087	0.173737	0.001264	0.283240	0.282771	16.6	16.6	1.2	15	22
LTA06-23	1.2	0.2	0.283275	0.000059	0.005192	0.000046	0.179736	0.002297	0.283274	0.282771	17.8	17.8	2.1	-40	-57
Lutao-Niutzushan volcanic breccia															
LTA07-04	2416	42	0.281374	0.000063	0.001571	0.000025	0.064992	0.001056	0.281302	0.281240	-49.4	2.2	2.2	2661	2801
LTA07-08	1.2	0.2	0.283240	0.000068	0.004273	0.000050	0.181366	0.003730	0.283240	0.282771	16.6	16.6	2.4	15	22
LTA07-10	2322	34	0.281482	0.000038	0.000292	0.000017	0.013139	0.000699	0.281469	0.281301	-45.6	6.0	1.3	2429	2497
LTA07-15	1.2	0.2	0.283258	0.000063	0.003874	0.000108	0.162039	0.003611	0.283258	0.282771	17.2	17.2	2.2	-13	-19
LTA07-19	1.0	0.2	0.283070	0.000027	0.001338	0.000029	0.061604	0.000759	0.283070	0.282771	10.5	10.6	1.0	259	410
LTA07-20	1.4	0.2	0.283148	0.000059	0.002264	0.000051	0.096395	0.001729	0.283147	0.282771	13.3	13.3	2.1	152	233
LTA07-21	1.1	0.2	0.283043	0.000031	0.001720	0.000086	0.072170	0.002229	0.283043	0.282771	9.6	9.6	1.1	301	472
LTA07-30	2631	46	0.281389	0.000060	0.001281	0.000026	0.049767	0.001400	0.281325	0.281100	-48.9	8.0	2.1	2620	2613
LTA07-33	1.1	0.2	0.283081	0.000043	0.002334	0.000084	0.095804	0.003497	0.283081	0.282771	10.9	11.0	1.5	250	384
LTA07-34	1.5	0.2	0.283092	0.000054	0.003168	0.000138	0.130446	0.004993	0.283092	0.282771	11.3	11.4	1.9	239	360
LTA07-35	1.5	0.2	0.282994	0.000027	0.001946	0.000091	0.080816	0.001836	0.282994	0.282771	7.9	7.9	1.0	375	583
LTA07-38	1.2	0.2	0.283119	0.000041	0.004276	0.000252	0.193383	0.008689	0.283119	0.282771	12.3	12.3	1.4	205	298
LTA07-39	2703	38	0.281270	0.000036	0.001003	0.000027	0.043159	0.001197	0.281218	0.281054	-53.1	5.9	1.3	2763	2799
LTA07-40	1.3	0.2	0.282998	0.000023	0.001633	0.000032	0.084633	0.002012	0.282998	0.282771	8.0	8.0	0.8	365	573
LTA07-41	1.3	0.2	0.282990	0.000025	0.002790	0.000052	0.128608	0.002649	0.282989	0.282771	7.7	7.7	0.9	390	593
LTA07-42	1.2	0.2	0.282954	0.000033	0.001534	0.000130	0.067804	0.004624	0.282954	0.282771	6.4	6.5	1.2	428	674
LTA07-44	1.5	0.2	0.283088	0.000019	0.002679	0.000038	0.158771	0.002256	0.283087	0.282771	11.2	11.2	0.7	243	370
LTA07-45	1.1	0.2	0.283237	0.000022	0.003150	0.000037	0.156217	0.000821	0.283237	0.282771	16.5	16.5	0.8	19	28
Lutao-beach sand															
LTS01-02	1.1	0.2	0.283198	0.000040	0.003263	0.000074	0.123652	0.002310	0.283198	0.282771	15.1	15.1	1.4	79	118
LTS01-04	1.2	0.2	0.283140	0.000064	0.002313	0.000067	0.081853	0.002254	0.283140	0.282771	13.0	13.0	2.3	163	251
LTS01-05	1.1	0.2	0.283072	0.000040	0.002026	0.000045	0.077240	0.001666	0.283072	0.282771	10.6	10.6	1.4	262	407
LTS01-15	1.2	0.2	0.283282	0.000073	0.002782	0.000072	0.100374	0.003551	0.283282	0.282771	18.1	18.1	2.6	-49	-75
LTS01-19	1.0	0.2	0.282961	0.000036	0.001586	0.000058	0.065089	0.001449	0.282961	0.282771	6.7	6.7	1.3	419	659
LTS01-20	1.5	0.2	0.283102	0.000058	0.001971	0.000014	0.076668	0.001016	0.283101	0.282771	11.7	11.7	2.0	218	338
LTS01-21	1.3	0.2	0.283126	0.000053	0.003009	0.000041	0.103550	0.001044	0.283126	0.282771	12.5	12.5	1.9	187	283
LTS01-22	1.4	0.2	0.283017	0.000039	0.002426	0.000059	0.099558	0.001216	0.283017	0.282771	8.6	8.7	1.4	346	532
LTS01-23	1.1	0.2	0.282909	0.000022	0.001746	0.000007	0.076194	0.000586	0.282909	0.282771	4.8	4.9	0.8	496	776
LTS01-27	1.1	0.2	0.282996	0.000034	0.001424	0.000069	0.055405	0.002031	0.282996	0.282771	7.9	7.9	1.2	367	579
LTS01-30	1.2	0.2	0.283088	0.000059	0.002756	0.000085	0.106448	0.004328	0.283088	0.282771	11.2	11.2	2.1	242	368
LTS01-32	1.1	0.4	0.283120	0.000093	0.001725	0.000021	0.058986	0.000962	0.283120	0.282771	12.3	12.3	3.3	190	297
LTS01-36	1.2	0.2	0.282919	0.000029	0.001201	0.000035	0.051229	0.000950	0.282919	0.282771	5.2	5.2	1.0	474	753
LTS01-37	1.3	0.2	0.283098	0.000034	0.001554	0.000040	0.062051	0.000660	0.283098	0.282771	11.5	11.6	1.2	220	345
LTS01-39	1.1	0.2	0.283047	0.000044	0.002607	0.000112	0.101498	0.003580	0.283047	0.282771	9.7	9.7	1.6	303	463
LTS01-40	0.8	0.2	0.282946	0.000028	0.001614	0.000031	0.063633	0.000562	0.282946	0.282772	6.2	6.2	1.0	441	693
LTS01-42	1.2	0.2	0.282927	0.000025	0.000964	0.000022	0.040229	0.001234	0.282927	0.282771	5.5	5.5	0.9	460	734
LTS01-44	1.2	0.2	0.282972	0.000028	0.002098	0.000055	0.097638	0.002998	0.282972	0.282771	7.1	7.1	1.0	409	634
LTS01-45	1.2	0.2	0.282956	0.000065	0.001985	0.000065	0.071280	0.001841	0.282956	0.282771	6.5	6.5	2.3	431	671

Table A2. (Continued)

Spot	Inferred age (Ma)	±2 s	Hf isotopes												
			$^{176}Hf/^{177}Hf$	±2 s	$^{176}Lu/^{177}Hf$	±2 s	$^{176}Yb/^{177}Hf$	±2 s	$^{176}Hf/^{177}Hf$ (T)	$^{176}Hf/^{177}Hf$ CHUR(T)	$\varepsilon_{Hf}(0)$	$\varepsilon_{Hf}(T)$	±2 s	T_{DM} (Ma)	T_{DM}^{C} (Ma)
LTS01-47	1.2	0.2	0.282972	0.000023	0.001519	0.000008	0.062913	0.000524	0.282972	0.282771	7.1	7.1	0.8	402	632
LTS01-48	1.9	0.6	0.283049	0.000026	0.001640	0.000076	0.070168	0.002160	0.283049	0.282771	9.8	9.8	0.9	292	458
LTS01-49	1.3	0.2	0.283169	0.000045	0.002709	0.000064	0.105405	0.001641	0.283169	0.282771	14.0	14.1	1.6	122	185
LTS01-52	1.4	0.2	0.282945	0.000021	0.000790	0.000018	0.039120	0.000823	0.282945	0.282771	6.1	6.1	0.8	433	695
LTS01-53	1.4	0.2	0.283048	0.000021	0.001657	0.000031	0.083320	0.001817	0.283048	0.282771	9.8	9.8	0.7	293	460
LTS01-54	1.2	0.2	0.282986	0.000021	0.001042	0.000019	0.053933	0.001165	0.282986	0.282771	7.6	7.6	0.7	378	602
LTS01-55	1.5	0.2	0.282992	0.000023	0.002301	0.000015	0.111751	0.000494	0.282992	0.282771	7.8	7.8	0.8	381	587
LTS01-56	1.1	0.2	0.283237	0.000031	0.003148	0.000062	0.161341	0.004792	0.283237	0.282771	16.4	16.5	1.1	20	30
LTS01-57	0.8	0.2	0.283025	0.000023	0.001824	0.000053	0.093391	0.003033	0.283025	0.282772	9.0	9.0	0.8	328	512
LTS01-58	1.3	0.2	0.283068	0.000028	0.001190	0.000107	0.061250	0.006252	0.283068	0.282771	10.5	10.5	1.0	262	415
Lutao-river sand															
LTS02-01	195	10	0.282830	0.000021	0.001057	0.000030	0.048477	0.001475	0.282826	0.282651	2.0	6.2	0.7	599	840
LTS02-02	227	10	0.282347	0.000022	0.000816	0.000008	0.044901	0.000303	0.282343	0.282631	-15.0	-10.2	0.8	1272	1905
LTS02-04	1.0	0.2	0.282945	0.000020	0.001015	0.000008	0.051054	0.000160	0.282944	0.282771	6.1	6.1	0.7	436	696
LTS02-05	1.4	0.4	0.282912	0.000021	0.000646	0.000008	0.031960	0.000380	0.282912	0.282771	4.9	5.0	0.7	478	770
LTS02-07	1.4	0.2	0.282950	0.000024	0.000890	0.000002	0.040203	0.000194	0.282950	0.282771	6.3	6.3	0.9	427	684
LTS02-09	127	6	0.282682	0.000028	0.003020	0.000033	0.163491	0.002212	0.282675	0.282693	-3.2	-0.7	1.0	853	1225
LTS02-11	2423	40	0.281381	0.000027	0.000828	0.000057	0.039088	0.002523	0.281343	0.281236	-49.2	3.8	1.0	2600	2708
LTS02-14	3.4	0.8	0.283097	0.000029	0.002758	0.000016	0.139283	0.001475	0.283097	0.282770	11.5	11.6	1.0	229	348
LTS02-15	768	32	0.282174	0.000025	0.002042	0.000077	0.114157	0.003933	0.282145	0.282293	-21.1	-5.2	0.9	1562	2002
LTS02-16	266	10	0.282488	0.000029	0.001502	0.000059	0.078144	0.001530	0.282481	0.282607	-10.0	-4.5	1.0	1094	1572
LTS02-17	250	10	0.282599	0.000029	0.001788	0.000066	0.105650	0.004626	0.282591	0.282617	-6.1	-0.9	1.0	944	1336
LTS02-22	248	10	0.282435	0.000032	0.001689	0.000055	0.090610	0.001530	0.282428	0.282618	-11.9	-6.7	1.1	1176	1703
LTS02-26	1.2	0.2	0.283016	0.000032	0.002513	0.000047	0.135251	0.002342	0.283016	0.282771	8.6	8.7	1.1	348	533
LTS02-27	1.0	0.2	0.282920	0.000033	0.000800	0.000019	0.040246	0.000445	0.282920	0.282771	5.2	5.3	1.2	467	750
Lutao-river sand															
LTS03-01	1.0	0.4	0.283062	0.000026	0.001973	0.000050	0.088534	0.001391	0.283062	0.282771	10.3	10.3	0.9	276	429
LTS03-08	1.3	0.2	0.282918	0.000086	0.001580	0.000033	0.054187	0.001179	0.282918	0.282771	5.2	5.2	3.1	481	756
LTS03-14	1.2	0.2	0.283084	0.000074	0.003565	0.000076	0.134146	0.004110	0.283084	0.282771	11.0	11.1	2.6	255	379
LTS03-20	1.2	0.2	0.283083	0.000027	0.002393	0.000083	0.116250	0.002067	0.283082	0.282771	11.0	11.0	1.0	249	382
LTS03-21	1.4	0.2	0.283135	0.000070	0.003565	0.000108	0.150443	0.003529	0.283135	0.282771	12.8	12.9	2.5	176	262
LTS03-23	1.2	0.2	0.283099	0.000039	0.002500	0.000078	0.112728	0.001953	0.283099	0.282771	11.5	11.6	1.4	225	345
LTS03-26	1.4	0.4	0.283146	0.000045	0.003462	0.000043	0.150134	0.001642	0.283146	0.282771	13.2	13.3	1.6	159	237
LTS03-27	1.3	0.2	0.283025	0.000044	0.001836	0.000054	0.084900	0.001620	0.283025	0.282771	9.0	9.0	1.6	328	512
LTS03-28	1.2	0.2	0.283084	0.000027	0.002947	0.000024	0.160918	0.000947	0.283084	0.282771	11.0	11.1	0.9	250	379
Lanyu-Shuangshihyen volcanic breccia															
LYA01-03	2504	34	0.281449	0.000060	0.002363	0.000090	0.103773	0.003553	0.281336	0.281183	-46.8	5.4	2.1	2612	2671
LYA01-05	2.5	0.2	0.283132	0.000030	0.001580	0.000019	0.072488	0.001301	0.283132	0.282770	12.7	12.8	1.0	171	268
LYA01-06	190	8	0.283195	0.000045	0.002745	0.000152	0.231362	0.006702	0.283185	0.282654	15.0	18.8	1.6	82	26
LYA01-07	96	4	0.282887	0.000020	0.000505	0.000002	0.029860	0.000094	0.282886	0.282712	4.1	6.1	0.7	511	768
LYA01-08	2.5	0.4	0.283133	0.000027	0.002573	0.000011	0.133044	0.000889	0.283133	0.282770	12.8	12.8	0.9	174	265

Table A2. (Continued)

Spot	Inferred age (Ma)	±2 s	Hf isotopes													
			$^{176}Hf/^{177}Hf$	±2 s	$^{176}Lu/^{177}Hf$	±2 s	$^{176}Yb/^{177}Hf$	±2 s	$^{176}Hf/^{177}Hf$ (T)	$^{176}Hf/^{177}Hf$ CHUR(T)	$\varepsilon_{Hf}(0)$	$\varepsilon_{Hf}(T)$	±2 s	T_{DM} (Ma)	T_{DM}^{C} (Ma)
Lanyu-Tungching andesite																
LYA02-01	2480	30	0.281268	0.000041	0.000687	0.000024	0.031241	0.000686	0.281235	0.281199	-53.2	1.3	1.5	2744	2905
LYA02-03	7.2	1.0	0.283314	0.000042	0.001783	0.000041	0.075210	0.001760	0.283314	0.282768	19.2	19.3	1.5	-94	-150
LYA02-04	2303	46	0.281461	0.000048	0.000893	0.000047	0.046806	0.002438	0.281422	0.281313	-46.4	3.9	1.7	2496	2612
LYA02-06	2468	42	0.281462	0.000041	0.002192	0.000080	0.114329	0.002831	0.281359	0.281206	-46.3	5.4	1.4	2582	2644
LYA02-07	61	4	0.283272	0.000029	0.003128	0.000036	0.157653	0.003027	0.283269	0.282734	17.7	18.9	1.0	-34	-82
LYA02-08	2435	32	0.281350	0.000019	0.000486	0.000017	0.026880	0.001548	0.281327	0.281228	-50.3	3.5	0.7	2620	2734
LYA02-09	2378	32	0.281343	0.000080	0.001788	0.000016	0.084606	0.001110	0.281262	0.281265	-50.5	-0.1	2.8	2719	2912
LYA02-10	2512	34	0.281361	0.000051	0.000809	0.000011	0.036832	0.000542	0.281322	0.281178	-49.9	5.1	1.8	2626	2695
LYA02-11	56	4	0.283060	0.000080	0.001635	0.000014	0.077756	0.001200	0.283059	0.282737	10.2	11.4	2.8	275	401
LYA02-12	2186	34	0.281425	0.000067	0.002212	0.000010	0.102055	0.001114	0.281333	0.281389	-47.6	-2.0	2.4	2635	2880
LYA02-13	2483	38	0.281417	0.000025	0.000735	0.000016	0.042104	0.001095	0.281382	0.281197	-47.9	6.6	0.9	2545	2583
LYA02-14	610	24	0.281385	0.000021	0.000645	0.000010	0.041019	0.001237	0.281377	0.282392	-49.1	-35.9	0.7	2583	3793
LYA02-15	2041	48	0.281454	0.000020	0.001249	0.000022	0.076717	0.000605	0.281405	0.281482	-46.6	-2.7	0.7	2529	2816
LYA02-16	2416	42	0.281439	0.000024	0.001236	0.000023	0.073457	0.001414	0.281382	0.281240	-47.1	5.0	0.9	2548	2626
LYA02-17	2223	84	0.281549	0.000039	0.001338	0.000028	0.082241	0.002906	0.281493	0.281365	-43.2	4.5	1.4	2403	2508
LYA02-18	14.8	1.2	0.283328	0.000032	0.002540	0.000118	0.120677	0.003607	0.283327	0.282763	19.7	20.0	1.1	-116	-186
LYA02-19	2263	38	0.281420	0.000024	0.000946	0.000011	0.051817	0.000735	0.281379	0.281339	-47.8	1.4	0.9	2555	2731
Lanyu-Lungtouyen volcanic breccia															
LYA03-06	2.3	0.4	0.283119	0.000046	0.001973	0.000057	0.088678	0.001277	0.283119	0.282771	12.3	12.3	1.6	192	297
LYA03-07	134	6	0.282680	0.000057	0.003033	0.000040	0.151885	0.002419	0.282673	0.282689	-3.2	-0.6	2.0	856	1225
Lanyu-Mantoushan andesite															
LYA04-03	130	6	0.282896	0.000109	0.008739	0.000201	0.327705	0.006136	0.282874	0.282691	4.4	6.5	3.9	636	772
LYA04-04	147	6	0.282427	0.000071	0.004027	0.000160	0.178015	0.004621	0.282416	0.282681	-12.2	-9.4	2.5	1268	1793
LYA04-05	155	6	0.282747	0.000055	0.002713	0.000052	0.123537	0.003819	0.282740	0.282676	-0.9	2.3	2.0	749	1061
LYA04-07	146	6	0.283346	0.000088	0.010799	0.000234	0.531592	0.015673	0.283317	0.282681	20.3	22.5	3.1	-187	-246
LYA04-08	2.7	0.2	0.283530	0.000105	0.010129	0.000308	0.491473	0.015756	0.283530	0.282770	26.8	26.9	3.7	-534	-646
LYA04-09	2090	66	0.281569	0.000048	0.000607	0.000008	0.026713	0.000313	0.281545	0.281451	-42.6	3.3	1.7	2331	2480
LYA04-10	140	10	0.282482	0.000041	0.005165	0.000217	0.241695	0.005973	0.282469	0.282685	-10.2	-7.7	1.5	1223	1679
LYA04-12	2.9	0.2	0.283663	0.000084	0.016058	0.000251	0.724013	0.011584	0.283662	0.282770	31.5	31.5	3.0	-999	-953
LYA04-13	2.6	0.2	0.283521	0.000066	0.008829	0.000248	0.415207	0.007320	0.283521	0.282770	26.5	26.5	2.3	-494	-624
LYA04-14	2529	38	0.281378	0.000026	0.000821	0.000020	0.044712	0.000335	0.281338	0.281167	-49.3	6.1	0.9	2604	2650
LYA04-15	2459	42	0.281366	0.000037	0.001169	0.000016	0.056484	0.000863	0.281311	0.281212	-49.7	3.5	1.3	2644	2753
LYA04-16	106	4	0.282670	0.000026	0.001821	0.000045	0.112772	0.001091	0.282666	0.282706	-3.6	-1.4	0.9	843	1258
LYA04-17	152	8	0.282515	0.000036	0.002253	0.000054	0.130064	0.004246	0.282509	0.282678	-9.1	-6.0	1.3	1078	1582
LYA04-18	2486	34	0.281368	0.000020	0.000636	0.000002	0.037689	0.000445	0.281338	0.281195	-49.6	5.1	0.7	2605	2677
Lanyu-Shuangshihyen volcanic breccia															
LYA05-02	2272	36	0.281536	0.000104	0.003953	0.000027	0.169392	0.002060	0.281365	0.281333	-43.7	1.1	3.7	2601	2756
LYA05-07	2111	34	0.281699	0.000044	0.002376	0.000026	0.111756	0.000953	0.281603	0.281437	-38.0	5.9	1.6	2258	2338
LYA05-11	2073	36	0.281491	0.000031	0.001029	0.000056	0.060328	0.001901	0.281450	0.281462	-45.3	-0.4	1.1	2464	2698
LYA05-12	1964	40	0.282041	0.000059	0.007154	0.000282	0.323887	0.013353	0.281774	0.281532	-25.8	8.6	2.1	2033	2056

Table A2. (Continued)

Spot	Inferred age (Ma)	±2 s	Hf isotopes												
			$^{176}Hf/^{177}Hf$	±2 s	$^{176}Lu/^{177}Hf$	±2 s	$^{176}Yb/^{177}Hf$	±2 s	$^{176}Hf/^{177}Hf$ (T)	$^{176}Hf/^{177}Hf$ CHUR(T)	$\varepsilon_{Hf}(0)$	$\varepsilon_{Hf}(T)$	±2 s	T_{DM} (Ma)	T_{DM}^{C} (Ma)
LYA05-15	1917	36	0.281546	0.000077	0.003776	0.000028	0.145942	0.001137	0.281408	0.281562	-43.4	-5.5	2.7	2573	2888
LYA05-16	1931	38	0.281674	0.000067	0.002226	0.000054	0.094357	0.002350	0.281592	0.281553	-38.8	1.4	2.4	2284	2477
LYA05-17	2178	38	0.281710	0.000060	0.001920	0.000059	0.083670	0.002183	0.281631	0.281394	-37.5	8.4	2.1	2214	2234
LYA05-20	2820	36	0.281034	0.000046	0.001602	0.000029	0.066610	0.001849	0.280947	0.280977	-61.5	-1.1	1.6	3132	3311
LYA05-22	1963	40	0.281597	0.000063	0.002108	0.000050	0.095371	0.003412	0.281518	0.281533	-41.6	-0.5	2.2	2386	2619
LYA05-24	2366	34	0.281767	0.000081	0.004533	0.000078	0.189334	0.004022	0.281562	0.281273	-35.5	10.3	2.9	2296	2264
LYA05-25	152	8	0.282885	0.000081	0.007680	0.000129	0.356262	0.009258	0.282863	0.282678	4.0	6.6	2.8	633	784
LYA05-26	147	10	0.282825	0.000084	0.005417	0.000172	0.233273	0.008989	0.282810	0.282681	1.9	4.6	3.0	686	906
LYA05-28	1966	34	0.281534	0.000063	0.003106	0.000045	0.129865	0.002197	0.281418	0.281531	-43.8	-4.0	2.3	2543	2837
LYA05-32	3197	32	0.280960	0.000059	0.002325	0.000037	0.102589	0.002419	0.280817	0.280730	-64.1	3.1	2.1	3296	3350
LYA05-33	2065	32	0.282001	0.000082	0.004250	0.000032	0.206549	0.002831	0.281834	0.281467	-27.3	13.0	2.9	1923	1858
Lanyu-River sand															
LYS01-01	2.3	0.4	0.283336	0.000072	0.003603	0.000054	0.124875	0.002449	0.283336	0.282771	20.0	20.0	2.5	-133	-199
LYS01-03	2.4	0.4	0.283072	0.000023	0.001523	0.000019	0.066944	0.001120	0.283072	0.282771	10.6	10.7	0.8	258	405
LYS01-04	2.1	0.6	0.283113	0.000024	0.001596	0.000023	0.069118	0.001215	0.283113	0.282771	12.1	12.1	0.9	199	311
LYS01-05	2.7	0.2	0.283219	0.000068	0.006133	0.000083	0.217964	0.002985	0.283219	0.282770	15.8	15.9	2.4	51	70
LYS01-06	2.8	0.6	0.283139	0.000031	0.001670	0.000060	0.069492	0.001515	0.283139	0.282770	13.0	13.1	1.1	161	251
LYS01-07	2.4	0.2	0.283211	0.000059	0.003691	0.000110	0.151925	0.003805	0.283211	0.282771	15.5	15.6	2.1	60	88
LYS01-08	2.6	0.2	0.283114	0.000046	0.003442	0.000069	0.128034	0.001750	0.283114	0.282770	12.1	12.2	1.6	207	309
LYS01-09	2.6	0.4	0.283105	0.000057	0.002307	0.000054	0.088969	0.001925	0.283105	0.282770	11.8	11.8	2.0	215	330
LYS01-10	2.7	0.4	0.283160	0.000045	0.002565	0.000088	0.100483	0.002326	0.283160	0.282770	13.7	13.8	1.6	134	204
LYS01-11	2.8	0.4	0.283077	0.000022	0.002136	0.000013	0.094970	0.000895	0.283077	0.282770	10.8	10.9	0.8	254	393
LYS01-12	2.4	0.6	0.283057	0.000022	0.001878	0.000010	0.086604	0.000638	0.283057	0.282771	10.1	10.1	0.8	283	440
LYS01-13	2.1	0.6	0.283046	0.000024	0.002107	0.000023	0.096846	0.000476	0.283046	0.282771	9.7	9.7	0.9	300	464
LYS01-15	2.6	0.2	0.283282	0.000030	0.006214	0.000053	0.296716	0.001079	0.283282	0.282770	18.0	18.1	1.1	-53	-74
LYS01-16	2.7	0.6	0.283024	0.000026	0.001470	0.000017	0.069951	0.001385	0.283024	0.282770	8.9	9.0	0.9	327	514
LYS01-17	2219	38	0.281526	0.000023	0.001161	0.000015	0.058460	0.001513	0.281477	0.281368	-44.1	3.9	0.8	2424	2545
LYS01-18	2.3	0.2	0.283074	0.000044	0.002406	0.000048	0.099708	0.001353	0.283074	0.282771	10.7	10.7	1.6	261	400
LYS01-19	2.4	0.2	0.283243	0.000029	0.002290	0.000049	0.109848	0.001741	0.283243	0.282771	16.7	16.7	1.0	11	15
LYS01-20	2.9	0.2	0.283261	0.000043	0.004633	0.000025	0.208554	0.003752	0.283261	0.282770	17.3	17.4	1.5	-18	-27
LYS01-21	2.9	0.2	0.283371	0.000091	0.004575	0.000099	0.189680	0.002693	0.283371	0.282770	21.2	21.3	3.2	-193	-280
LYS01-22	2.4	0.6	0.282983	0.000021	0.001442	0.000026	0.069707	0.000740	0.282983	0.282771	7.5	7.5	0.7	386	608
LYS01-23	2.4	0.4	0.283047	0.000023	0.001690	0.000011	0.078926	0.000212	0.283047	0.282771	9.7	9.8	0.8	295	462
LYS01-24	2.4	0.4	0.283094	0.000041	0.002425	0.000072	0.099465	0.001995	0.283093	0.282771	11.4	11.4	1.4	232	356
LYS01-25	3.2	0.2	0.283141	0.000028	0.002893	0.000069	0.143330	0.002155	0.283141	0.282770	13.1	13.1	1.0	164	247
LYS01-26	2.4	0.2	0.283275	0.000109	0.009340	0.000077	0.369351	0.005194	0.283274	0.282771	17.8	17.8	3.8	-45	-57
LYS01-27	2.9	0.2	0.283279	0.000039	0.003744	0.000069	0.185477	0.001202	0.283279	0.282770	17.9	18.0	1.4	-45	-68
Lanyu-Beach sand															
LYS02-03	2521	34	0.281888	0.000131	0.005047	0.000097	0.190476	0.004929	0.281644	0.281172	-31.3	16.8	4.7	2144	1984
LYS02-04	542	26	0.282610	0.000070	0.003917	0.000062	0.108927	0.002199	0.282570	0.282434	-5.7	4.8	2.5	986	1196
LYS02-05	2488	62	0.281593	0.000055	0.004186	0.000037	0.156353	0.002380	0.281394	0.281193	-41.7	7.1	1.9	2533	2554

Table A2. (Continued)

Spot	Inferred age (Ma)	±2 s	Hf isotopes												
			$^{176}Hf/^{177}Hf$	±2 s	$^{176}Lu/^{177}Hf$	±2 s	$^{176}Yb/^{177}Hf$	±2 s	$^{176}Hf/^{177}Hf$ (T)	$^{176}Hf/^{177}Hf$ CHUR(T)	$\varepsilon_{Hf}(0)$	$\varepsilon_{Hf}(T)$	±2 s	T_{DM} (Ma)	T_{DM}^{C} (Ma)
LYS02-06	2500	36	0.281660	0.000066	0.003567	0.000070	0.138151	0.002449	0.281490	0.281186	-39.3	10.8	2.3	2390	2336
LYS02-07	2546	32	0.281540	0.000065	0.002795	0.000038	0.114379	0.002403	0.281404	0.281156	-43.6	8.8	2.3	2513	2495
LYS02-09	2560	34	0.281683	0.000059	0.003911	0.000137	0.166478	0.006571	0.281492	0.281147	-38.5	12.3	2.1	2380	2294
LYS02-10	2552	32	0.281476	0.000046	0.003569	0.000071	0.147075	0.003785	0.281302	0.281152	-45.8	5.3	1.7	2660	2713
LYS02-11	2558	32	0.281636	0.000077	0.004230	0.000070	0.175512	0.003384	0.281430	0.281148	-40.2	10.0	2.7	2471	2431
LYS02-12	2543	34	0.281710	0.000061	0.003275	0.000067	0.130839	0.003654	0.281551	0.281158	-37.5	14.0	2.2	2298	2175
LYS02-13	2524	32	0.281619	0.000081	0.002671	0.000010	0.094716	0.000847	0.281490	0.281170	-40.8	11.4	2.9	2391	2322
LYS02-14	2.6	0.4	0.283065	0.000042	0.001922	0.000056	0.071727	0.001520	0.283065	0.282770	10.4	10.4	1.5	271	421
LYS02-15	2497	40	0.281728	0.000116	0.003588	0.000066	0.133507	0.003072	0.281556	0.281188	-36.9	13.1	4.1	2293	2193
LYS02-16	2552	36	0.281746	0.000060	0.002932	0.000036	0.116539	0.001721	0.281603	0.281152	-36.3	16.1	2.1	2224	2055
LYS02-22	2401	36	0.281507	0.000042	0.002942	0.000028	0.115630	0.002513	0.281372	0.281250	-44.7	4.4	1.5	2570	2657
LYS02-27	2540	34	0.281548	0.000041	0.003745	0.000030	0.171299	0.001090	0.281366	0.281160	-43.3	7.3	1.4	2568	2581
LYS02-29	3.0	0.4	0.283041	0.000074	0.001994	0.000030	0.070179	0.001337	0.283041	0.282770	9.5	9.6	2.6	307	475
LYS02-30	772	32	0.282493	0.000059	0.002697	0.000028	0.107466	0.001589	0.282454	0.282290	-9.9	5.8	2.1	1124	1309
LYS02-33	2555	38	0.281622	0.000051	0.004041	0.000036	0.174526	0.002635	0.281424	0.281150	-40.7	9.8	1.8	2480	2445
LYS02-34	2531	32	0.281622	0.000073	0.002770	0.000069	0.109027	0.003665	0.281488	0.281166	-40.7	11.5	2.6	2393	2322
LYS02-36	2452	32	0.281933	0.000059	0.004550	0.000054	0.192832	0.001729	0.281720	0.281217	-29.7	17.9	2.1	2044	1862
LYS02-37	2525	40	0.281703	0.000067	0.002102	0.000042	0.081084	0.002009	0.281601	0.281169	-37.8	15.4	2.4	2236	2077
LYS02-38	2522	36	0.281625	0.000059	0.004283	0.000100	0.181963	0.005138	0.281419	0.281171	-40.6	8.8	2.1	2492	2478
LYS02-39	2364	34	0.281522	0.000048	0.003628	0.000069	0.153812	0.003639	0.281358	0.281274	-44.2	3.0	1.7	2598	2711
LYS02-41	2450	52	0.281641	0.000059	0.004472	0.000066	0.177961	0.004509	0.281432	0.281218	-40.0	7.6	2.1	2482	2496
LYS02-42	2301	32	0.281902	0.000087	0.004762	0.000212	0.181689	0.008717	0.281693	0.281315	-30.8	13.4	3.1	2105	2019
LYS02-44	2528	32	0.281753	0.000049	0.003748	0.000049	0.156152	0.003266	0.281572	0.281167	-36.0	14.4	1.8	2265	2138
LYS02-46	2.8	0.8	0.283026	0.000062	0.002622	0.000059	0.094599	0.001836	0.283026	0.282770	9.0	9.0	2.2	334	509
LYS02-47	2605	32	0.281618	0.000042	0.003030	0.000066	0.134450	0.003483	0.281467	0.281117	-40.8	12.4	1.5	2416	2319
LYS02-48	4.8	0.8	0.283023	0.000055	0.002606	0.000069	0.101161	0.001579	0.283022	0.282769	8.9	9.0	1.9	339	516
LYS02-49	2.9	0.6	0.283087	0.000048	0.002015	0.000042	0.089257	0.001085	0.283087	0.282770	11.2	11.2	1.7	239	370
LYS02-50	3.0	0.2	0.283245	0.000064	0.004198	0.000057	0.150834	0.002272	0.283245	0.282770	16.7	16.8	2.3	8	10
LYS02-51	816	34	0.282493	0.000053	0.004180	0.000118	0.195348	0.005747	0.282429	0.282262	-9.9	5.9	1.9	1172	1337
LYS02-53	2.6	0.6	0.283030	0.000033	0.001632	0.000088	0.078353	0.002677	0.283030	0.282770	9.1	9.2	1.2	319	500